THE EFFECT OF WELD PENETRATION ON THE TENSILE STRENGTH OF FILLET WELDED JOINTS

by

Robb C. Wilcox

B.S., Naval Architecture and Marine Engineering
United States Coast Guard Academy, 1991

Submitted to the Departments of Ocean Engineering and Mechanical Engineering
in Partial Fulfillment of the Requirements for the Degrees of

MASTER OF SCIENCE
IN NAVAL ARCHITECTURE AND MARINE ENGINEERING

AND

MASTER OF SCIENCE
IN MECHANICAL ENGINEERING

at the
Massachusetts Institute of Technology
May 1995

Signature of Author_____
Department of Ocean Engineering
May 1995

Certified by _____
Professor Koichi Masubuchi
Department of Ocean Engineering, Thesis Supervisor

Certified by_____
Professor Frank A. McClintock
Department of Mechanical Engineering, Thesis Reader

Accepted by_____
Professor A. Douglas Carmichael
Department Graduate Chairman, Department of Ocean Engineering

THE EFFECT OF WELD PENETRATION ON THE TENSILE STRENGTH OF FILLET WELDED JOINTS

by

Robb C. Wilcox

Submitted to the Departments of Ocean Engineering and Mechanical Engineering on May 12, 1995 in partial fulfillment of the requirements for the degrees of Master of Science in Naval Architecture and Marine Engineering and Master of Science in Mechanical Engineering

Abstract

Fillet welds joining ship hull plating to longitudinal stiffeners have failed in the grounding of very large crude oil carriers (VLCC). A tension mode of fillet weld failure has been observed in some grounding accidents. Deeper penetration welds are shown to be an effective and inexpensive way to increase fillet weld joint strength and tearing resistance.

Specimens were fabricated to determine the welding parameter effects on geometry and quality of fillet welds. Flux Cored Arc Welding (FCAW) was chosen as the welding process due to its popular use for fillet welds in shipbuilding. Full scale 6 mm leg length fillet welds corresponded to typical design standards for VLCC ships. Specimens were constructed using A-36, DH-36, and EH-36 steel. Two grades of 0.045 inch diameter welding wire were used for the appropriate base plate as specified by American Bureau of Shipping (ABS). Polished profiles of the fabricated welds showed that weld penetrations as deep as 4.0 mm can be achieved without beveling the joint.

Tests determined the tensile strength of fillet welded joints with penetration. Seven test specimens were fabricated using EH-36 base plate and Excel-Arc 71 (E71T-1) welding electrode. Three test specimens were fabricated using DH-36 base plate and Fabco 802 (E71T-1) welding electrode. Results with the Excel-Arc 71 electrode showed a 63% increase in tensile joint strength with 3.2 mm of penetration. This was a 50% increase in the tensile strength of the joint as compared to the 1.1 mm penetration obtained from manufacturer-recommended parameters. Results with the Fabco 802 electrode showed a 37% increase in the weld tensile strength with an increase of 3.3 mm in weld penetration.

Load versus displacement diagrams for the ten tests showed similar trends. A plastic limit load was achieved by the welded joints prior to breaking the specimens. Deeply penetrating welds showed three to four times the plastic extension as compared to welds without penetration. Deformation increased the work to deform the deeper penetrating welds by a factor of three to five.

Limit loads of the test specimens were compared to theoretical predictions using an exact and a least upper bound solution. Methods are based on the assumptions of plane strain conditions, homogeneous welds, and non-strain hardening material. The exact solution is based on slip-line theory described by curved lines of shear in yield when the weld deforms

plastically. The upper bound solution simplifies calculations by assuming two linear slip planes of shear oriented to give the least upper bound in plastic deformation. The upper bound solution overpredicts the slip line solution by 5% for the largest penetrations achieved. The upper bound method was used for comparison to test results due to its simplicity with good accuracy.

To calculate the limit load, the shear strength of the weld material in yield was necessary. Manufacturer and Rockwell A hardness estimates for tensile strength calculated the values of yield strength in shear. Welds without penetration showed a 10% underprediction and deeper penetrating welds showed a 30% underprediction in shear strength for manufacturer strengths as compared to hardness estimated values. Hardness estimated strengths reflected the increase in hardness with deeper penetrating welds giving a more realistic weld strength. For deep penetration welds, the upper bound solution overpredicts weld strength by 25% using hardness determined values of yield strength. Low penetration welds showed a 22% underprediction based on hardness determined weld strength.

Deposition rate and specific energy for tested welds showed the relative costs of producing the deeper penetration welds. The deepest penetrating welds showed an increase of 70% in deposition rate of weld metal as compared to manufacturer recommended weld parameters. Deepest penetrating welds with higher currents showed the energy needed to weld a given length of weld decreased by 5% as compared to power consumed using the manufacturer recommended parameters.

Thesis Supervisor: Dr. Koichi Masubuchi
Title: Kawasaki Professor of Engineering

Acknowledgments

I would like to thank Professor Masubuchi for his guidance and support as a thesis advisor. I also give thanks to Professor McClintock for his patience and valuable insight that helped me better understand plasticity and the limit load theory and improve the quality of my thesis calculations. I appreciate the assistance of Tony Zona in welding the test specimens. Thanks are also due to the welding engineers at Bath Iron Works, Newport News Shipbuilding, Ingalls Shipbuilding, Mitsubishi Heavy Industries, and Kawasaki Heavy Industries for their insight into this research and willingness to share relevant information with me. I would also like to thank the staff at the Army Arsenal in Watertown Massachusetts; with special thanks to Wayne Bethany for assistance in performing the tensile tests using the Arsenal's test equipment. Thanks are also due to my family and Maryann for their support and my father for engineering advice.

TABLE OF CONTENTS

LIST OF FIGURES

LIST OF FIGURES (CONTINUED)

LIST OF TABLES

CHAPTER 1
INTRODUCTION

1.1 Background

Despite advancing technology in navigation equipment and improvements in the control of ships, collision and grounding incidents of vessels have continued to present a problem in the safe transportation of cargo at sea. The grounding of the Exxon Valdez at Prince William Sound in 1989 showed the damage that can occur from a vessel accident. Millions of gallons of oil were spilled into the delicate marine ecosystem; the damaging effects will be felt for many years to come. Despite a large scale clean up effort and billions of dollars in funding, the environment of Prince William Sound is far from its original condition. Although it is difficult to say that a ship is fully ground proof or unsinkable, as shown by the disaster of the Titanic, naval architects can continue to learn from maritime accidents to improve ship structures.

Ship design in the past has focused on the strength required to withstand expected forces at sea and in loading, however, the environmental concerns and a better understanding of uncommon ship forces are becoming more influential in vessel design today. Shipbuilding has developed design standards for the selection of materials, sizing of vessel components, and methods for welding ship structures. The effect of grounding as a significant problem in ship design prompted the U. S. Congress to pass the Oil Pollution Act of 1990 requiring the use of double hull ships to protect against the loss of oil in ship grounding.

The design of ships to better withstand damage due to grounding should not be limited to the use of double bottom hulls. An open mind should be considered for the best solution (s) to prevent grounding damage from leading to oil outflow and damage to the environment. The need to better understand the effects of grounding on ship structures prompted a joint M.I.T.-Industry Program on Tanker Safety. The research at M.I.T. was divided into two teams: one focusing on the prediction of damage to hull plating and the other team focusing on the better understanding of weld design in ships and improving weld strength as needed for grounding failure loads.

Investigations of the damage encountered in the grounding of the Exxon Valdez and the Charles B. Renfrew have shown failure of the fillet welds in the damaged area. Fillet welds attaching the longitudinal stiffeners to the lower hull have primarily been designed to withstand the longitudinal shear stresses encountered by the hogging and sagging moments encountered by the ship in waves. The better understanding of the longitudinal stresses and use of stronger materials has pushed for the reduction in the required size of fillet welds for the determined joint efficiencies. However, the occurrence of grounding loads should be considered for the better design of ship resistance to hull damage.

Research of the welding team at M.I.T. has worked towards the improvement and understanding of weld design. A literature survey was performed by McDonald (1993) on existing requirements for the design of fillet welds in ships. Inspection of vessel grounding damage showed that a prominent mode of fillet weld failure was the tearing of longitudinal stiffeners away from the hull plating. The desire to increase joint strength and shift deformation away from the weld prompted the tearing test performed by Kirkov (1994). Results showed that it would be necessary to increase the typical leg length from 6 mm to 12 mm to shift the failure from the weld to the stiffener in tension loading.
If the work to deform the weld is larger than the work to fold the hull plate, the weld will not fail in a peeling mode. An examination of various ways to improve weld joint strength including increasing leg length, weld penetration, and strength of weld material raised interest in the advantages of increasing weld strength through larger weld penetrations

1.2 Objectives

Understanding the strength of fillet welded joints is important in the design of ships. Achieving a weld joint strength that is sufficient to shift the plastic deformation failure into the longitudinal web is desirable. In a grounding the result would be the increase in the work absorbed by the deformation of welded stiffeners, a reduction in the size of hull damage, and less oil spillage.

The scope of this research was divided into two main parts including the methods of obtaining deeper penetrating welds and the determination of the added strength due to

the deeper penetrating welds. Weld parameters were varied for the FCAW process to obtain varying penetrations. Full scale fillet weld tension tests were performed to determine the experimental value of increased weld strength with penetration. A theoretical analysis of weld strength was performed using plasticity theory.

There are several different theoretical approaches available for the design of fillet welds. Conventional design treated all fillet welds as if the load was oriented in the weakest direction (longitudinally). The result of this method was an oversizing of fillet welds loaded transversely since transverse loaded welds are stronger than welds loaded longitudinally as shown by Kato & Morita (1974). Krumpen and Jordan (1984) approximate the tensile strength of fillet welds based on the throat thickness of the fillet weld and a determined allowable tension yield stress. Kato and Morita (1974) approximated the strength of a weld in tension to be 1.46 times the longitudinal strength applying certain boundary conditions to the compatibility equations of elasticity.

While Krumpan and Jordan give an approximation to weld joint strength, there are theoretical tools that can be used to approximate strength of fillet welds with plastic deformation. The use of plastic mechanics with slip line theory satisfies equilibrium equations and yield conditions to give an exact solution to the limit load assuming plane strain and a nonhardening material. Another theoretical approach using plasticity, the block sliding method, satisfies displacement boundary conditions for an upper bound solution to the limit load. This study uses the block sliding method and slip line theory as theoretical tools for determining the limit load of fillet welds. Assumptions include non-hardening material properties and a homogeneous weld.

1.3 Organization of Paper

Chapters are used to identify the separate areas of research in this thesis. At the end of each chapter are the relevant tables and figures that relate to the information contained in the chapters. Appendices offer more detailed information as needed in clarifying the text.

CHAPTER 2
FILLET WELD DESIGN IN SHIPBUILDING

2.1 Current Design Standards

The design of structural details in merchant ships is influenced greatly by standards of classification societies. There are about thirteen larger classification societies in the world that govern vessel design within their country. The majority of merchant vessels are governed by the American Bureau of Shipping, Lloyd's Register of Shipping, and Nippon Kaiji Kyokai (McDonald, 1993). Another source of ship construction standards in welding is the U.S. Navy for the construction of military vessels. It is important to compare the design standards between classification societies for possible improvements in ship design.

Classification societies direct the size and type of material used in constructing commercial ship welds. The standards are based on theory, experience, and factors of safety used to simplify weld design for normal operating stresses. Standards used in the sizing of fillet welds in commercial vessels are largely controlled by the American Bureau of Shipping, Lloyd's Register of Shipping, and Nippon Kaiji Kyokai.

2.1.1 ABS

The American Bureau of Shipping specifies the appropriate weld geometry, material, and conditions for specified joints encountered in ship construction. Size requirements of fillet welds are found in Part 3 Section 23 "Weld Design" of the ABS rules. Specifications for acceptable filler metals for ABS steels are described in Part 2 Appendix 2/C. Standards show a qualification test is required to demonstrate the ability of welders and evaluate the welding process to ensure good quality fillet welds free from porosity, undercut, and other weld defects.

In order to determine the size of fillet welds required without penetration ABS (1993) uses the following formula:

w = leg length of fillet weld

$w_{min} = 0.3 \times t_{pl}$ *or* 4.5 mm

w_{min} (tanks of oil carriers) = 6 mm

l = length of fillet weld

S = the distance between successive weld fillets, from center to center

S/l = 1.0 for continuous fillet welding

t_{pl} = thickness of the thinner of the two members being joined

C = weld factors (Table 3/23.1 in ABS Standards Publication)

C = .25 for frames, beams, and stiffeners attached to the bottom shell

$$w = t_{pl} \times C \times \frac{s}{l} + 2.00 \qquad (2.1)$$

ABS takes the effect of a deeper penetration weld into consideration with a reduction in the required weld size. Where automatic double continuous fillet welding is used and quality control facilitates working with a maximum of 1 mm gap between members being attached, a reduction in weld size of 1.5 mm is allowed provided that the penetration at the root is at least 1.5 mm into the members being attached (American Bureau of Shipping, 1993).

2.1.2 Lloyd's Register of Shipping

In order to determine the size of fillet welds without penetration the following formula is used as shown in Lloyd's Register, 1992:

S = intermittent welds length of the fillet

d = intermittent welds distance between start positions of successive fillet welds

$\frac{d}{s} = 1.0$ for double continuous fillet welding

t_p = thickness of the thinner of the two members being joined

weld factor: = 0.21 for longitudinal attached to plating in oil tanks

= 0.34 for primary structure in oil tanks

$$\text{throat thickness} = t_p \times \text{weld factors} \times {}^{d}/_{s} \quad \text{(mm)} \qquad (2.2)$$

Lloyd's Register of Shipping requires the use of deep penetration or full penetration welds in highly stressed connections as specified by the standards. A leg length reduction for deeper penetrating fillet welds allows a decrease of the weld factors by as much as 15 per cent. Beveling of the plate is to be performed as required.

2.1.3 Nippon Kaiji Kyokai

NKK specifies the welding material that can be used on specific grades of steel. The sizes of fillet welds are based on the thickness of the web member for stiffeners. A table shows the leg length required for varying web thickness. The use of deeper penetration welds is not specified as a way of decreasing fillet weld size in the NKK standards. However, a deep penetration fillet weld test assembly is shown to examine the weld quality and penetration of deeper penetrating welds. Figure 2.1 shows a midship section of a typical double hull tanker design and the required weld sizes as specified by NKK. (NKK, 1986)

2.1.4 Comparison of Regulatory Agencies

The size of fillet welds attaching longitudinal stiffeners to the hull varies between classification societies as shown in Table 2.1. The design of fillet welds has traditionally been based on a weld with no penetration. Classification societies specify the leg length of

a fillet weld in order to estimate a certain weld strength. This method of designing welds makes it is easy to inspect for the required weld sizes.

Welds with deeper penetrations decrease the required leg length by varying amounts. ABS shows a 25% reduction in weld leg length due to a minimum of 1.5 mm penetration. LR shows a 15% reduction in weld leg length with deep penetrating fillet welds, however, the definition of "deep penetration" is not mentioned in the standard. NKK did not state any size reduction due to penetration in fillet welds. Differences with the fillet weld standards concerning weld penetration are significant. The effect of weld penetration on the size of a fillet weld should vary with the depth of penetration.

2.2 Grounding Failure Modes

McDonald (1993) estimated that the American Bureau of Shipping standards typically design fillet welds with a 40% efficiency in strength when loaded in the longitudinal direction. Longitudinal shearing is the loading condition that typically governs the size of fillet welds for stiffeners. A combination of the primary shear and bending stresses with secondary stresses from pressure on the hull can be combined using the Von Mises Combined Stress Condition to estimate the shear stress at the weld location (Krumpen and Jordan, 1984). ABS is not sizing welds based on full efficiency due to the increase in cost and the apparent adequacy of the weld design based on common ship operation. However, the failure of fillet welds in ship grounding has raised the question of how to increase the strength of the welds and to what extent.

Figure 2.2 shows the various deformation and fracture modes possible for fillet welds in ships. Web folding and bending are modes that have been observed in grounding. Both the Exxon Valdez and Charles B. Renfrew showed a bending mode of deformation of the stiffeners at the location of the damage on the hull. McClintock (1994) predicted that the leg length required to prevent weld failure in folding for homogeneous welds is 0.366 times the web thickness which is marginally met by standards up to a web thickness of 19 mm. Web folding is observed in the damage of the Exxon Valdez and Charles B. Renfrew, however, the failure of the welds was not observed in photographs. Further

analysis and testing of the strength of fillet welds in bending has been done by Brooks (1995).

Tearing and tension loadings on fillet welded joints are also possible deformation modes as shown in Fig. 2.3. The tearing and tension modes were observed in the damage in the grounding of the Exxon Valdez and Charles B. Renfrew. Tearing work of welds must exceed the complimentary hull folding work to prevent weld failure. The required leg length to shift failure from the weld to the intercostal (web) of the stiffener was determined by Kirkov (1994). Results by Kirkov showed that for a 15 mm web thickness the fillet weld leg length would need to be increased to 12 mm in order to create a 100% efficient joint in tension. The benefit of creating a 100% efficient weld joint is the increase in strength of the structure and the amount of work needed to deform the ship. As a result, a tanker would have less damage and oil outflow.

2.3 Improving Weld Joint Strength

Improving the tearing work or tensile strength of fillet welds to shift the deformation and fracture to areas surrounding the weld is desirable in the grounding of ships. To improve the fillet weld strength there are several alternatives as shown in Fig. 2.4. Longer leg length is a customary way to increase the strength of a fillet weld, however, there are several difficulties. One of the problems is the increase in the amount of weld consumable. In order to double the strength of a fillet weld without penetration the leg length of the weld needs to generally be doubled with a fourfold increase in volume. The extra welding cost from the consumable as well as increased welding time due to multiple welding passes makes this method expensive for fully efficient joints in tension.

The effect of varying the fillet angle affects the strength of a welded fillet joint. McClintock (1994) used upper bound solutions to show that as the fillet angle (angle of fillet weld surface above the continuous member) is increased above 45 degrees, the strength of the weld slightly increases. However, the increase in weld material consumed outweighs the benefit from weld strength. A 45 degree fillet weld with equal leg lengths is the most efficient use of weld material.

Weld penetration is a promising method of increasing weld joint strength in tension loading. Full penetration welds typically formed by beveling plate, welding, backgouging, and then welding the opposite side to achieve full penetration have been used for full efficient fillet weld joints in shipbuilding (MIL-STD-1628). The use of partial penetration welds through beveling joints to increase the strength of fillet welds to 100% has been included in Navy standards in situations where beveling is more economical than increasing the leg size.

Penetration without beveling the plate is another consideration. With relevant depths of penetration a weld can increase joint strength without adding any weld material. Theory and experiments presented in this research paper focus on the amount of penetration that can be achieved using Flux Cored Arc Welding; a process used in shipbuilding. Added tearing work and strength achieved by using partial penetration welds are presented by theory and compared to experimental results in Chapter 5. The effect of the cost of producing deeper penetration welds is covered in Chapter 6.

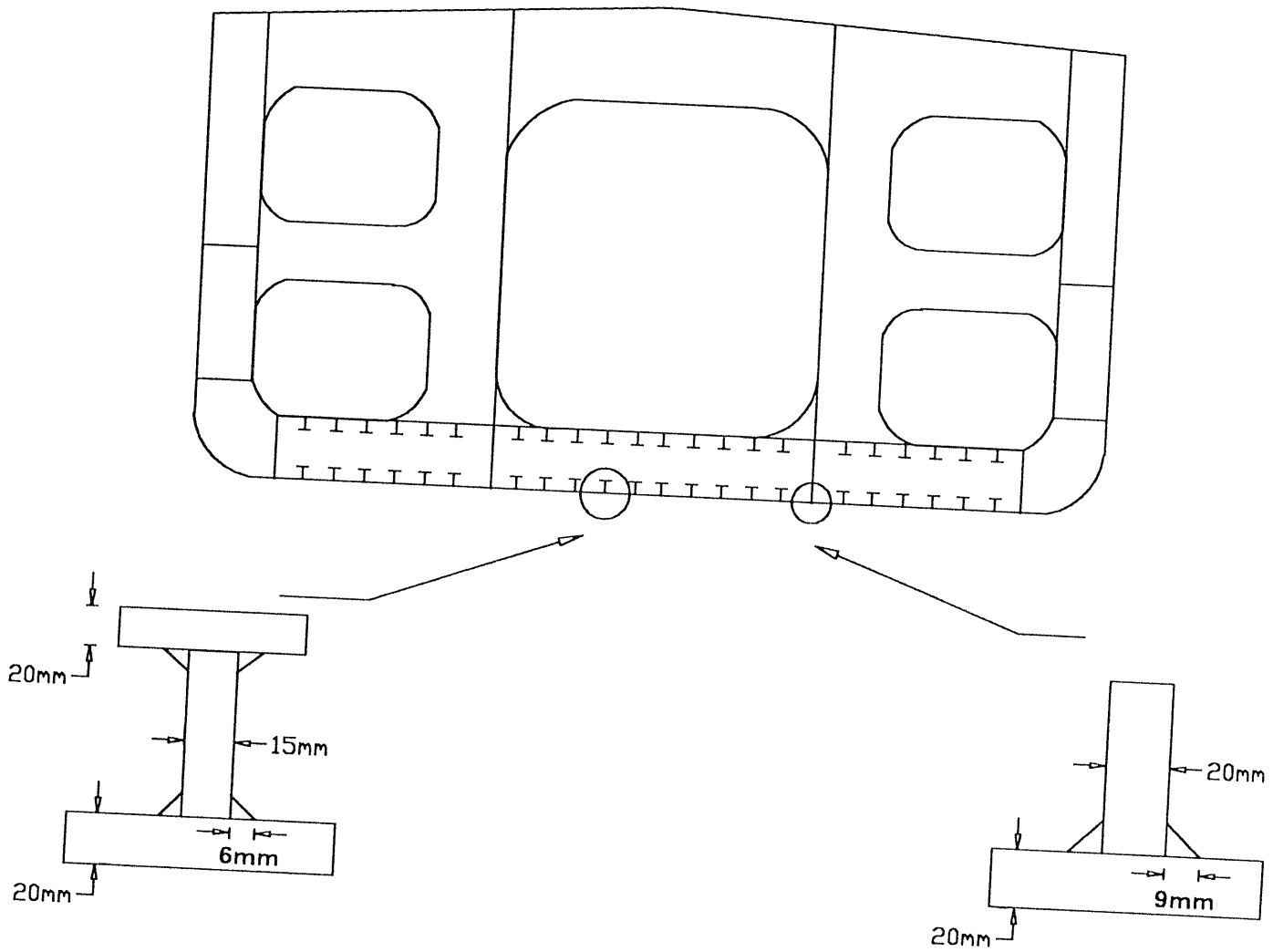

FIGURE 2.1 Midship Section of Double Hull Tanker

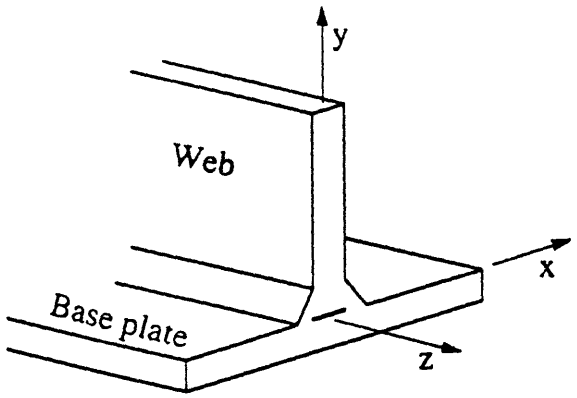

Coordinate axes for a T-joint

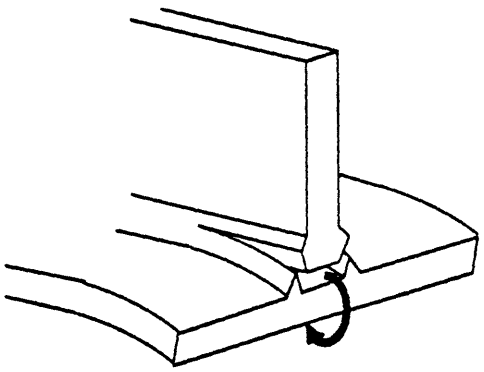

(a) Tearing

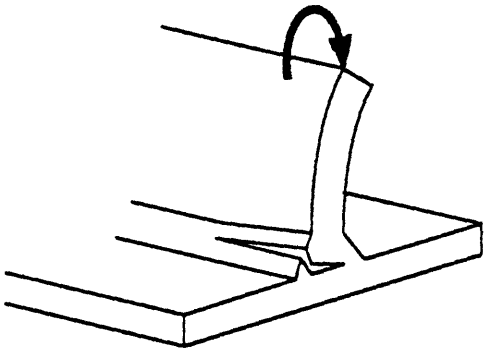

(b) Web folding

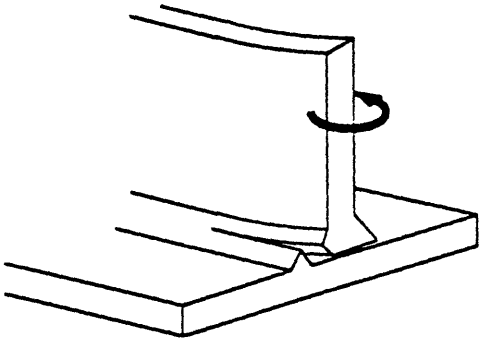

(c) Web bending

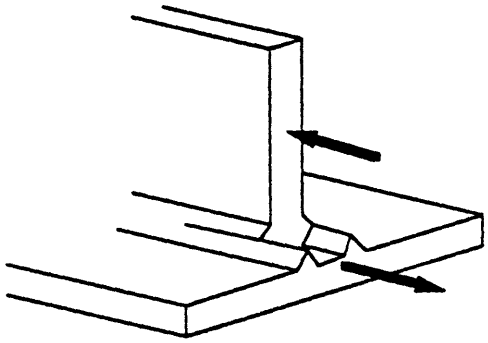

(d) Longitudinal shearing

FIGURE 2.2 Deformation and Fracture Modes of T-Joints [McClintock, 1994]

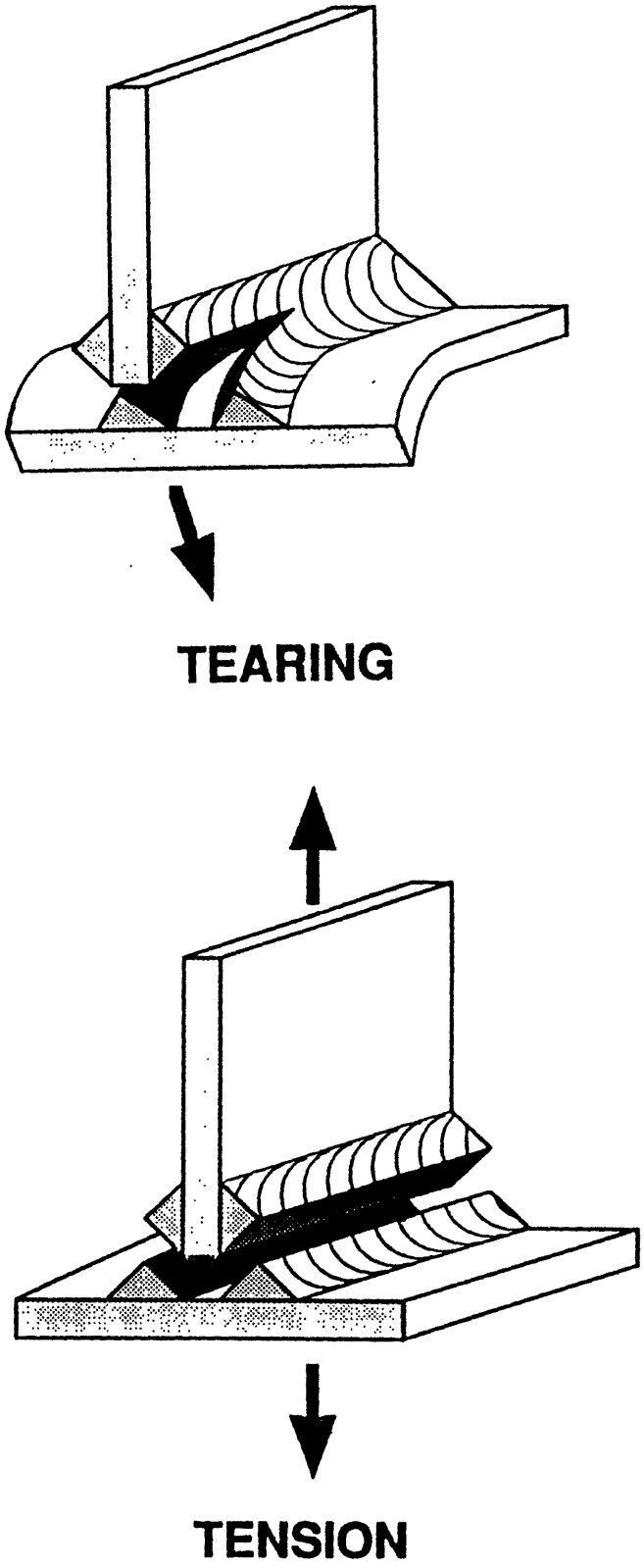

FIGURE 2.3 Deformation Modes Observed in Tanker Grounding

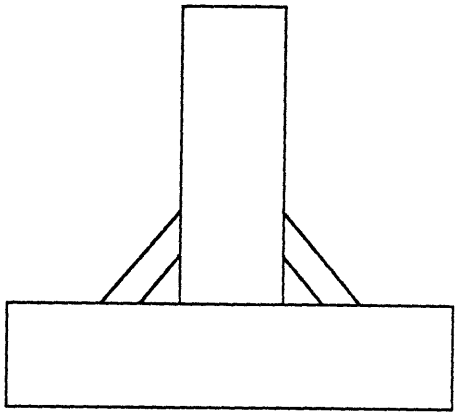

LONGER LEG LENGTH

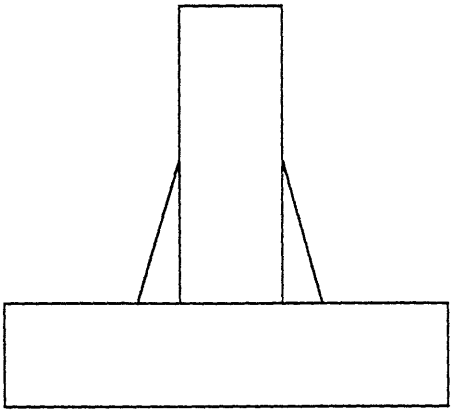

VARYING FILLET ANGLE

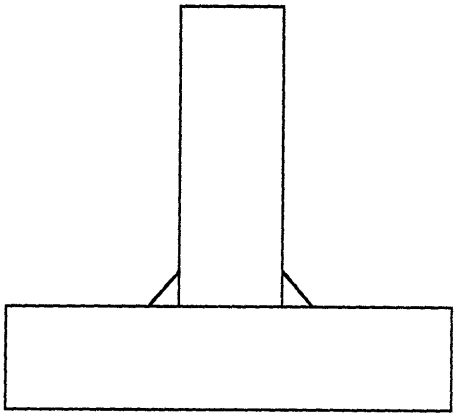

STRONGER WELD METAL

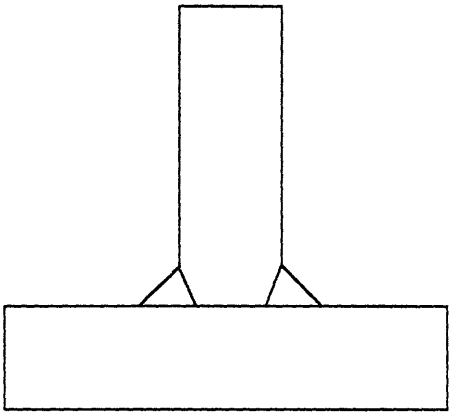

DEEPER PENETRATION

FIGURE 2.4 Improving Fillet Weld Joint Strength

Table 2.1. Comparison of Stiffener Weld Sizes by Classification Societies

(Thickness of intercostal = 15 mm)

AGENCY	LEG LENGTH (Penetration = 0)	LEG LENGTH (Penetration)
American Bureau of Shipping	5.75 mm	4.25 mm (> 1.5mm)
Lloyd's Register of Shipping	5.10 mm	4.34 mm (unstated)
Nippon Kaiji Kyokai	6.00 mm	not specified

CHAPTER 3
ANALYSIS OF TENSION LIMIT LOAD FOR FILLET WELDS

3.1 Introduction

It is important in fillet weld design to be able to predict weld tearing work and strengths. As shown in Fig. 3.1, the force-displacement curve of a plastic structure levels off at a force called the limit load, prior to thinning down or cracking failure. (McClintock, 1994).

The limit load in tension loading of a welded T-joint is a concern for the weld strength of ship stiffeners in grounding. Comparing the limit load of a fillet weld to the strength of the stiffener web predicts which member will fail in extreme loading. The work to tear the weld can also be compared to the work of bending the shell plating in order to determine if the weld will tear or complementary bending of the hull plate will occur (Kirkov, 1994).

The development of estimates for the strength of fillet welds is largely based on a combination of theoretical and experimental results. Theory predicting fillet weld strength varies with different assumptions. Current accepted fillet weld strength analysis for transversely (tension) loaded fillet welds is based on simplified stress calculations for a single failure plane of a fillet weld. The steels used in shipbuilding and welding are generally ductile enough so the failure occurs in the plastic flow region of a load-displacement diagram. Therefore, fully plastic mechanics is needed to determine the strength and tear resistance of fillet welds.

3.2 Conventional Fillet Weld Design

Fillets welds are designed to withstand loading either in longitudinal shear or transverse tension. Strength predictions of longitudinally loaded fillet welds are based on the strength in shear across the weld throat. This is also the exact solution based on non-hardening plasticity theory as long as the web is strong enough to shift shear deformation to the weld. The method of calculating the longitudinal weld strength is accurate and straight forward to calculate . (Krumpen and Jordan, 1984)

Fillet weld design for transversely loaded joints has traditionally been based on longitudinal strength calculations giving conservative weld strength estimates (Krumpen and Jordan, 1984). During the 1920's, testing was performed on fillet welds showing fillet weld transverse loads are of the order of 40% greater than required longitudinal loads to break welded joints. (Kato & Morita, 1974). In order to simplify calculations, all fillet welds were treated as if oriented in the weakest direction (longitudinally). It is excessively conservative because it is not possible to load the web transversely in tension in a way that will fail the weld in longitudinal shear. The resulting design formula for this conservative assumption is (Krumpen and Jordon, 1984):

D = fillet weld leg length (w for ABS notation)

τ_{wl} = weld metal ultimate shear strength

σ_{ui} = tensile stress of intercostal material

T = thickness of the intercostal member (t_{pl} for ABS notation)

$$2 \times D \times \sin(45) \times \tau_{wl} = T \times \sigma_{ui} \tag{3.1}$$

A proposal was presented by Krumpen and Jordan (1984) that made weld joint approximate strength less conservative by accounting for the increase in transverse weld strength as compared to longitudinal loaded strength. From theory and testing it was determined that the transverse strength of a fillet weld is 1.44 times as great as the longitudinal strength. The resulting changes in the transverse strength equation are:

$$\tau_{wt} = \text{weld transverse shear strength} = 1.44 \times \tau_{wl} \tag{3.2}$$

$$2 \times D \times \sin(45) \times \tau_{wt} = T \times \sigma_{ui} \tag{3.3}$$

It is important to note that Eq. 3.3 is still an estimate assuming that weld failure in shear acts on throat of the fillet. Experiments have shown that the fracture path in welds

loaded transversely is about $22\frac{1}{2}$ degrees; not the 45 degree assumption used in Eq. 3.3 (Kato & Morita, 1974). Kato and Morita (1974) show the calculations for the ratio of longitudinal and transverse failure loads of fillet welds to be 1.46. The recommendation by Krumpen and Jordan (1984) is more conservative by taking a smaller ratio of 1.44.

Equations 3.1, 3.2, and 3.3 are based on fillet welds without penetration. Gaines (1990) included estimates for the limit load of such welds that used the same approach as suggested by Krumpen and Jordan, however, for the design of beveled fillet weld joints with penetration. Further explanation of the estimates by Gaines (1990) is shown in Appendix A.

Estimates for limit load by assuming failure regions in the heat affected zone have also been considered by Krumpen and Jordan (1984) and Gaines (1990). Failure in a heat affected zone would occur when the weld strength is large enough to shift crack failure from the weld metal to the HAZ. The intercostal member and continuous member of the welded joint are considered separately. Equations for the estimates of weld strength if failure occurs in a HAZ are included in Appendix A.

3.3 Slip Line Solution

The exact solution for satisfying the limit load must satisfy the following conditions (e.g. McClintock ,1994):

1) the partial differential equations of equilibrium of stress gradients
2) the definitions of components of strain in terms of displacement gradients
3) boundary conditions in terms of displacement of tractions
4) a yield locus which limits the deformation tendency of the stress components
5) linear functions relating only the increments of strain components to current stress components, not the total strain components to the to the current stress components as in elasticity

In plasticity the exact theoretical solution for plane strain with negligible strain-hardening is expressed in terms of lines parallel to the two directions of maximum shear at

each point (Chakrabarty, 1987). The slip lines are under pure shear without any normal distortional stresses. For tension on a homogeneous fillet weld with equal leg lengths the slip lines form sets of parallel lines meeting the surface at 45 degrees as shown in Fig. 3.2. Deformation with deeper penetrating welds forms some curved slip lines as shown in Fig. 3.3.

In order to solve for the plane strain plastic flow of a weld , a slip line field is necessary for the region where deformation will occur. The slip line fields are determined by meeting the plasticity equations and can be verified by observing the deformations. A field defined by circular arcs of equal radii has been found (e.g. Chakrabarty, 1987, p 448) which has the same geometry slip lines as formed in the tension loading of fillet welds with penetration. Figure 3.4 shows the slip line field solutions as determined by Chakrabarty. Appendix B shows the method used to calculate slip-line fields by notes from McClintock (1988). Further explanation of the slip line solution method is covered by Chakrabarty (1987) and Johnson et al. (1982).

For the problem of plasticity in fillet welds the slip line field defined by circular arcs of equal radii was utilized (Chakrabarty, 1987). This eliminated the task of using slip line theory to develop slip line solutions. Chakrabarty's solution was limited to welds with equal leg lengths. The solution for welds with unequal leg lengths is possible but beyond the scope of this thesis.

Integrating the forces along a slip line gives the limit load for the structure. Chakrabarty showed the final forces P and Q along the β slip line from E to N Fig. 3.4 to be:

P = X direction component of force

Q = -Y direction component of force

α = slip lines originating from point D

β = slip lines originating from point E

x_N = *x coordinate of point N*

y_N = *y coordinate of point N*

t = the angle turned through along the slip line

a = throat thickness of the weld

$$P = k[x_N + 2(\alpha+\beta)y_N - 2\beta\alpha - 2y\int_0^{\alpha} y(t,\beta)dt] \tag{3.4}$$

$$Q = k[a - y_N + 2(\alpha+\beta)x_N - 2\int_0^{\alpha} x(t,\beta)dt] \tag{3.5}$$

Normalized values of the P and Q components of force are shown in Table 3.1. These force components along slip lines were found by Chakrabarty (1987) for the intersection of α and β lines in 10 degree increments. These force components were used to interpolate for slip lines occurring at various weld penetrations. Transformation of the P and Q force components to be consistent with the direction of tension loading was used to determine the limit load for different penetration welds as shown in Appendix C. The limit load results are shown in Table 3.2; which also gives the upper bound limit loads as found in section 3.4.

3.4 Upper Bound from Block Sliding

Bounds to the limit load are determined from satisfying fewer conditions than the exact solutions for the slip plane theory. Lower bounds to the limit load are determined if equilibrium equations and yield criterion are satisfied everywhere, including force boundary conditions. Lower bound calculations are often difficult to obtain due to difficulty in satisfying these conditions even throughout the rigid regions. Upper bounds to the limit load must satisfy strain-displacement and incompressibility equations and meet any displacement boundary conditions. McClintock (1994) specifies that an upper bound to the limit load must have displacement fields that:

1) satisfy any displacement boundary conditions
2) give no change in volume anywhere
3) give an integral of the plastic work increment throughout the body that is an upper bound times the corresponding displacement component in the direction of load

Applying the upper bound solution to the fillet weld limit load prediction is a relatively easy process as compared to the exact or slip line solutions. One upper bound method subdivides the deforming weld into three separate rigid regions as shown in Fig. 3.5. The intersecting lines of deformation (shear) do not need to be perpendicular as in the slip line solution. The three solid regions are separated by slip planes. Relative velocities as shown in Fig. 3.6 and slip plane lengths are used to define the rate of work being dissipated. Based on the selected orientation of the slip planes an upper bound solution was determined by the following method (Guerra and McClintock, 1994):

P_{ub} = upper pound to the limit load

k = shear strength of the weld in yield

b = length of the weld segment

L_{AB} = length of the slip plane from A to B

θ_{AB} = angle from the root of the weld to the intersection of the web and weld surface

θ_{BC} = angle from the root of the weld to the intersection of the continuous member and weld surface

L_{BC} = length of the slip plane from B to C

$$P_{ub}\vec{V}_A = 2kb[L_{AB}\left|\vec{V}_A - \vec{V}_B\right| + L_{BCy}\left|\vec{V}_B - \vec{V}_C\right| \tag{3.6}$$

$$\left|\vec{V}_A - \vec{V}_B\right| = \left|\vec{V}_A\right|\frac{\left|\cos(\theta_{BC})\right|}{\sin(\theta_{AB} - \theta_{BC})} \tag{3.7}$$

$$\left|\vec{V}_B - \vec{V}_C\right| = \left|\vec{V}_A\right|\frac{\left|\cos(\theta_{AB})\right|}{\sin(\theta_{AB} - \theta_{BC})} \tag{3.8}$$

Substituting Eq. 3.8 and Eq. 3.7 into Eq. 3.6 and canceling out $\vec{V}_A$ gives limit loads for a double fillet weld loaded in tension for the slip angles defined in Fig. 3.5:

$$P_{ub} = 2kb\left[L_{AB} \frac{|\cos(\theta_{BC})|}{\sin(\theta_{AB} - \theta_{BC})} + L_{BC} \frac{|\cos(\theta_{AB})|}{\sin(\theta_{AB} - \theta_{BC})} \right] \qquad (3.9)$$

Equation 3.9 expresses upper bounds to the limit load for a variety of weld geometries. For welds with equal leg lengths vertically and horizontally as well as with no penetration, the upper bound for a double sided fillet weld reduces to: $P_{ub} = 2kd$ (d = leg length of the weld). The upper bound for welds with penetration can be found by substituting dimensions for the weld geometry. Calculations considering penetration have shown least upper bound solutions found from an upper slip plane with an angle defined from the crack tip (penetration) to the intersection point between the web and weld surface, and a lower slip plane at an angle defined by the crack tip (penetration) and intersection of the weld and base plate surface (Guerra and McClintock, 1994). Limit loads for welds with unequal leg lengths can be found by the upper bound solution for limiting cases as described by Guerra and McClintock (1994). Application of the upper bound method to calculate the limit load of fillet weld joints is shown using Mathcad in Appendix D and results are shown in Table 3.2.

3.5 Comparison of Upper Bound and Slip Line Solution

In order to determine the accuracy of the upper bound solution, a comparison was made with the slip line solution for similar weld geometries. In order to compare the theoretical methods, dimensionless values of penetration/(leg length) with values ranging from 0 to 0.67 were entered for both solution methods. Calculations using the upper bound method are included in Appendix D. Appendix C has calculations for the slip line solution. Table 3.2 and Fig. 3.7 show a comparison of the two solution methods. Slip line and upper bound calculations for welds without penetration are exactly the same. This is due to the same 45 degree field and same active vertical slip plane by either method. As penetrations were increased the upper bound method exceeded the slip line results by as much as 5% for a penetration/(leg length) ratio of 0.67.

3.6 Estimates of Penetration to Shift Yielding to the Web

For fillets welds joints loaded in tension it is desirable to have the weld at least as strong as the web to prevent weld failure in tension loading. If the weld joint is stronger than the web, deformation from tension loading will be shifted to the web and the amount of work to deform the structure will be much larger. Using the upper bound theorem for weld strength and knowing the properties of the web and weld metal gives the tools necessary to predict the required weld geometry for such a 100% efficient joint. The strength of the web is the product of the tensile strength, cross sectional area of the web, and a $\frac{2}{\sqrt{3}}$ factor for plane strain conditions.

As presented by Masubuchi et al. (1993) a typical stiffener has a 15 mm web thickness and a welding leg length of 6 mm as required for VLCC hull design in Japan. Material properties used for the calculation of limit loads was based on EH 36 steel and manufacturer strength properties of AWS E71T-1 (Excel Arc 71) flux cored arc welding electrode. Fig. 3.8 shows the joint strength increasing with longer weld leg lengths with no penetration. The intersection of the weld limit load and the strength of the web gives a required leg length of 12 mm for 100% joint efficiency. This requires doubling the leg length of the fillet weld and a fourfold increase in welding material. Figure 3.9 shows the effect of weld penetration on the limit load for a 6 mm weld leg length. The intersection of the weld limit load and the strength of the web shows that a penetration of 3 mm is necessary to achieve 100% joint efficiency based on the upper bound solution. If weld penetrations of at least 3 mm can be achieved without beveling the plate, the upper bound theory predicts the weld should achieve full joint efficiency.

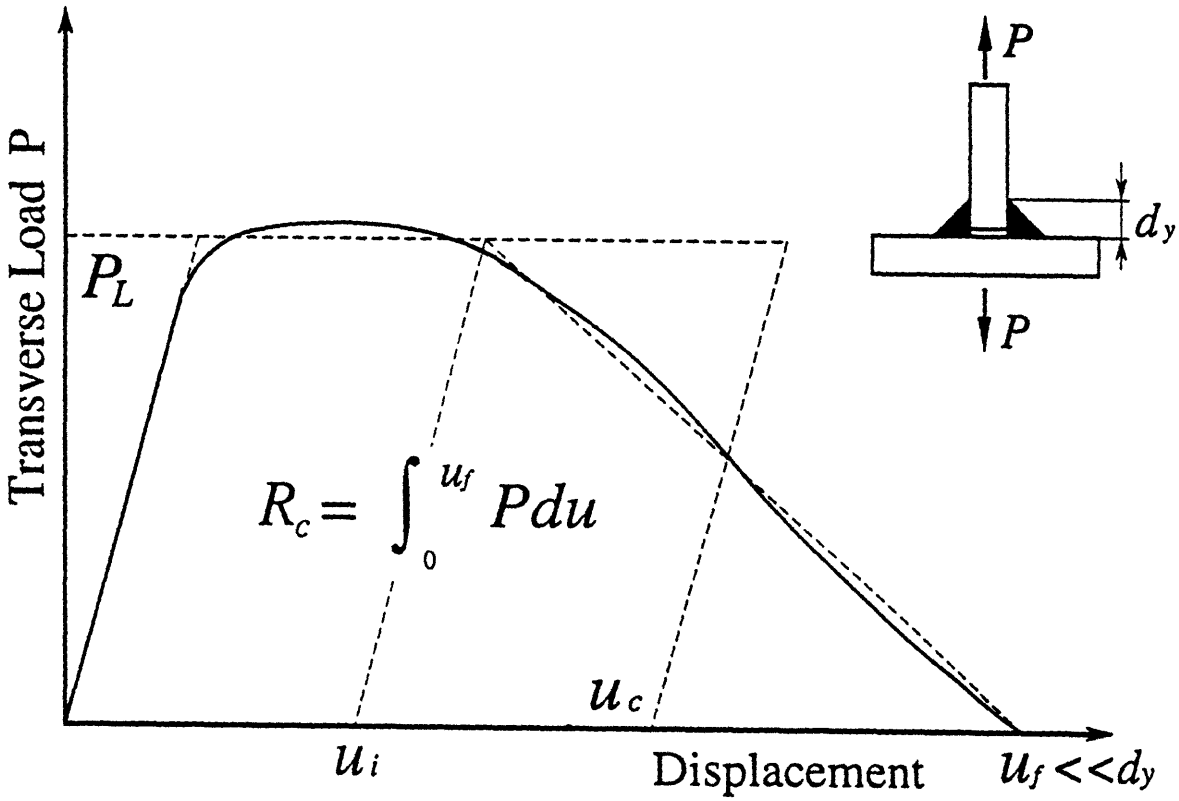

FIGURE 3.1 Force-Displacement Curve for T-Joint Tension
[McClintock, 1994]

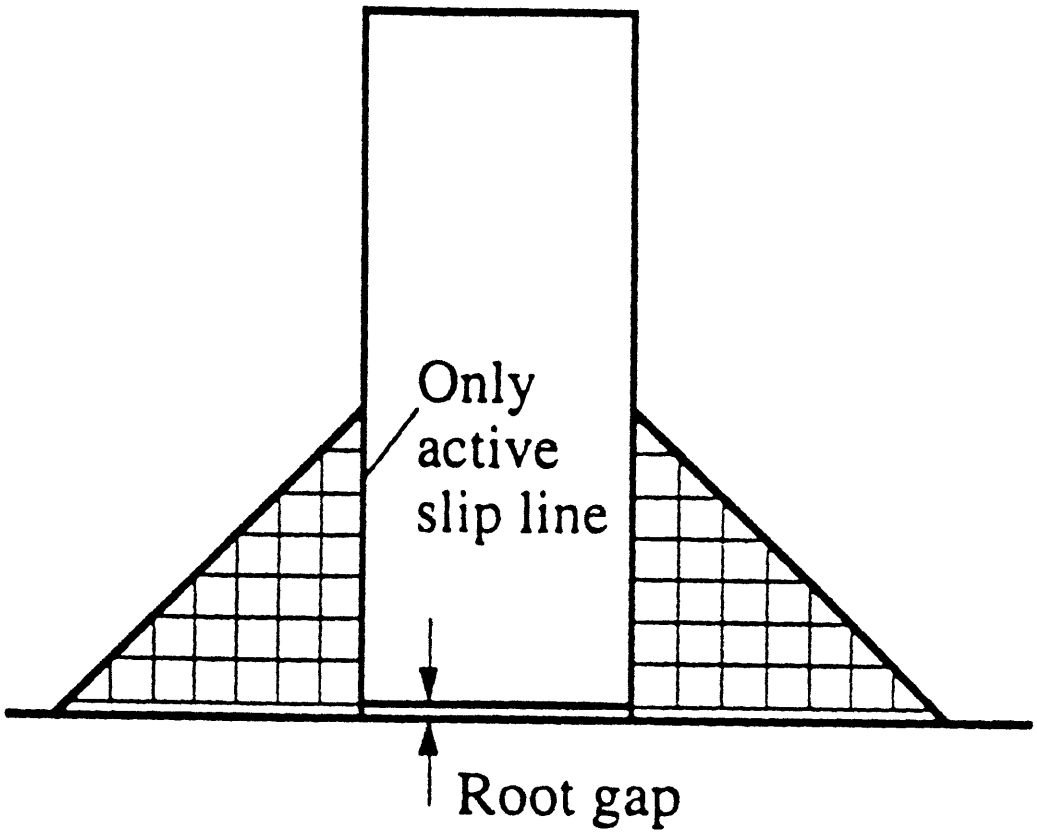

FIGURE 3.2 Slip Line Fields for Symmetric Welds Without Penetration [McClintock, 1994]

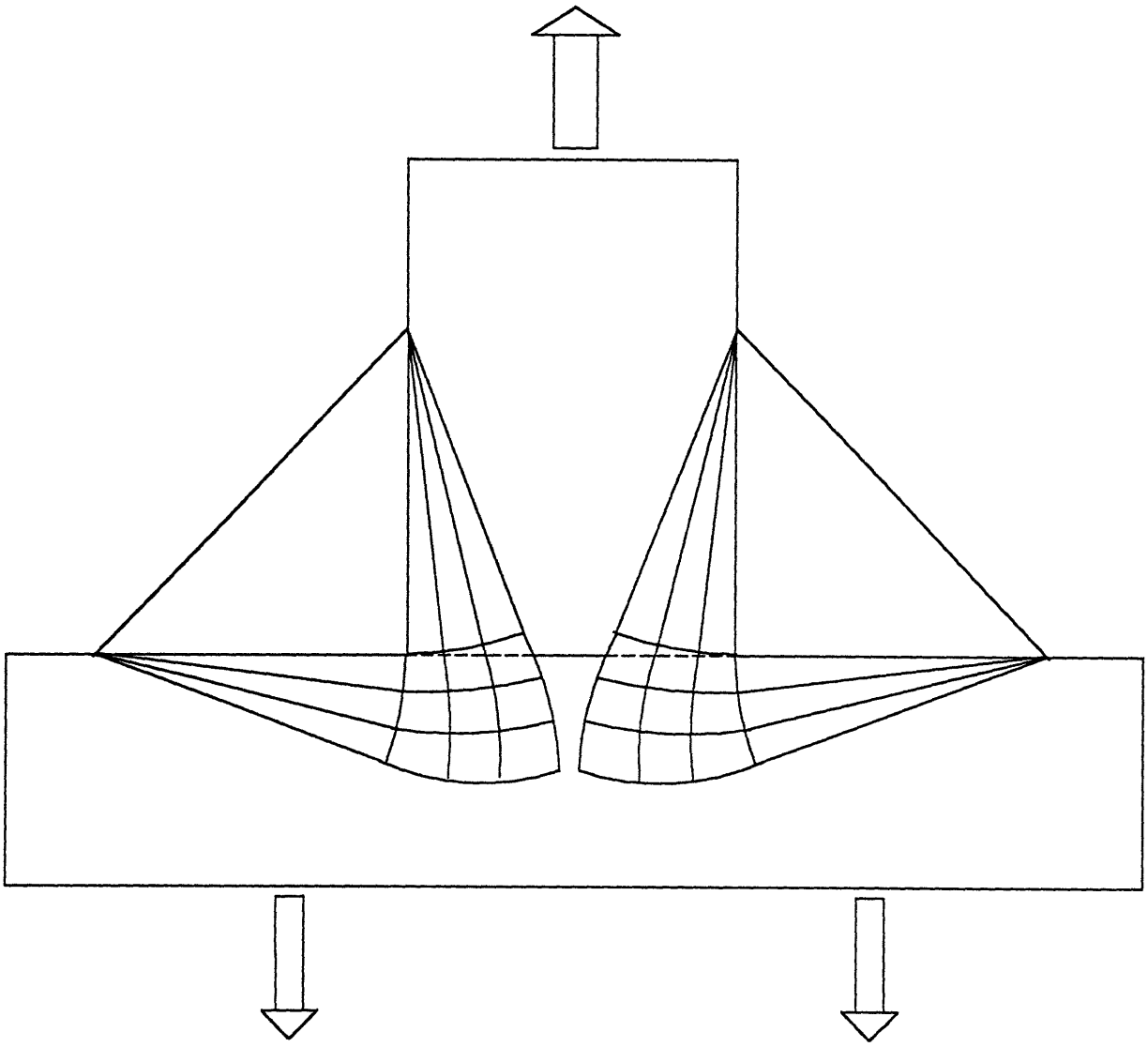

FIGURE 3.3 Slip Line Fields for Welds With Penetration

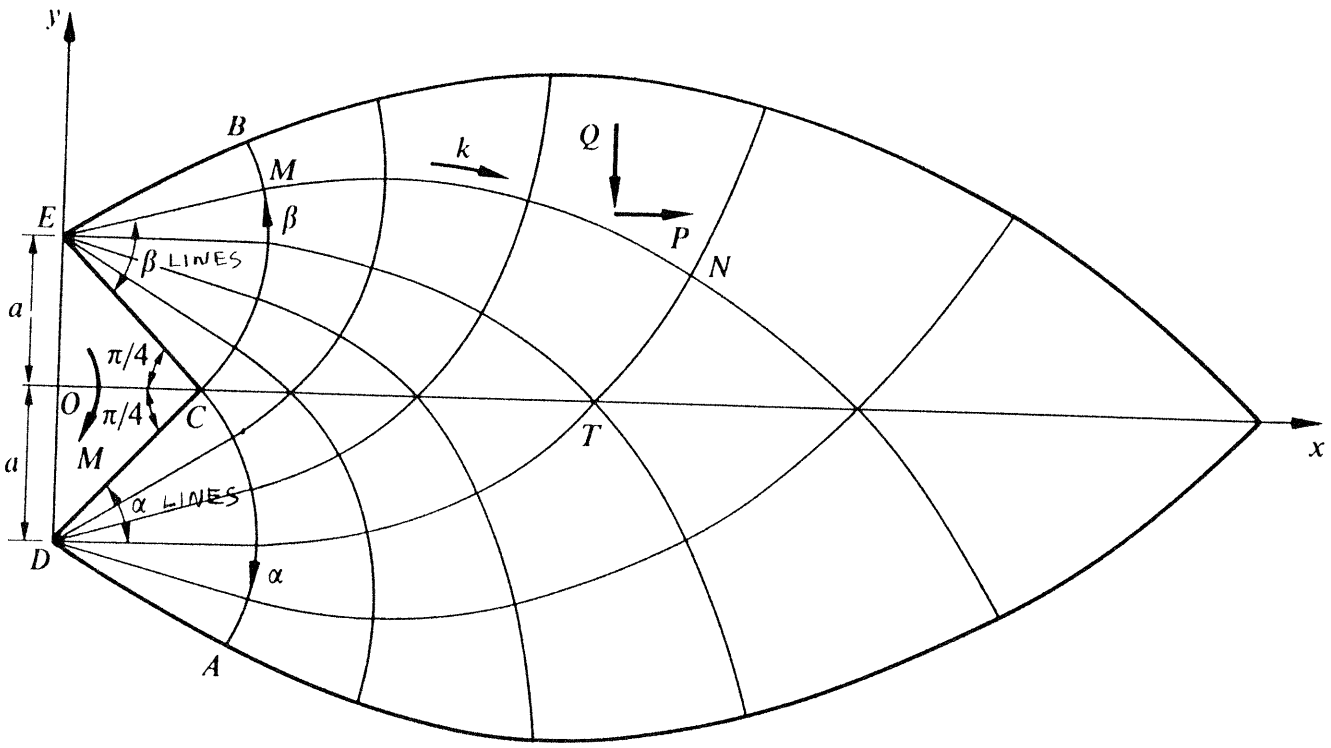

FIGURE 3.4 Symmetrical Slip Line Field Defined by Circular Arcs of Equal Radii [after Chakrabarty, 1987, p 448]

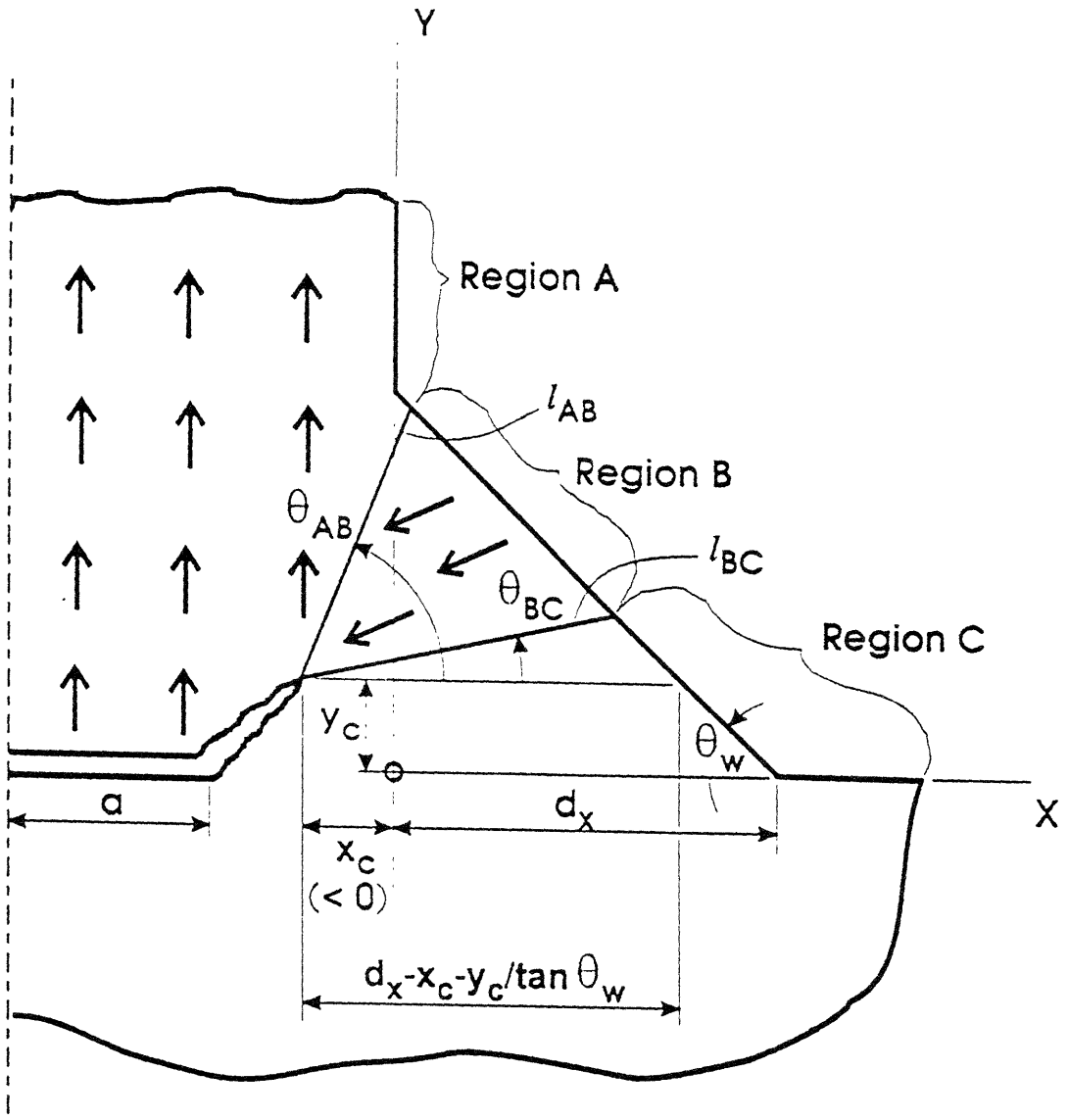

FIGURE 3.5 Planar Block Sliding for Upper Bounds to the Limit Load for Web Tension [McClintock, 1994]

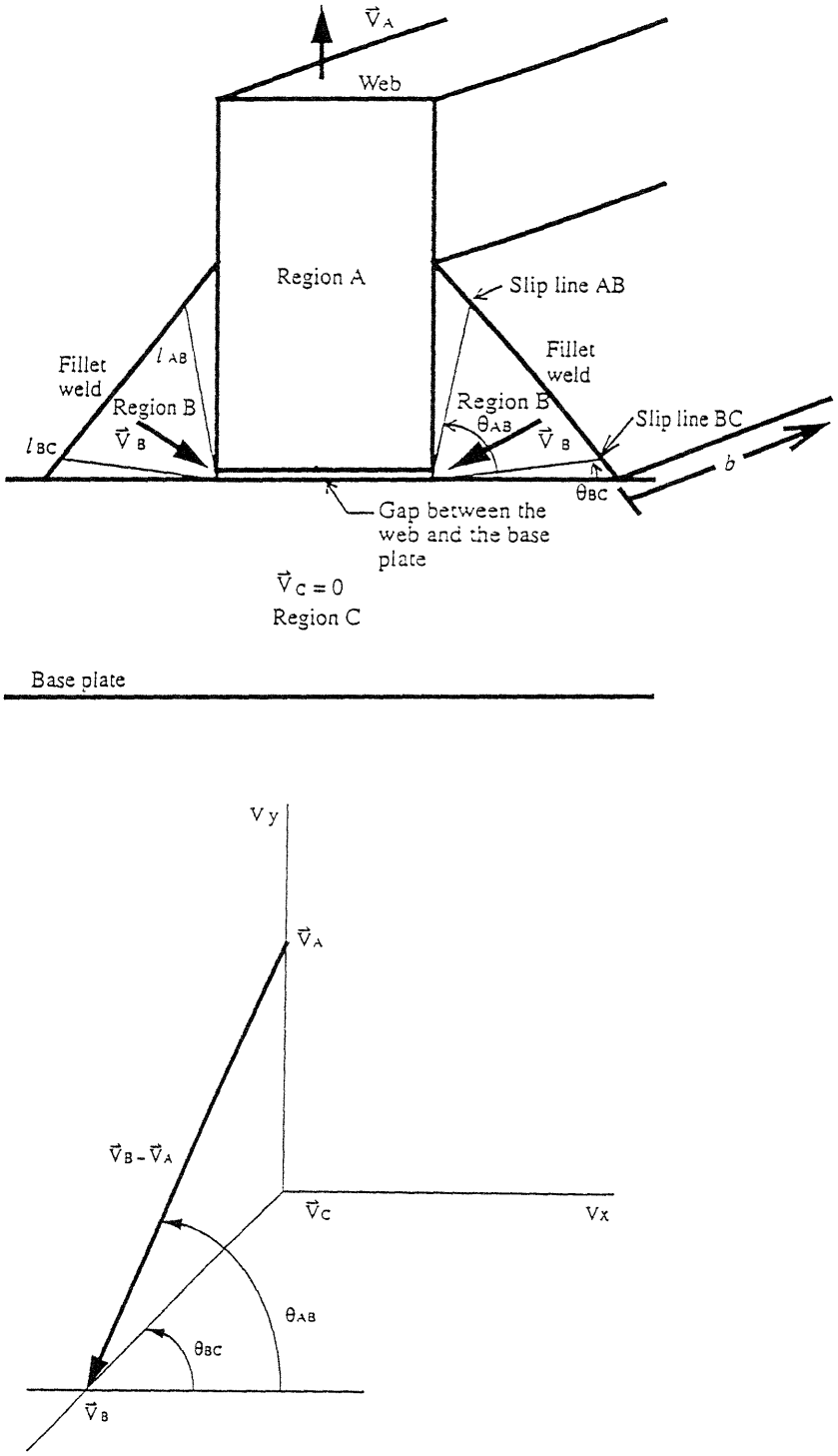

FIGURE 3.6 Relative Velocities of Regions in the Block Sliding Method [Gurerra, 1994]

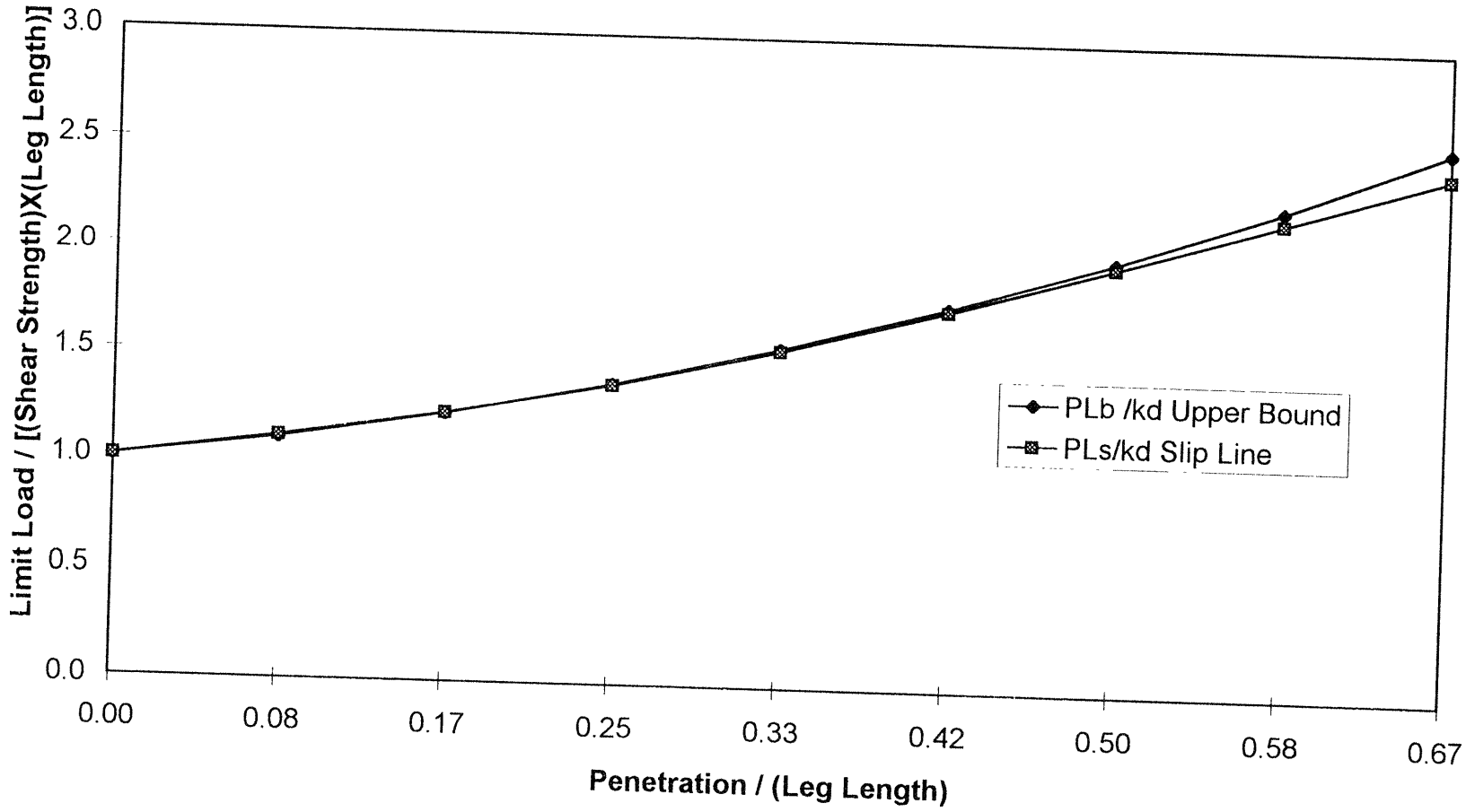

FIGURE 3.7 Upper Bound and Slip Line Solution for Single Fillet Weld Limit Load vs. Penetration

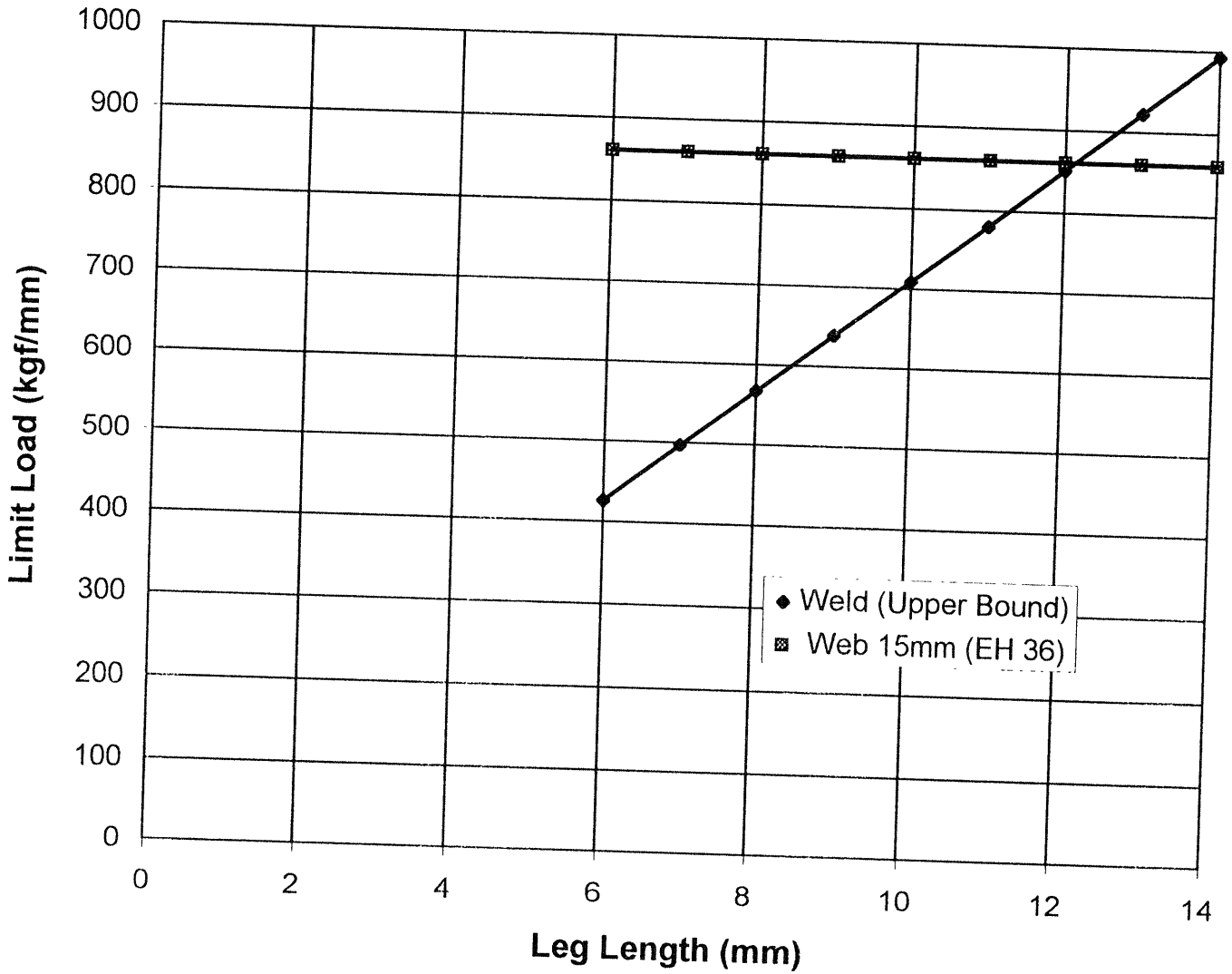

FIGURE 3.8 Limit Load vs. Weld Leg Length

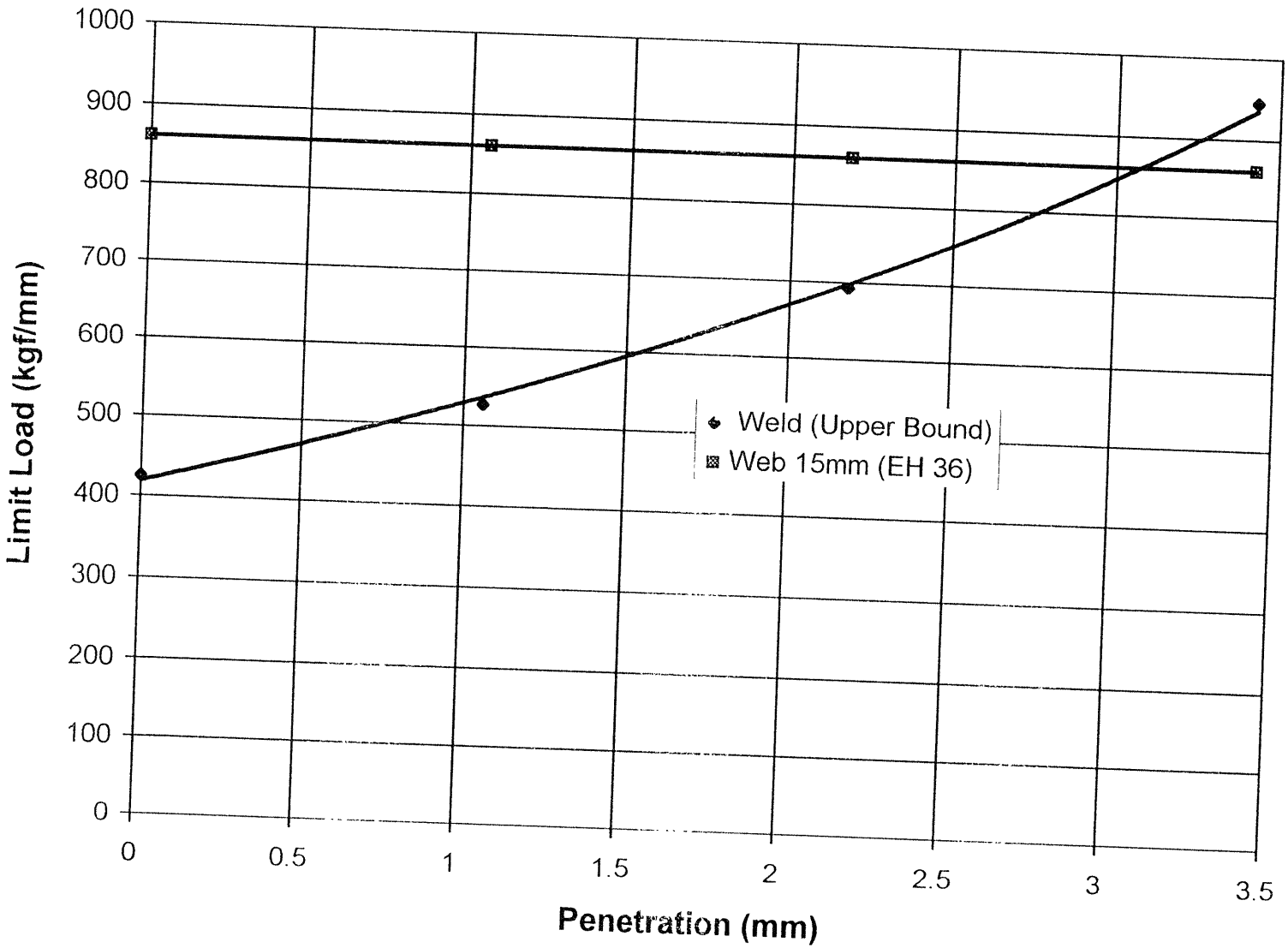

FIGURE 3.9 Limit Load vs. Weld Penetration (Leg = 6 mm)

TABLE 3.1 Slip Line Field Solution for Field Defined by Fig. 3.4 [Chakrabarty, 1987, p. 765]

(α^0, β^0)	x/a	y/a	$\int_0^s \frac{x}{a}\,dt$	$\int_0^s \frac{y}{a}\,dt$	$P/2ka$	$Q/2ka$	M/ka^2
(10, 10)	1.38332	0.00000	0.22220	0.01713	0.50000	0.76067	1.6298
(10, 20)	1.57730	0.23137	0.24971	0.05618	0.50455	0.96049	2.2247
(10, 30)	1.73236	0.50019	0.27033	0.10005	0.59173	1.18900	3.0534
(10, 40)	1.84131	0.79987	0.28323	0.14751	0.77302	1.42368	4.1338
(10, 50)	1.89806	1.12245	0.28777	0.19721	1.05457	1.63865	5.4850
(10, 60)	1.89793	1.45876	0.28357	0.24768	1.43630	1.80580	7.1114
(10, 70)	1.83785	1.79872	0.27051	0.29736	1.91132	1.89626	9.0036
(10, 80)	1.71656	2.13158	0.24872	0.34470	2.46558	1.88186	11.1382
(10, 90)	1.53472	2.44626	0.21864	0.38817	3.07791	1.73683	13.4778
(20, 20)	1.85262	0.00000	0.54940	0.07724	0.50000	1.24397	3.2065
(20, 30)	2.09558	0.28998	0.60453	0.17015	0.60710	1.57921	4.5695
(20, 40)	2.29410	0.63439	0.64393	0.27405	0.83920	1.94125	6.3825
(20, 50)	2.43655	1.02661	0.66542	0.38628	1.21358	2.29807	8.7025
(20, 60)	2.51224	1.45763	0.66731	0.50374	1.74042	2.61163	11.5740
(20, 70)	2.51193	1.91614	0.64841	0.62301	2.42109	2.83925	15.0264
(20, 80)	2.42827	2.38877	0.60814	0.74039	3.24668	2.93561	19.0680
(20, 90)	2.25626	2.86043	0.54660	0.85206	4.19690	2.85490	23.6943
(30, 30)	2.44045	0.00000	1.00076	0.19663	0.50000	2.05487	6.7079
(30, 40)	2.75042	0.37015	1.08423	0.36321	0.76609	2.59096	9.6027
(30, 50)	3.00816	0.81758	1.14022	0.54898	1.22398	3.15118	13.3881
(30, 60)	3.19622	1.33579	1.16458	0.74947	1.89971	3.68814	18.1924
(30, 70)	3.29774	1.91460	1.15386	0.95930	2.80944	4.14448	24.1329
(30, 80)	3.29717	2.54004	1.10551	1.17239	3.95646	4.45459	31.3103
(30, 90)	3.18117	3.19459	1.01807	1.38201	5.32851	4.54726	39.8045
(40, 40)	3.19044	0.00000	1.60306	0.39709	0.50000	3.35163	14.0424
(40, 50)	3.59178	0.47948	1.71618	0.66415	1.01224	4.18605	19.9700
(40, 60)	3.93022	1.06725	1.78593	0.96148	1.81912	5.03998	27.6681
(40, 70)	4.18047	1.75724	1.80519	1.28227	2.95989	5.84212	37.4273
(40, 80)	4.31724	2.53793	1.76789	1.61812	4.45967	6.50515	49.5398
(40, 90)	4.31632	3.39212	1.66929	1.95924	6.32460	6.92807	64.2927
(50, 50)	4.16156	0.00000	2.39319	0.70812	0.50000	5.37010	28.9370
(50, 60)	4.68742	0.62844	2.53785	1.11209	1.39095	6.64714	40.8364
(50, 70)	5.13587	1.40755	2.61736	1.56150	2.73267	7.93540	57.2701
(50, 80)	5.47104	2.33214	2.62031	2.04645	4.58426	9.12701	75.8899
(50, 90)	5.65607	3.38925	2.53668	2.55444	6.98430	10.08908	100.3936
(60, 60)	5.43401	0.00000	3.42154	1.16981	0.50000	8.45941	58.6747
(60, 70)	6.12961	0.83152	3.60020	1.76042	1.96931	10.39168	82.3086
(60, 80)	6.72822	1.87186	3.68369	2.41738	4.12428	12.32054	113.0190
(60, 90)	7.17956	3.11739	3.65436	3.12667	7.05361	14.08301	152.2482
(70, 70)	7.11722	0.00000	4.75666	1.83668	0.50000	13.13398	117.5106
(70, 80)	8.04448	1.10870	4.97238	2.68222	2.84634	16.03367	164.1977
(70, 90)	8.84843	2.50624	5.05131	3.62287	6.22928	18.90505	225.0838
(80, 80)	9.36106	0.00000	6.49179	2.78427	0.50000	20.14922	233.4019
(80, 90)	10.60500	1.48762	6.74819	3.97780	4.16776	24.47367	325.4187
(90, 90)	12.37126	0.00000	8.75376	4.11483	0.50000	30.61170	461.3014

Table 3.2. Tensile Limit Load for T-Joints with Penetration

$\frac{\text{Penetration}}{a}$	0.0	0.35	0.71	0.94
$\frac{\text{Slip Line Limit Load}}{2ka}$	.707	.968	1.40	1.72
$\frac{\text{Upper Bound to Limit Load}}{2ka}$	.707	.972	1.41	1.81

TABLE 3.3 Comparison of the Slip Line and Upper Bound Limit Load Methods for Single Fillet Welds

Variables:

d = throat thickness of the weld wiithout penetration
k = yield stress of weld in pure shear
PLb = limit load using the upper bound method
PLs = limit load using the slip line solution

Penetration (mm)	Penetration/d	PLb /kd Upper Bound	PLs/kd Slip Line	PLb/PLs (Ratio of upper bound to slip line solution)
0.0	0.000	1.000	1.000	1.000
0.5	0.083	1.097	1.103	0.995
1.0	0.167	1.222	1.223	0.999
1.5	0.250	1.375	1.369	1.004
2.0	0.333	1.556	1.546	1.006
2.5	0.417	1.764	1.749	1.008
3.0	0.500	2.000	1.973	1.014
3.5	0.583	2.264	2.206	1.026
4.0	0.667	2.555	2.437	1.049

CHAPTER 4

PRODUCING DEEPER PENETRATION WELDS

4.1 Process

In order to determine the effect of weld penetration on joint strength it was necessary to determine how to produce deep penetrating welds. Beveling plate is currently used for developing welds with penetration. Beveled joints are costly due to the labor and equipment needed to bevel both sides of the intercostal (web) member as well as the added weld material required to fill the bevel area. In order to increase weld penetration without machining the plate, a welding process needs to provide adequate depth of penetration. A comparison of different welding methods and varying parameters was used to determine favorable conditions to create deep penetrating welds. The comparison of different welding processes is based on a limited literature survey.

4.1.1 Shielded Metal Arc Welding

SMAW has traditionally been used to weld ship structures. Transfer of weld metal is accomplished by an electric arc between the electrode tip and the base metal. The metal core of the rod provides the filler metal for the joint. The electrode is covered with material that aids in the stability of the arc as well as shields the molten metal from the atmospheric gases. Advantages of this process are the low equipment costs and use in all welding positions. Disadvantages include the frequent replacement of electrodes, decreasing welding operating time, and the restriction to lower welding currents. Recently the use of automated machines has reduced the use of SMAW in the shipbuilding industry. (Welding Handbook, 1987)

4.1.2 Gas Metal Arc Welding

GMAW melts a continuous electrode wire from the heat generated by an electrical arc at the electrode tip. A shielding gas is used to protect the weld puddle from

contamination by the atmosphere. One advantage is the good arc maneuverability in all welding positions. The electrode is continuously fed to the weld location making it suitable for automation. The electrode allows for high current densities at the electrode tip, increasing the weld deposition rate and depth of penetration. In the spray transfer of weld material, deeper penetration is possible as compared to SMAW. GMAW does not require the removal of flux after welding but the lack of flux makes controlling the weld bead shape more difficult. GMAW is more expensive than SMAW as a result of added equipment and shielding gas costs. (Welding & Fabricating Data Book, 1988/89)

4.1.3 Flux Cored Arc Welding

FCAW combines characteristics of shielded metal arc welding and gas metal arc welding as shown in Fig. 4.1. FCAW uses flux inside a hollow electrode to shield the weld pool from contamination by the atmosphere. Some electrodes are designed to be dual shielded, using a shielding gas in addition to the flux material. The addition of the flux generally gives better control of the weld shape as compared to GMAW. Automation is possible due to the continuous supply of electrode. Higher current densities than SMAW promote higher deposition rates and weld penetration. Faster weld speeds reduce the amount of workpiece distortion. The process requires less precleaning than GMAW. The high cost of the welding equipment as compared to SMAW is a disadvantage of this process. FCAW is limited to ferrous allows and produces slag that must be removed after welding. The cost of the shielding gas in addition to the more costly flux cored wire are disadvantages to be considered in process selection. (Welding & Fabrication Data Book 1988/1989)

In the gas shielded method of FCAW the production of narrow, deep penetrating welds is possible. The shielding gas options include carbon dioxide (CO_2) and a combination of Argon (A) and CO_2. A pure CO_2 shielding gas generates deeper penetration welds than the A/CO_2 mixture. However, the weld quality and deposition rate is generally slightly higher with an Ar/CO_2 combination. (Welding Handbook)

Higher productivity compared to SMAW and GMAW is the main appeal of the FCAW process. Despite added costs of equipment and electrodes, FCAW is more cost efficient. Ingalls Shipbuilding, Newport News Shipbuilding, Bath Iron Works, and Kawasaki Heavy Industries have all reported using FCAW for the automated production of fillet welds.

4.2 Weld Parameters (FCAW)

Altering welding parameters controls the properties of welds. Penetration, bead geometry, and weld quality are controlled by the following variables (Welding Handbook):

1) Welding current (electrode feed speed)
2) Polarity
3) Arc voltage - arc length
4) Travel speed
5) Extension of electrode
6) Electrode orientation
7) Weld joint position
8) Electrode diameter
9) Shield gas composition and flow
10) Base metal
11) Electrode composition

Selecting optimum weld parameters is often difficult. Parameters are frequently interdependent. The ascending order of parameter influencing penetration as stated in the Welding Handbook are: wire size, voltage, travel speed, electrode orientation, and current. (Welding Handbook, 1987) Factors leading to the optimum design of welds requires numerous experimental tests.

4.2.1 Electrode Size

Electrode size influences the weld bead shape and penetration. High currents lead to a larger current density for smaller electrodes in FCAW. This higher concentration of heat tends to cause deeper penetration welds. (Welding Handbook)

4.2.2 Voltage

Arc voltage is proportional to the arc length of a weld when all other variables are constant. Increasing arc voltage tends to flatten the weld and reduce penetration. Decreasing arc voltage creates narrower weld beads with deeper penetration. Arc voltage settings vary depending on the material, shielding gas, and transfer mode of the electrode. In order to determine proper arc voltages experimentation must be used to develop the desired weld geometry. (Welding Handbook)

4.2.3 Travel Speed

The travel speed is the rate that the welding arc is moved along the welded joint. When the travel speed of the arc is slow the increase in weld pool size inhibits the penetration into the base plate. At fast weld travel the heat energy transferred to the base plate decreases and the penetration is decreased. (Welding Handbook) The determination of optimum travel speed setting must be determined from test experiments.

4.2.4 Electrode Orientation

The electrode orientation has a large influence on weld bead shape and penetration. The travel angle represents the relationship of the electrode axis to with respect to the direction of travel. The work angle represents the angle between the electrode axis and the adjacent joint surface. Travel angle and work angle orientations for fillet welds are shown in Fig. 4.2. For fillet welds welded in the horizontal position (Figure 4.3) maximum penetration of welds generally occurs with travel between 5 to 15 degrees using the backhand technique shown in Fig 4.4. When welding in the horizontal position the work angle should be 45 degrees. (Welding Handbook)

4.2.5 Current

Welding current has the most influence on the depth of weld penetration. FCAW controls the welding current by the feed speed of the electrode. If all other variables are held constant, increasing the weld current increases the depth of penetration and width of the weld. In addition the deposition rate increases and fillet weld size increases. The deeper penetration is due to the higher heat provided by the increased current. (Welding Handbook, 1987)

4.3 Selection of FCAW Electrode

The selection of the FCAW electrode depends on a variety of factors including base plate composition, welding position, and desired weld qualities.
A 0.045 inch diameter FCAW wire was selected for a fillet weld leg length of 6 mm (1/4 inch). Based on the Welding Handbook smaller diameter electrodes should produce higher current densities and deeper penetrating welds. FCAW material classification for electrodes is determined by filler metal grades. The American Bureau of Shipping specifies acceptable filler metal grades to be used with welding various grades of commercial hull steels as shown in Table 4.1.

Tensile strength of the filler metal is required to be at least as strong as the base material. Three metal grades for welding ordinary and high strength steels differ by the notch toughness. Filler metal grades are matched to steel grades using the Charpy V-notch test to estimate the toughness of the material. Testing to ensure that the properties of welding manufacturers meet the ABS standards is performed biannually. (American Bureau of Shipping, 1993)

High strength steels are currently being used in the design of tanker ships. High strength steels reduce the weight of the ship hull, allowing for an increase in cargo weight. Masubuchi et al. (1993) reported that KA32 (AH32) and KA36 (AH36) steels are being used in the construction of tanker ships in Japan. Terai (1970) reported that for a large tanker ship (210,000 D.W.T.) the bottom shell plate grade is often DH and EH (Fig. 4.5).

Due to the availability of EH36 from research performed by Kirkov (1994) the base plate selection for testing was EH36. Toughness and strength make EH36 the best steel grade used in commercial shipbuilding. Table 4.4 shows the acceptable ABS filler metal grade required for this steel is 3Y. Hobart Welding Products recommended the use of Excel -Arc 71 electrode for a FCAW electrode that meets the ABS standards for 3Y grade. The electrode is designated as E71T-1 by the American Welding Society (AWS) allowing for welding in all positions. The full description of E71T-1 is shown in Fig. 4.6. An added feature of Excel-Arc 71 is the use of either CO2 or 75% Ar / 25% CO2 gas shielding. Many electrodes are designed for a specific gas shield. This allowed for flexibility in testing welds with different shielding gases. The manufacturer recommended settings and material properties of Excel-Arc 71 are shown in Appendix E.

Experimental testing was also performed on DH36 plate. The manufacturer classified the plate used as either AH36 or DH36 as shown in Appendix E. DH36 grade plate requires 2Y or 3Y grade electrodes according to ABS standards. Hobart Welding Product engineers recommended the use of Fabco 802 FCAW electrode for this steel and the desired fillet weld leg length of 6 mm.. This electrode is rated with the 2Y grade by ABS and is designated as E71T-1 by the AWS. It is an all-position welding electrode designed to be used with 100% CO_2 shielding gas. Further description of Fabco 802 is in Appendix E.

4.4 Weld Testing Results

Testing two different electrode and base plate combinations allowed for a broader range of testing data for materials used in the building of tanker ships. Table 4.2 shows weld parameters currently used by several ship manufacturers. The Welding Handbook shows weld parameter trends that can be used to achieve deeper weld penetration as discussed in section 4.2. However, the maximum depth of penetration achievable in fillet welds was not available. Welding engineers at Hobart Welding Products and Lincoln Electric did not have information on the fillet weld penetrations achievable for specified weld parameters of FCAW electrodes. Changes in weld parameters were used to

estimate the effect on penetration; further testing should be carried out to optimize weld parameters for penetration with different materials.

4.4.1 Test Setup

The machine used for experimental welding allowed for fully automated welding of fillet welds. Figure 4.7 contains a photograph of the welding machine assembly used for experimentation. The welding power source was a Miller Delta Weld 650 constant potential, direct current machine. A Miller Radiator-1 cooling system was used to provide water cooling to the welding nozzle. The control of the position and speed of the welding nozzle was by a Jetline carriage system. The calibration curve shown in Fig. 4.8 was developed to convert the travel speed dial settings to an actual speed. Millermatic digital controls were used to set the voltage and wire feed speed. The amperage was determined by a gauge on the power source.

4.4.2 Trial on A36 Steel

Preliminary runs involved the use of A36 plate, 19 mm thick. This plate was used for trials because of its abundance and the limited supply of EH36 and DH36 steels. Trial welding specimens were formed by cold saw-cutting the steel plate to form rectangular plates 127 mm long and 90 mm wide. Two rectangular plates were placed in a T-joint configuration and tack welded at the ends to give a rigid joint for stability in welding. Figure 4.9 was developed from the manufacturers recommended voltage settings at various feed speeds for the electrode. This gave some basis for selecting voltage settings at the various feed speeds. Table 4.3 shows the parameters used, resulting weld sizes, and weld penetrations for welding the A36 plate with the Excel-Arc 71 electrode. The maximum penetration, without slag inclusions, was 3.7 mm on Trial 17.

4.4.3 Trial on EH36 Steel

After experimenting with the parameters necessary for deeper penetration with the A36 plate, welds were performed on EH36 steel with the Excel-Arc 71 electrode. The 20 mm thickness test plate was cold saw cut into rectangular sections 127 mm long and

90 mm wide. The same procedure of tack welding the ends to give a secure T-joint was used. Trial runs were more organized than tests on the A36 plate. Weld current was increased from minimum to maximum setting. Different voltage values were used at each feed speed (current) to try to optimize the weld geometry and penetration. Maintaining the fillet weld size was accomplished by trying to provide the same deposition rates for welds. This was accomplished by changing the travel speed by maintaining the ratio of feed speed to travel speed. Resulting penetrations and weld sizes for varying weld parameters are shown in Tables 4.4 and 4.5. Trial 44 showed the best penetration, 3.6 mm, without any slag inclusion.

4.4.4 Test Specimens

Parameters used for the final test specimens were based on those determined in the trial specimens producing good quality welds with varying penetrations. Different weld penetrations were developed to test the effect on the tensile strength of the welded joint. Table 4.5 shows the resulting weld penetrations and leg lengths for the test specimens. Test specimen fabrication is described in Chapter 5.

It is important to note that weld penetrations for the test specimens was less than trial specimens with similar weld parameters. Maximum weld penetration without slag inclusion was determined to be 3.6 mm for Trial 44. However, the same parameters only generated a penetration of 3.2 mm for Test 6. The weld sections for the test specimens were taken 0.75 inch from the end of the weld; trial specimens were taken at the midsection of the weld specimen. Observation of the failed welds showed that penetrations were greater in the middle of the of the welded joint. Table 4.6 shows averages of weld penetrations for the test specimens taken from measurements of the failed welds.

4.4.5 Developing Pictures of Weld Profiles

Welds were sectioned in the center part of the weld for trial specimens and 0.75 inch from the ends for test specimens to get a good view of the weld profile. T-joints were sectioned using a water-cooled cutting disk in order to keep temperatures low and maintain the physical properties of the weld. The cut surface was polished using a Stuers

polishing machine and a series of wet sanding disks in the following order: 180, 320, 500, 1500, and 4000 grit. Specimens were further polished using a .1μ polishing liquid.

In order to show the depth of penetration and location of the heat affected zone an etchant was used. Ammonium persulfate steel etchant was used as directed by ASTM Standards (1992). This etchant consisted of 10g of ammonium persulfate in 100 ml of water. The solution was applied with cotton swabs for approximately 20 seconds and then rinsed off with cold water.

Test specimen pictures were developed using Leitz Polaroid photography equipment. The weld sections were magnified six times in order to better examine weld qualities. Weld dimensions for leg length and penetration were taken by measuring the distances with a scale magnified at the same power as weld photographs giving an accuracy of 0.1 mm. Photographs of the trial and test specimens are included in Appendix F.

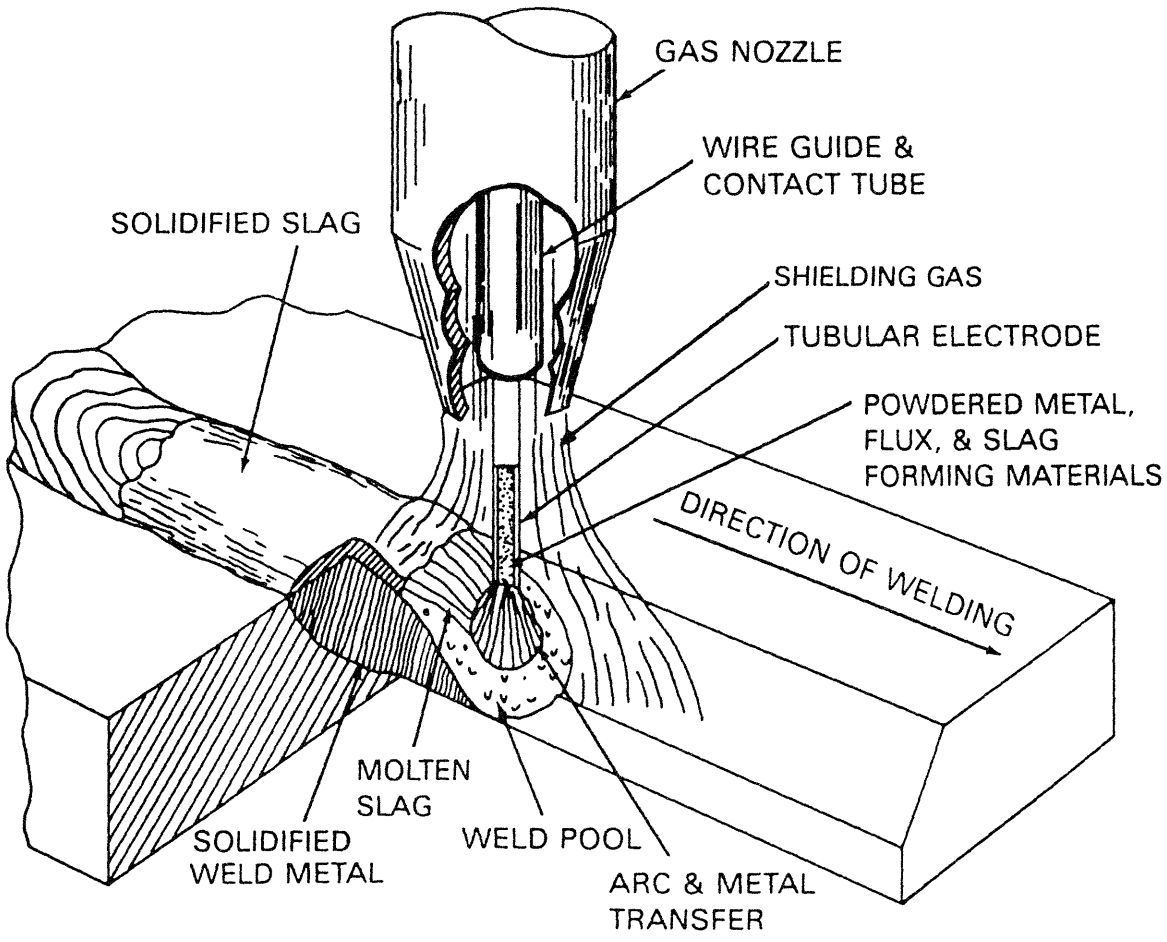

FIGURE 4.1 Gas Shielded Flux Cored Arc Welding
[Welding Handbook, 1991]

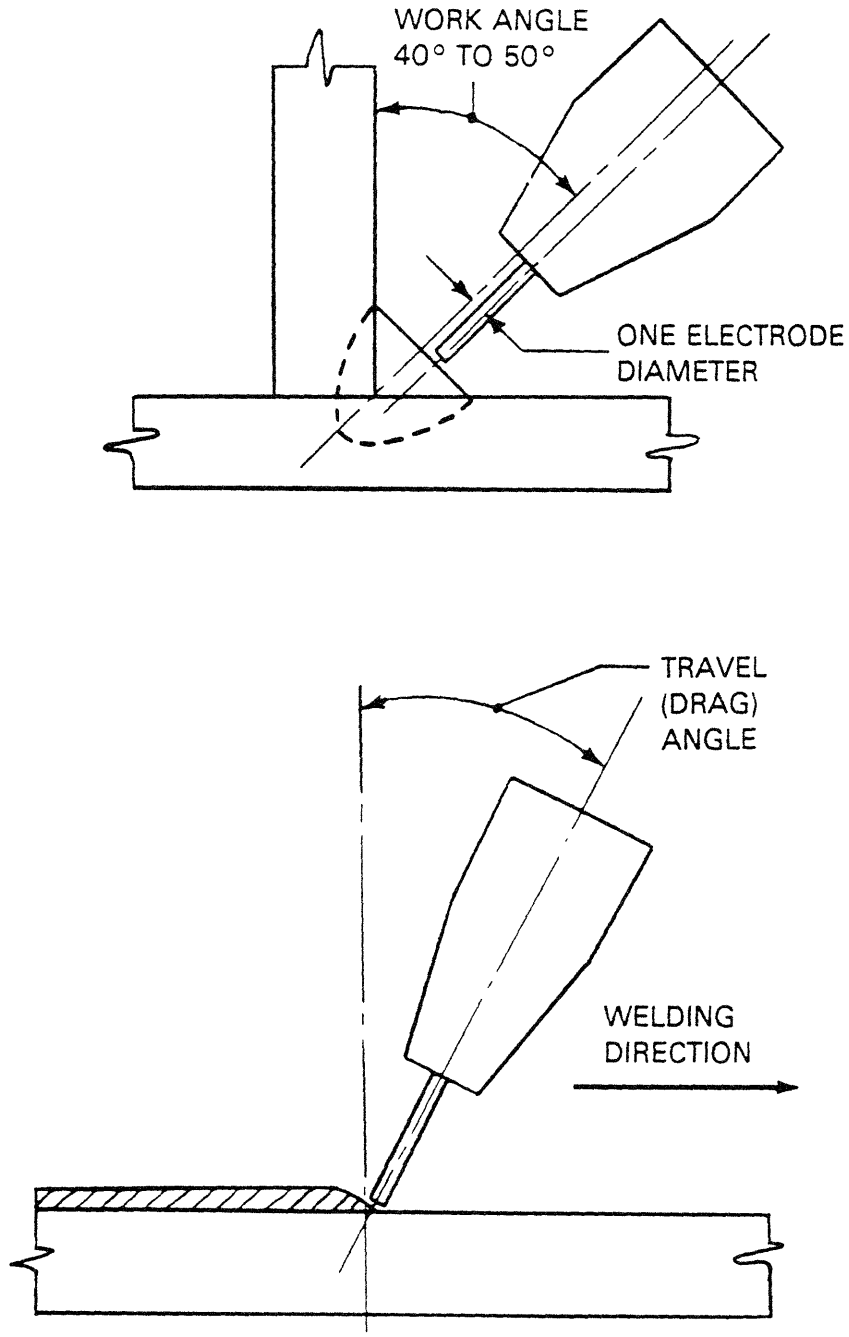

FIGURE 4.2 Welding Electrode Positions
[Welding Handbook, 1991]

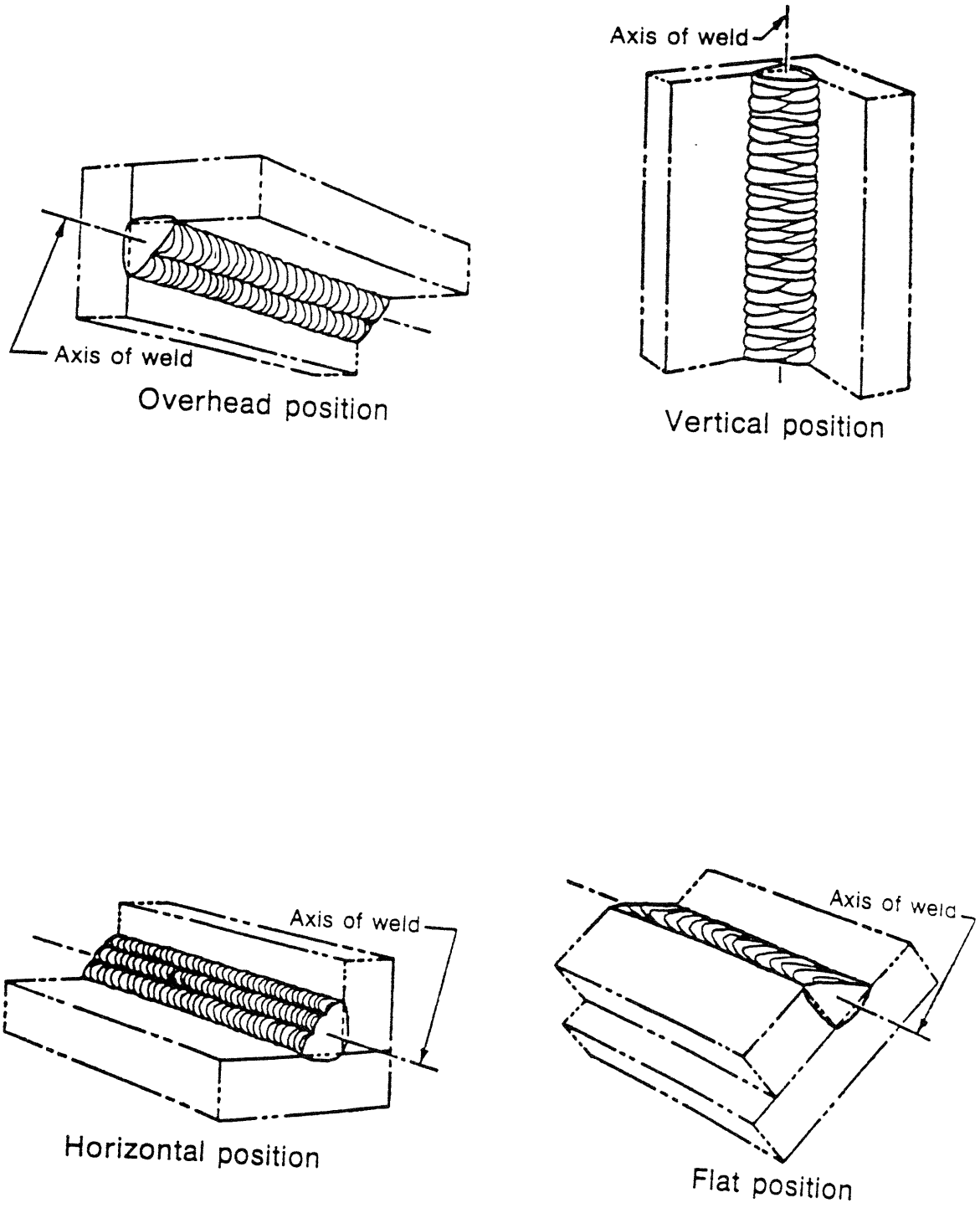

FIGURE 4.3 Welding Positions for Fillet Welds

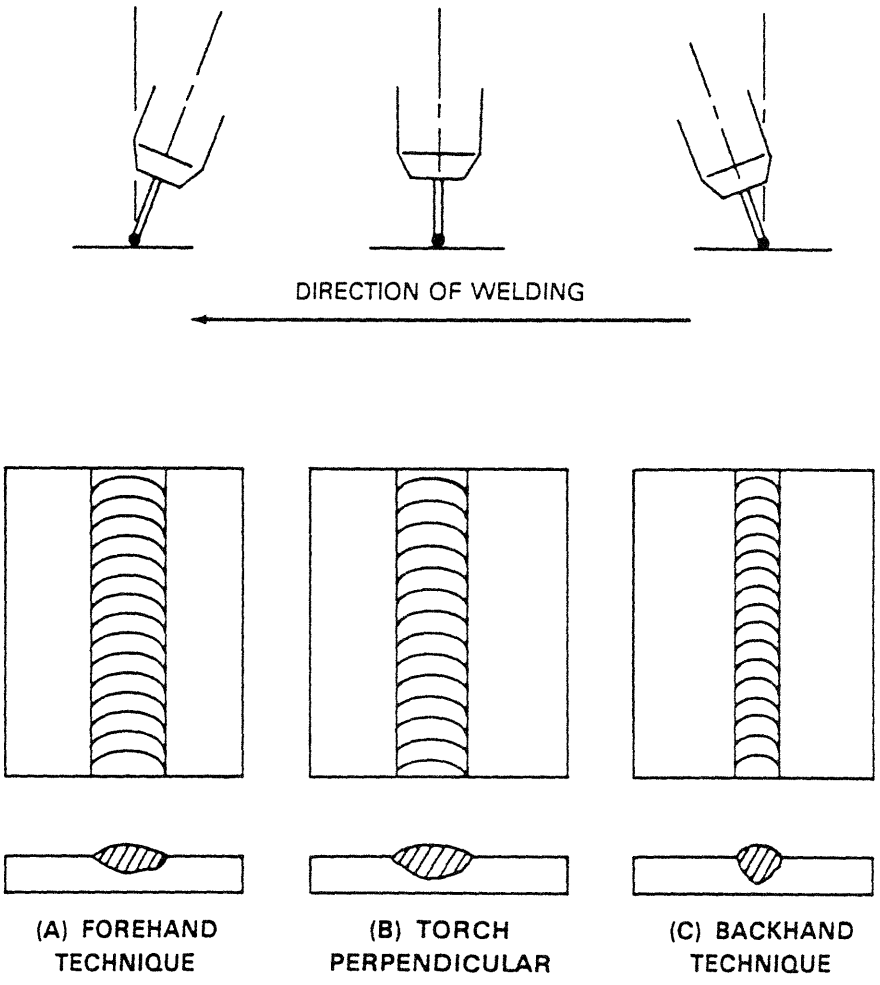

FIGURE 4.4 Effect of Electrode Position on Weld Geometry [Welding Handbook, 1991]

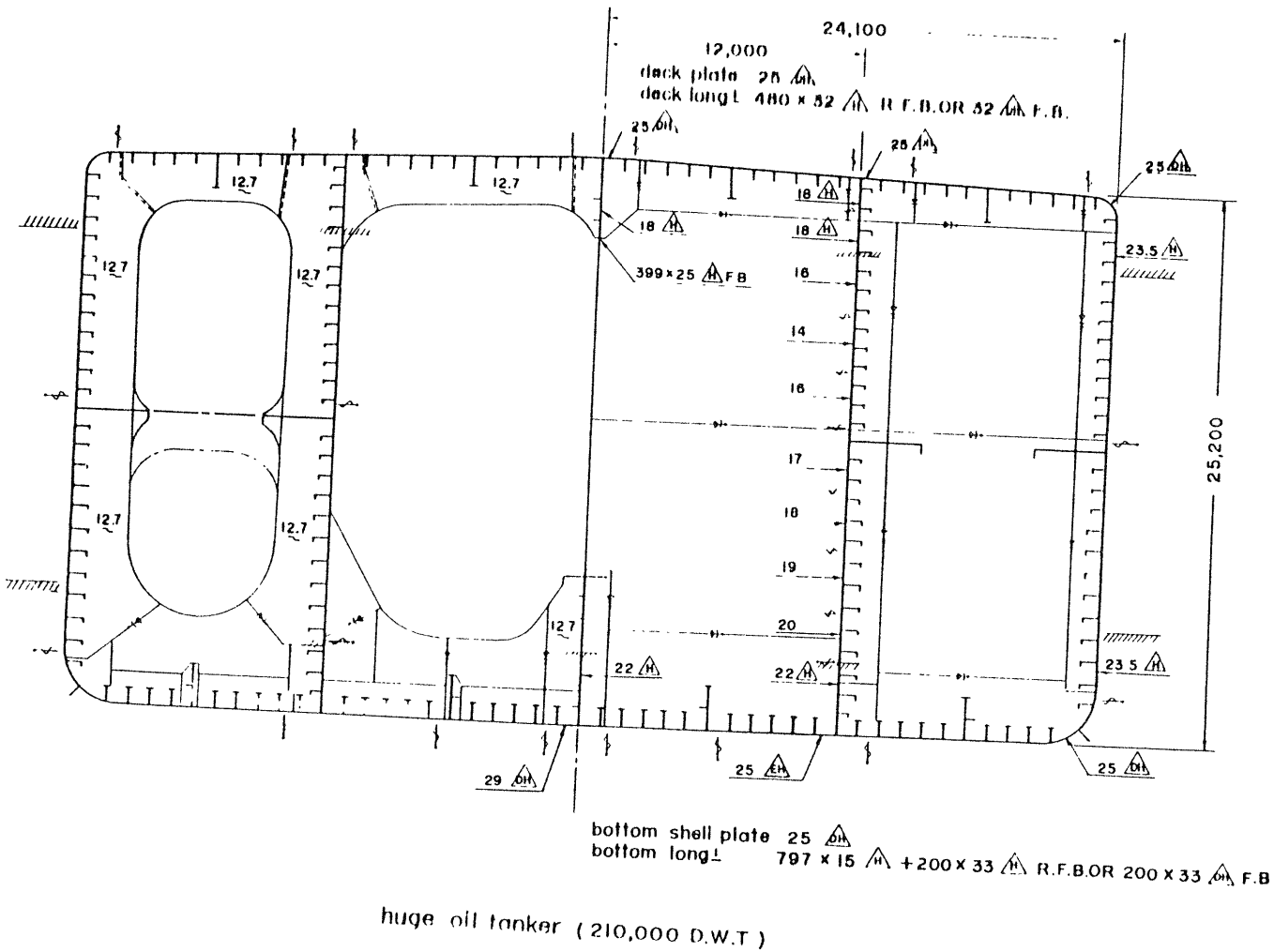

FIGURE 4.5 Midship Section of Oil Tanker [Terai, 1970]

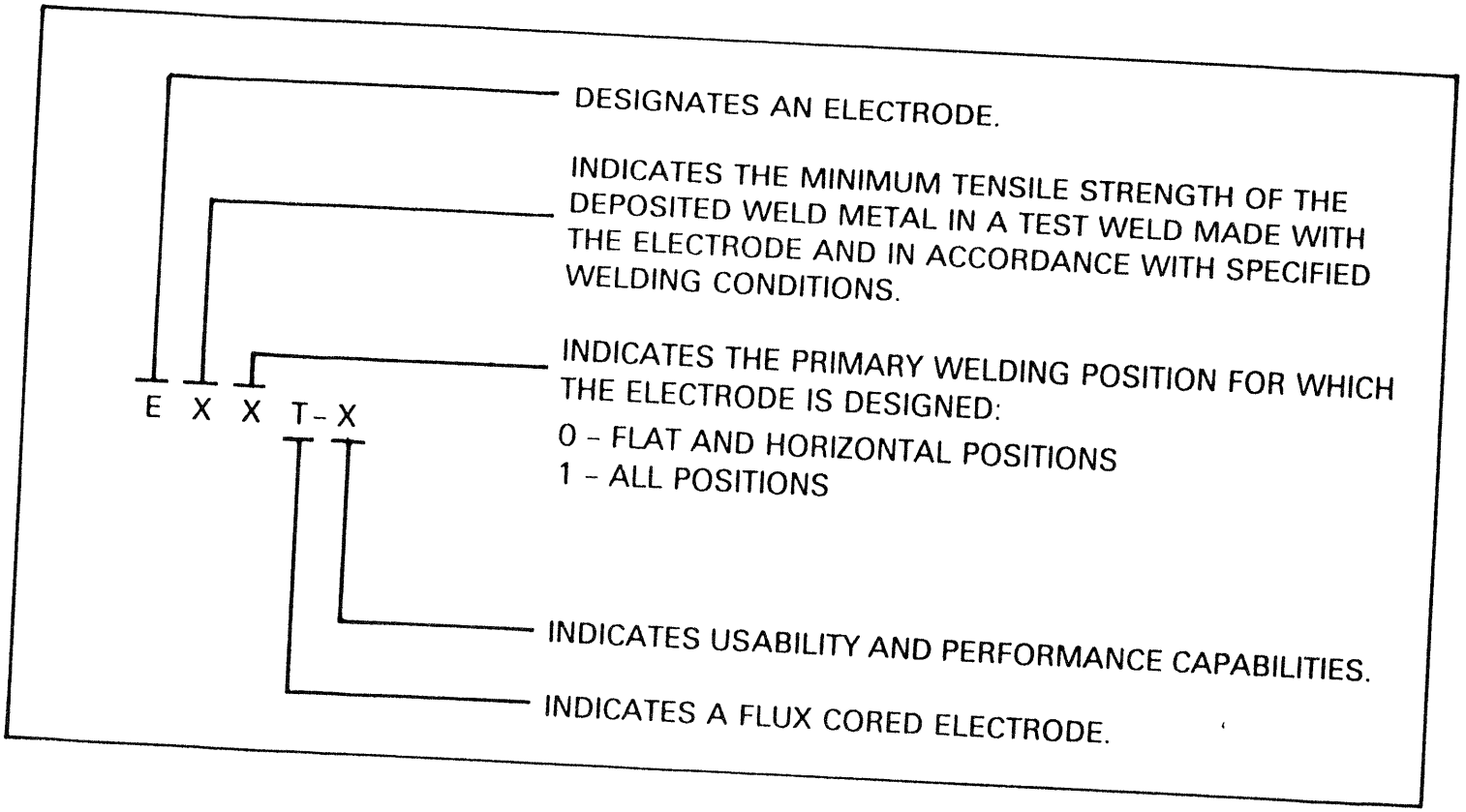

FIGURE 4.6 Identification System for FCAW Electrodes
[Welding Handbook, 1991]

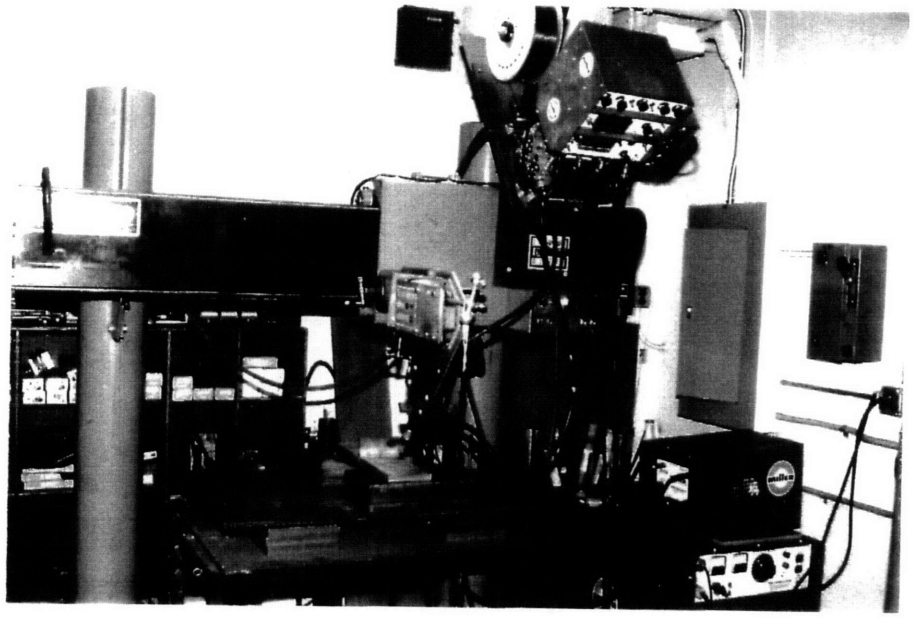

Flux Cored Arc Welding Machine Assembly

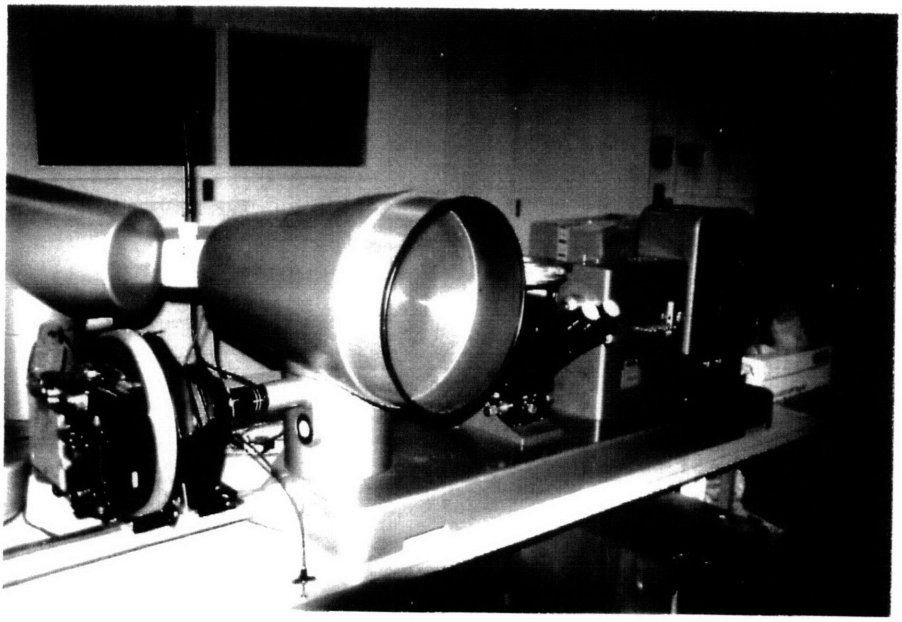

Leitz Photography Equipment

FIGURE 4.7 Pictures of Welding and Photography Equipment

CALIBRATION OF AUTOMATED WELDING MACHINE TRAVEL SPEED

$i := 0..11$

$SETTING_i :=$	$SPEED_i :=$
0	0
300	4.96
400	8.43
450	11.19
500	13.06
550	16.15
600	18.99
650	23.52
700	27.97
750	34.39
800	42.86
900	71.43

The speed was measured using a stop watch to measure the time to the nearest tenth of a second to travel 36 inches. The speed is in inches per minute.

(inches per minute)

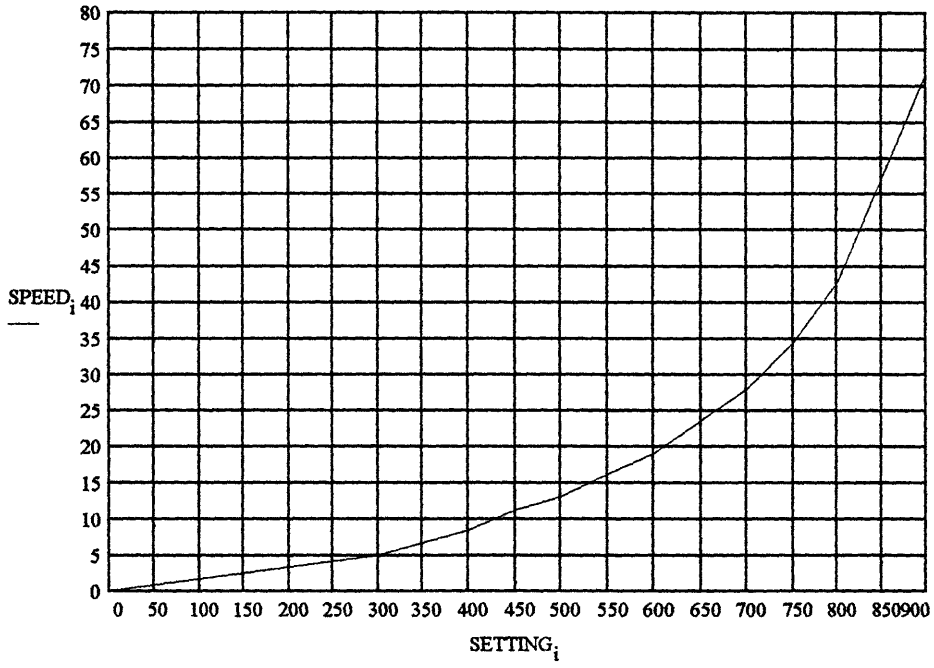

FIGURE 4.8 Travel Speed Determination from Machine Setting

MANUFACTORERS GIVEN RELATIONSHIPS FOR VOLTAGE AND FEED
FOR EXCEL -ARC 71

$i := 0..2$

$volt_i :=$

21
27
30

$feed_i :=$

168
500
625

The benefit of graphing the relationship between volatage and feed speed was to estimate reasonable values of voltage for various wire feed speeds and extrapolate. The wire feed speed is in units of inches per minute.

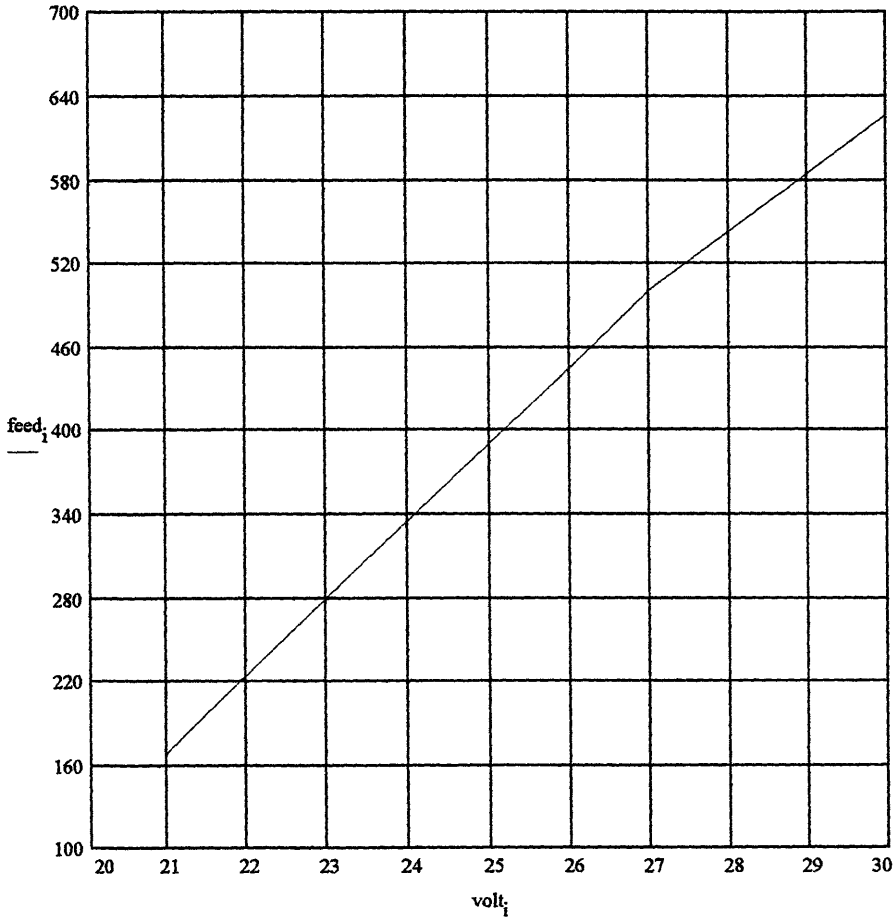

Slope=53.6
Y-Intercept=-955.33

Extrapolations:
Feed: 700 ipm Voltage: 30.9 V
Feed: 800 ipm Voltage: 32.8 V

FIGURE 4.9 Manufacturer Recommendations for Voltage and Feed Speed (Excel-Arc 71)

TABLE 4.1. Acceptable Filler Metal Grades for ABS Steels

ABS Hull Structural Steel	Acceptable Filler Metal Grade
Ordinary Strength Steel	
A (< 12.5 mm)	1, 2, 3
A (> 12.5 mm)	2, 3
CS, E	3
Higher Strength Steel	
AH (<12.5 mm)	1Y, 2Y, 3Y
AH (>12.5 mm), DH	2Y, 3Y
EH	3Y

TABLE 4.2 Comparison of Fillet Weld Parameters in Shipbuilding

	INGALLS SHIPBUILDING	NEWPORT NEWS SHIPBUILDING	MITSUBISHI HEAVY INDUSTRIES, LTD.
Process	FCAW	FCAW	FCAW
Filler	E71T-1-HY	E71T-1	N/A (Not Available)
Electrode Diam.	1.32 mm .052 in	1.14 mm .045 in	N/A
Shielding Gas	CO2	CO2	CO2
Travel Speed (mm/s)	5	8-8.5	8.3
Stick Out (mm)	N/A	19	20
Travel Angle (degrees fwd)	N/A	5-10	5
Work Angle (degrees)	N/A	40-50	N/A
Amperage (A)	240	290	300-320
Voltage (V)	26-27	28	32
Fillet Size (mm)	6.4	6.4	5
Shell Plate Thickness (mm)	16	16	22-25
Web Thickness (mm)	N/A	14	12.5
Type Steel	Lower Strength Grade A	Lower Strength Grade A	High Strength

TABLE 4.3 Weld Parameters for Trial Specimens 1 thru 24

TRIAL	Steel	FCAW	Volt	AMP	FEED (ipm)	TRAVEL (setting)	SHIELD (psi)	TRAV ANG (degrees)	WK ANG (degrees)	STICK OUT (mm)	ROOM TEMP (fahrenheit)	LEG (Horiz*Vert) (mm)	PEN (mm)
1	A36	Excel-Arc 71	26	300	625	650	C25 (35)	15 aft	45	21	73	6.5*6.5	1.4
2	A36	Excel-Arc 71	24	295	625	650	C25 (35)	15 aft	45	21	73	5.5*5.7	2.0
3	A36	Excel-Arc 71	28	300	625	650	C25 (35)	15 aft	45	21	75	6.2*6.0	1.5
4	A36	Excel-Arc 71	30	300	625	650	C25 (35)	15 aft	45	21	75	6.8*5.9	0.4
5	A36	Excel-Arc 71	26	260	500	600	C02 (35)	15 aft	45	18	75	5.8*5.6	1.6
6	A36	Excel-Arc 71	27	270	500	600	C02 (35)	15 aft	45	18	75	5.9*5.6	1.1
7	A36	Excel-Arc 71	27	300	625	650	C02 (35)	15 aft	45	18	75	5.6*5.9	2.4
8	A36	Excel-Arc 71	30	300	625	650	C02 (35)	15 aft	45	18	75	5.8*5.9	2.3
9	A36	Excel-Arc 71	30	310	650	650	C02 (35)	15 aft	45	18	65	6.0*6.5	2.8
10	A36	Excel-Arc 71	30	315	675	650	C02 (35)	15 aft	45	18	65	7.0*6.0	0.8
11	A36	Excel-Arc 71	30	315	700	650	C02 (35)	15 aft	45	18	65	5.7*7.0	2.8
12	A36	Excel-Arc 71	30	320	725	650	C02 (35)	15 aft	45	18	65	6.0*5.8	2.8
13	A36	Excel-Arc 71	30	325	750	650	C02 (35)	15 aft	45	18	65	6.0*6.3	2.2
14	A36	Excel-Arc 71	30	330	775	650	C02 (35)	15 aft	45	18	65	6.3*6.3	2.1
15	A36	Excel-Arc 71	32	340	775	650	C02 (35)	15 aft	45	18	65	7.2*5.5	2.4
16	A36	Excel-Arc 71	32.5	340	775	650	C02 (35)	15 aft	45	18	65	7.1*7.0	2.4
17	A36	Excel-Arc 71	30	300	625	650	C02 (35)	15 aft	45	16	74	5.5*6.2	3.7
18	A36	Excel-Arc 71	32.5	340	775	650	C02 (35)	15 aft	50	16	74	5.1*7.0	3.3
19	A36	Excel-Arc 71	32.5	340	775	650	C02 (35)	15 aft	50	16	74	6.5*7.0	2.6
20	A36	Excel-Arc 71	30	300	625	650	C02 (35)	15 aft	45	16	74	6.0*6.5	2.4
21	A36	Excel-Arc 71	27	270	500	575	C02 (35)	15 aft	45	16	74		
22	A36	Excel-Arc 71	27	160	200	370	C02 (35)	15 aft	45	16	74		
23	A36	Excel-Arc 71	27	340	800	710	C02 (35)	15 aft	45	16	74		
24	A36	Excel-Arc 71	22	150	200	370	C02 (35)	15 aft	45	16	74		

Note: FEED is the feed speed of the electrode.
TRAVEL is the travel setting on the the automatic welding machine.
SHIELD is the the type of shielding gas and the pressure. (C25= 25%CO2 / 75% Ar)
TRAV ANG is the travel angle of the the electrode nozzle rotated forward or aft from the travel direction.
WK ANG is the work angle of the of the electrode from the vertical (web) plate.
STICK OUT is the electrode stickout length from the wire guide.

TABLE 4.4 Weld Parameters for Trial Specimens 25 thru 52

TRIAL	Steel	FCAW	Volt	AMP	FEED (ipm)	TRAVEL (setting)	SHIELD (psi)	TRAV ANG (degrees)	WK ANG (degrees)	STICK OUT (mm)	ROOM TEMP (fahrenheit)	LEG (Horiz*Vert) (mm)	PEN (mm)
25	EH36	E71T-1	20.0	150	200	370	C02 (35)	15 aft	45	16	74	5.8*5.7	0.0/-0.8
26	EH36	E71T-1	21.5	150	200	370	C02 (35)	15 aft	45	16	74	5.7*5.8	0.0/-1.0
27	EH36	E71T-1	23.0	160	200	370	C02 (35)	15 aft	45	16	74	6.3*6	0.2/-0.5
28	EH36	E71T-1	22.0	200	300	440	C02 (35)	15 aft	45	16	74	6.5*6.7	0.0/-1.0
29	EH36	E71T-1	23.5	200	300	440	C02 (35)	15 aft	45	16	74	6.4*6.0	0.0/-0.8
30	EH36	E71T-1	25.0	200	300	440	C02 (35)	15 aft	45	16	74	7.0*7.0	0.0/-0.7
31	EH36	E71T-1	23.5	235	400	530	C02 (35)	15 aft	45	16	74	5.8*6.2	0.9
32	EH36	E71T-1	25.0	230	400	530	C02 (35)	15 aft	45	16	74	6.0*6.5	0.5
33	EH36	E71T-1	26.5	240	400	530	C02 (35)	15 aft	45	16	74	6.6*6.7	0.3/0.7
34	EH36	E71T-1	25.5	275	500	575	C02 (35)	15 aft	45	16	74	6.4*7.0	1.8/2.4
35	EH36	E71T-1	27.0	280	500	575	C02 (35)	15 aft	45	16	74	6.4*7.1	2.2
36	EH36	E71T-1	29.5	280	500	575	C02 (35)	15 aft	45	16	74	7.8*7.0	1.2/1.7
37	EH36	E71T-1	28.0	300	600	630	C02 (35)	15 aft	45	16	74	6.5*6.6	2.2
38	EH36	E71T-1	29.5	300	600	630	C02 (35)	15 aft	45	16	74	6.6*6.3	2.5
39	EH36	E71T-1	31.0	305	600	630	C02 (35)	15 aft	45	16	74	6.5*6.5	4.0/4.5
40	EH36	E71T-1	29.5	330	700	660	C02 (35)	15 aft	45	16	74	6.4*6.5	3.1
41	EH36	E71T-1	31.0	330	700	660	C02 (35)	15 aft	45	16	74	6.6*6.6	3.2
42	EH36	E71T-1	33.5	340	700	660	C02 (35)	15 aft	45	16	74	7.2*6.7	3.0
43	EH36	E71T-1	31.0	360	800	710	C02 (35)	15 aft	45	16	74	5.5*6.2	3.5
44	EH36	E71T-1	32.5	365	800	710	C02 (35)	15 aft	45	16	74	6.0*6.7	3.6
45	EH36	E71T-1	34.0	370	800	710	C02 (35)	15 aft	45	16	74	5.7*6.8	3.6/4.0
46	EH36	E71T-1	35.5	375	800	710	C02 (35)	15 aft	45	16	74	6.8*6.4	3.5/4.0
47	EH36	E71T-1	35.0	345	700	660	C02 (35)	15 aft	45	16	74	6.9*6.7	2.8
48	EH36	E71T-1	29.5	330	700	660	C02 (35)	15 aft	45	16	74	5.5*7.3	2.7
49	EH36	E71T-1	33.5	330	700	660	C02 (35)	15 aft	45	16	74	5.3*7.4	3.6
50	EH36	E71T-1	33.5	330	700	660	C02 (35)	15 aft	45	16	74	6.0*7.0	3.5/5.0
51	EH36	E71T-1	33.5	320	700	660	C02 (35)	15 aft	45	16	74	5.0*9.5	0.0/1.5
52	EH36	E71T-1	34.0	360	800	710	C02 (35)	15 aft	45	16	74	4.5*7.8	1.7/2.0

Note: **PEN** is the penetration of the weld. A negative penetration is due to a slag inclusion or porosity.
Order as shown = (Penetration w/o slag)/(Penetration w/ slag)
Trials 48 - 52 had electrode raised at joint (48 -3mm, 49-3mm, 50-1.5mm, 51-5mm, 52-3mm)

TABLE 4.5 Weld Parameters for Test Specimens

TEST	Steel	FCAW	Volt	AMP	FEED (ipm)	TRAVEL (setting)	SHIELD (psi)	TRAV ANG (degrees)	WK ANG (degrees)	STICK OUT (mm)	ROOM TEMP (fahrenheit)	LEG (MM)(Horiz*Vert) (mm)	PEN (mm)
1	EH36	Excel-Arc 71	23	170	200	355	CO2(35)	15 aft	45	16	75	5.7*5.7	0
2	EH36	Excel-Arc 71	26	230	400	530	CO2(35)	15 aft	45	16	75	5.9*5.9	0
3	EH36	Excel-Arc 71	27	270	500	575	CO2(35)	15 aft	45	16	75	7.0*7.0	1.1
4	EH36	Excel-Arc 71	31	300	600	630	CO2(35)	15 aft	45	16	75	7.2*7.2	2.2
5	EH36	Excel-Arc 71	32	330	700	675	CO2(35)	15 aft	45	16	75	6.6*6.8	2.7
6	EH36	Excel-Arc 71	33	350	800	710	CO2(35)	15 aft	45	16	75	6.9*6.6	3.2
7	EH36	Excel-Arc 71	34	330	700	660	CO2(35)	15 aft	45	16	75	7.8*7.5	2.1
8	DH36	Fabco 802	23	160	200	355	CO2(35)	15 aft	45	16	75	4.9*5.4	0
9	DH36	Fabco 802	27	260	500	575	CO2(35)	15 aft	45	16	75	7.1*6.3	2.2
10	DH36	Fabco 802	33	350	800	710	CO2(35)	15 aft	45	16	75	5.6*6.3	3.3

Note: PEN is the penetration of the weld. Penetrations in tests 1, 2, and 8 were not used due to slag inclusions. This resulted in penetration = 0. Leg lengths were determined from the point of the slag inclusions. The penetration values were determined from average measurements from the failed test specimens.

TABLE 4.6 Average Test Specimen Penetration

TEST	Penetration (End 1) (mm)	Penetration (Middle) (mm)	Penetration (End 2) (mm)	Average Penetration (mm) (10% End 1, 80% Middle, 10% End 2)	Penetration (Etched Specimens) (mm)
1	0.0	0.0	0.0	0.0	0.0
2	0.0	0.0	0.0	0.0	0.0
3	0.6	1.2	0.9	1.1	0.5
4	1.6	2.3	1.8	2.2	1.1
5	2.3	2.8	1.8	2.7	2.2
6	2.6	3.3	2.7	3.2	2.7
7	1.8	2.2	1.6	2.1	1.1
8	0.0	0.0	0.0	0.0	0.0
9	2.0	2.2	1.9	2.2	0.9
10	2.7	3.4	2.9	3.3	2.9

CHAPTER 5

TENSION TESTING FILLET WELDS WITH PENETRATION

5.1 Tension Test Design

Full scale fillet weld tests were necessary in order to compare theoretical tensile strength predictions to actual testing. Table 4.5 and Appendix F show the results of changing welding parameters on penetration. Tests were welded in the horizontal welding position shown by Figure 4.3. Two different electrode and base plate combinations were used for testing. Tests 1-7 were performed with Excel-Arc 71 FCAW electrode and EH36 plate. Tests 8-10 were performed on DH36 plate with Fabco 802 FCAW electrode. Test specimens were designed with varying weld penetrations.

5.1.1 Base Plate and Weld Metal

The material used for the tension test specimens was based on actual materials used in the building of large tanker ships. The selection of EH36 and DH36 plate was based on the tanker ship design shown by Terai (1970). Material properties for the two steels are shown in Appendix E. Masubuchi et al. (1993) determined typical tanker ship stiffener web sizes of 15 mm and shell plate sizes of 20 mm. Plate thickness used in testing was 20 mm for EH36 and 19 mm for DH36. A larger web size than 15 mm was needed for the tension tests in order to determine limit loads of the welds and not of the web.

Chapter 4 described the use of FCAW as the dominant welding process being used in producing fillet welds for longitudinal stiffeners. The size of 0.045 inch diameter wire was based on ship practice used today as shown in Table 4.2. Welding electrode selection was based on ABS standards for compatible welding wire grades with the specific steels.

Attempts were made to keep fillet weld leg lengths nearly constant in order to focus the effect of weld penetration on weld strength. Masubuchi et al. (1993) reported that 6 mm leg lengths were being used for tanker ships in Japan. The comparison of fillet

weld sizes for tanker ships displayed in Table 2.1 shows that a 6 mm leg length is common for stiffener fillet welds. Therefore, a 6 mm leg lengths based the leg length size for the test specimens.

5.1.2 Test Equipment

Finding a test machine capable of creating large tension forces to fail full scale fillet welds led to the assistance of the Watertown Army Arsenal. A Baldwin Testing Machine shown in Fig. 5.1 was capable of a 600,000 pound (272,000 kgf) testing load. The mechanical grips used for holding test pieces were capable of specimens with 160 mm width (160 mm weld length).

A data acquisition system, computer, and a linear-variable differential transformer (LVDT) were used to obtain load and displacement for testing. In order to get estimates of the load-displacement relation, a Megadec 5517A data acquisition system was used. A displacement voltage was determined with a Bourns LVDT. Load and displacement data was channeled through the data acquisition system and into a computer that transformed the voltage values for load and displacement into load and displacements signals. Using calibration data in order to transform actual testing data into loads and displacements. Calibration data for displacements using the Bourns LVDT is shown in Fig. 5.2. The load data was determined by a 600, 000 lb. load cell. The same process used for the determination of displacement by the LVDT was used for the determination of loads. Load cell calibration was performed at the National Institute of Standards (NIST).

5.1.3 Test Specimen Configuration

Test specimen design required consideration for the desired test conditions within limitations of the testing machine. The size of the specimen was limited to less than 160 mm in length due to the size restriction of the gripping mechanism. Even if a fully efficient joint were tested, the expected load to fail EH36 plate 20 mm thick and 160 mm wide would be 212,000 kgf; less than the machine capacity of 272,000 kgf.

One possibility for the design of the test specimen was a single T-joint. The wedges of the testing machine could grip the upper portion of the web while the flange

(representing the ship hull) would be supported by the exterior surface of the lower gripping structure. The disadvantage of this method is the amount of material needed to make the T-joint. The specimen would need to have a 900 mm web and a 400 mm flange. Another disadvantage would be the safety in controlling the flange when the weld failed.

A cruciform joint was chosen as the design for the test specimens as shown in Fig. 5.4. The cruciform joint consists of two T-joints symmetrically welded onto a common continuous plate. Tension failure occurs in these joints when tensile forces are applied to the two symmetrically welded joints. Limiting failure to only one set of fillet welds required reinforcing one set of welds as shown in Fig. 5.3. The overmatched welds were formed using three weld passes at the same parameters as the single pass welds. The length of the fillet weld section were 127 mm for the cruciform joints in order to allow the specimen to fit in the testing machine. A web width of 127 mm was used in order to give an adequate plate size for plane strain loading of the fillet welds. The lengths of the webs were 228 mm to allow for enough surface area for the grips to hold. Positioning of the test specimen in the test machine is shown in Fig. 5.4.

Special attention was given in forming the cruciform joints to insure symmetry of the welded plates. Precision in the positioning of the web plates reduced bending effects that would result from off-center loading. The use of cruciform joints for tension testing of welded joints is described by Hicks (1979) and Davies (1992).

5.1.4 Manufacturing the Test Specimens

The procedure used to weld all ten test specimens was the same. Plate was cold cut using a circular saw. Base plates were cut to be 165 mm long and 127 mm wide. Web plates were cut to be 228 mm long and 165 mm wide. Tack welds were performed at the end of the T-joint using a Gas Tungsten Arc in order to provide joint stability for FCAW with the automatic machine. Single fillet welds were applied with the appropriate weld parameters to form a T-joint. The plate was allowed to cool for 10 minutes between each weld pass. End sections of the T-joints were cut off by 19 mm using a water-cooled band saw; creating weld cross section specimens and minimizing weld end effects for the test specimens. The second web for the cruciform joint (cut to

meet 127 mm weld length) was symmetrically positioned to the existing web and tack welded in place. Single fillets were first performed and then second and third weld passes were applied to each side to form the reinforced welds. Figure 5.3 shows the resulting specimen configuration.

Test specimens showed good quality welds using the automated welding system. The leg lengths of the test welds remained constant to within 1 mm along the length of each specimen. There were no visible weld defects including: porosity, undercut, and overlap. The rotation of the web plates from perpendicular to the continuous plate was measured to be less than 1 degree for all specimens. This lack in distortion of the T-joints was important because a significant positioning of the web away from the perpendicular would cause bending as well as tension in loading.

5.2 Test Results

Load and displacement data were saved by the testing computer in ASCII format. The data sampling rate was set to twenty samples per second. With tests as long as five to eight minutes the total number of data samples was often over ten thousand. This allowed for a good coverage for the load displacement diagram. However, the unloading was so fast when the weld ultimately failed that the load vs. displacement data could not be determined.

The amount of data needed to be reduced in order to use Excel program for graphing the load and displacement relations. Excel program is limited to 4,000 data entries in its graphics program. In order to reduce the data, Microsoft recommended a computer subroutine to select every nth row of data. The subroutine is shown in Appendix G. The data were reduced to near one thousand samples for each test. Data in the unstable failure region were not reduced, but this did not provide much more information.

5.2.1 Load vs. Displacement Diagrams

Results of testing on the ten specimens are shown in Figure 5.5 through

Figure 5.14. Each figure shows similar trends in the load vs. displacement relation. Initially welded joints reacted elastically to a point where yielding occurred. After yielding the load began to level off with increasing displacement due to plastic deformation and then failed at some critical displacement. Although the welds behaved similarly in loading, there were differences in displacement of the plastic deformation regions prior to joint failure.

The length of the plastic deformation is significant because an increase in displacement with a constant limit load increases the amount of work absorbed by the welded joint. McClintock (1994) determined that if the work to tear the weld is greater than the complementary work to bend the shell plate, deformation will occur by bending the plate rather than tearing the welds.

5.2.2 Limit Loads

The limit load of the welded joint is the highest load experienced in testing. The limit loads for all tests are shown in Table 5.1. The table shows that limit loads increased with welded joints having deeper weld penetrations. However, part of the changes in joint strength is due to changes in leg length of the welds. A comparison of tested results to theoretical predictions was necessary to better understand experimental results for the effect of weld penetration on joint strength.

5.3 Limit Load Analysis

Theoretical analysis helps to understand the benefit of penetration to fillet welds. The direct comparison of the limit loads from calculations and test results was not the only use of upper bound calculations. Test specimen welds did not all have equal leg lengths of 6 mm. Theoretical calculations for the actual weld geometries were used in order to normalize the effect of varying fillet weld sizes on the effect of penetration.

5.3.1 Determination of Weld Shear Strength in Yield

Yield strength in shear specifies the maximum shearing stress that can be sustained by a non-strainhardening material. In the upper bound and slip line solutions this specifies the stress required for material to deform along slip planes/lines. Values for shear strength in yield can be estimated from (tensile strength)/($\sqrt{3}$) for nonhardening materials (Kato and Morita, 1974). Approximation for the strength in shear is based on the determination of the tensile strength of the weld material.

Two approaches were used to determine the weld tensile strength. One source of determining the tensile strength is the manufacturer's recommended values from testing. The welding manufacturer performed tension tests from machined multi-pass weld specimens and included the values with the electrode specifications. Manufacturer-estimated tensile strengths are included in Appendix E.

Weld tensile strength can also be estimated with the use of hardness tests. The Rockwell A scale was used to take hardness values for sectioned test specimens. The values of the hardness readings are included in the photographs in Appendix F. Average hardness values were used to convert the readings to estimated tensile strengths. Table 5.2 shows the conversion of hardness reading to tensile strengths from the ASTM Standards (1992).

A comparison of weld strength in shear for hardness and manufacturer estimates is shown in Table 5.1. Deep penetrating welds showed hardness strength estimates 30% to 40% larger than the manufacturer's estimate. Welds without penetration showed a 10% larger strength estimate determined by hardness tests as compared to manufacturer estimates.

Hardness estimates of weld metal tensile strength were used in the upper bound calculations. Hardness values showed that the deeper penetration welds gave higher hardness readings. Therefore, the tensile strength of the welds should have increased with deeper penetration. This trend was not shown with the manufacturer's weld strength estimate. Weld material differences may also occur because manufacturer test specimens were formed with multi-pass welding whereas testing performed in this research involved single pass welds.

5.3.2 Benefit of Penetration

The upper bound solution of section 3.4 was used to determine theoretical limit loads. Upper bound calculations shown in Appendix D determine weld penetration effects for welds with equal leg lengths. Appendix H uses the upper bound solution to calculate tensile strengths based on actual test specimen weld geometry. Appendix I uses tested weld geometries without penetration to give limit loads as a baseline

Table 5.1 contains the data used for comparison of the upper bound and test results. Figure 5.15 shows the ratio of the tested limit loads to upper bound solutions from block sliding with hardness estimated weld strength. Deeper penetrating welds show the theoretical solutions tend to overestimate the weld strength. Figure 5.15 shows a 40% overprediction of theoretical tensile strength results for the deep penetration welds with their hardnesses compared to welds without penetration. Figure 5.16 shows that the expected benefit using the upper bound method for the deepest penetrating welds was 100%. A net benefit of 60% is determined for the deepest penetrating weld of 3.3 mm.

Figure 5.17 compares the tested load to the upper bound solution without penetration. Using an average of the hardness determined tensile strength estimates for welds without penetration gives a 60% benefit in the strength of welds with a penetration of 3.3 mm. Figure 5.17 also shows the ratio of the tested limit load to the upper bound solution without penetration based on varying hardness values at different penetrations to estimate weld strength. Results here only show around a 30 % increase in the tensile strength of the 3.3 mm penetration fillet welds because the effect of increasing joint strength with harder welds is effectively normalized out. The 60% increase in joint strength with a penetration of 3.3 mm is the best estimate for the overall effects of penetration on joint strength.

The increase in the plastic work required to fail a fillet joint with penetration is significant. Test load-displacement diagrams shown from Figure 5.5 to Figure 5.14 indicate the deepest penetrating welds give three to five times the plastic displacements compared to welds without penetration. Figure 5.18 shows that the deepest penetrating welds increased the amount of work by threefold to fourfold.

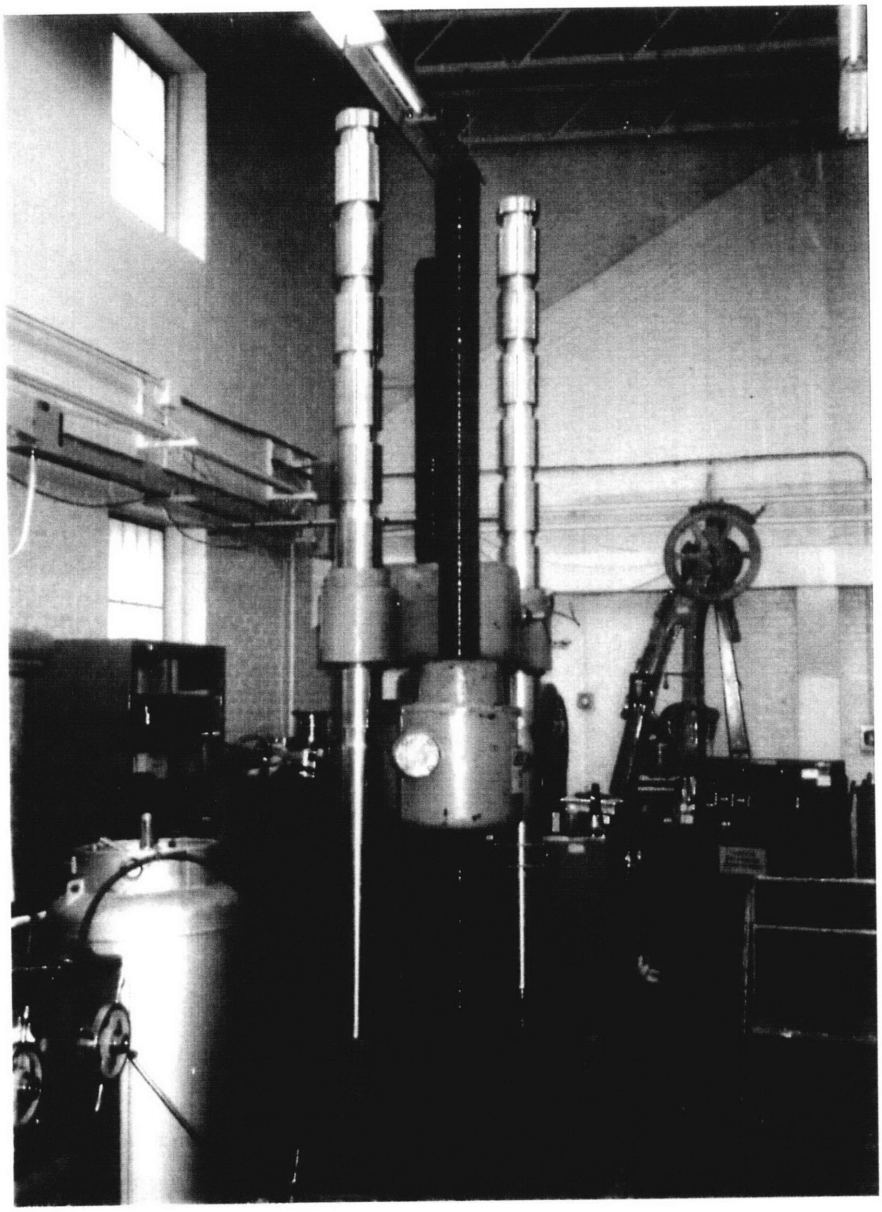

FIGURE 5.1 Tension Test Machine

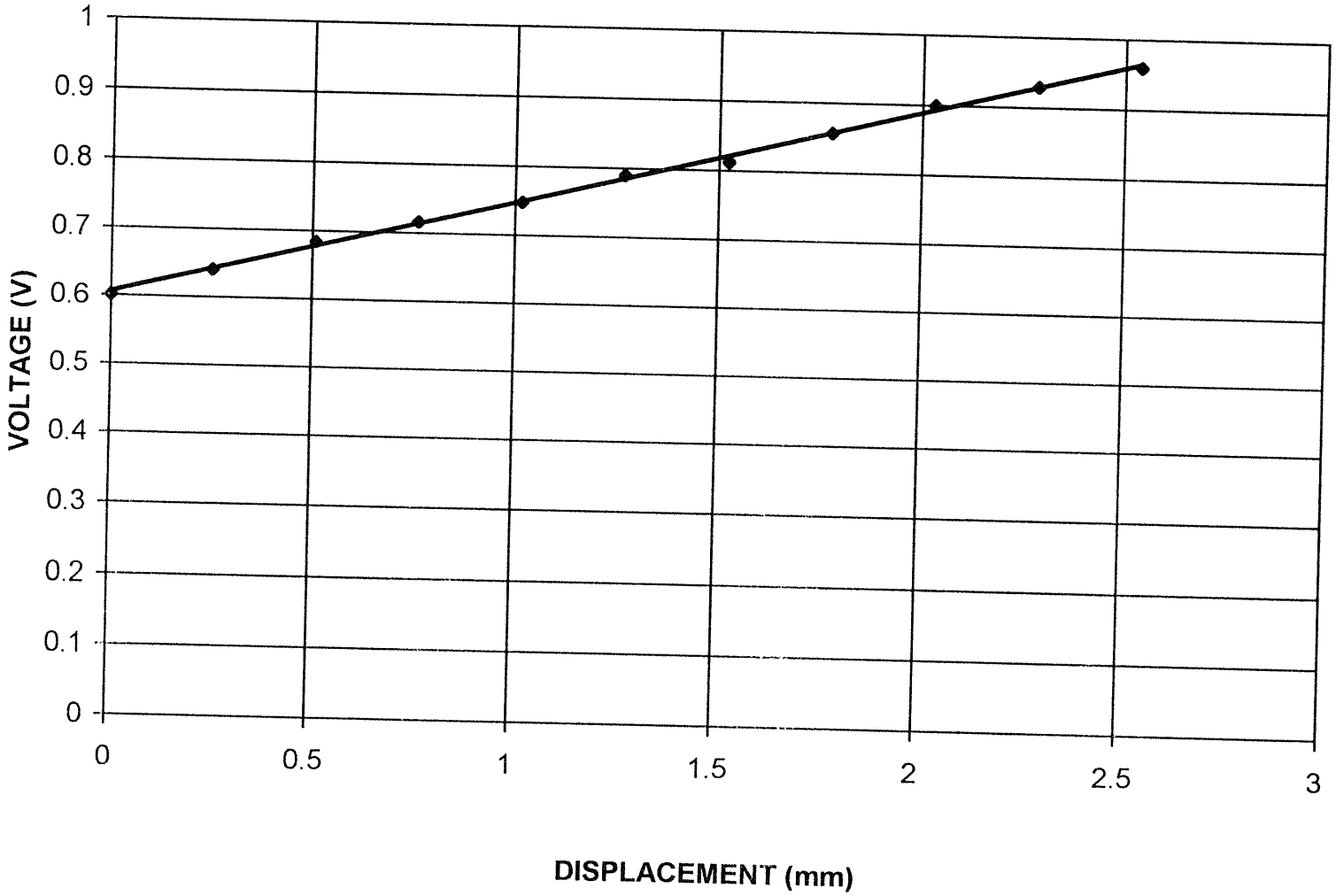

FIGURE 5.2 Calibration Curve for LVDT

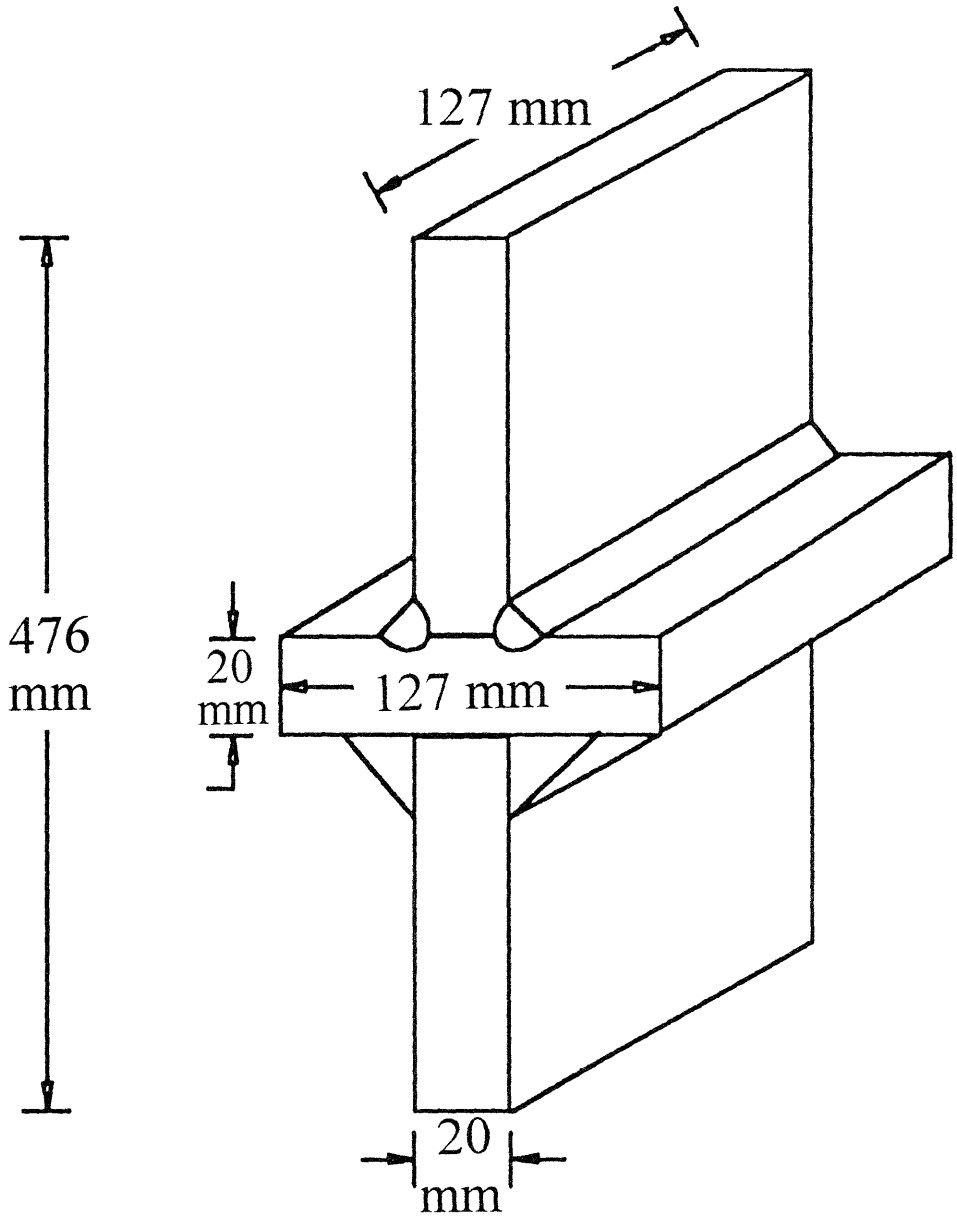

FIGURE 5.3 Tensile Strength Test Specimen

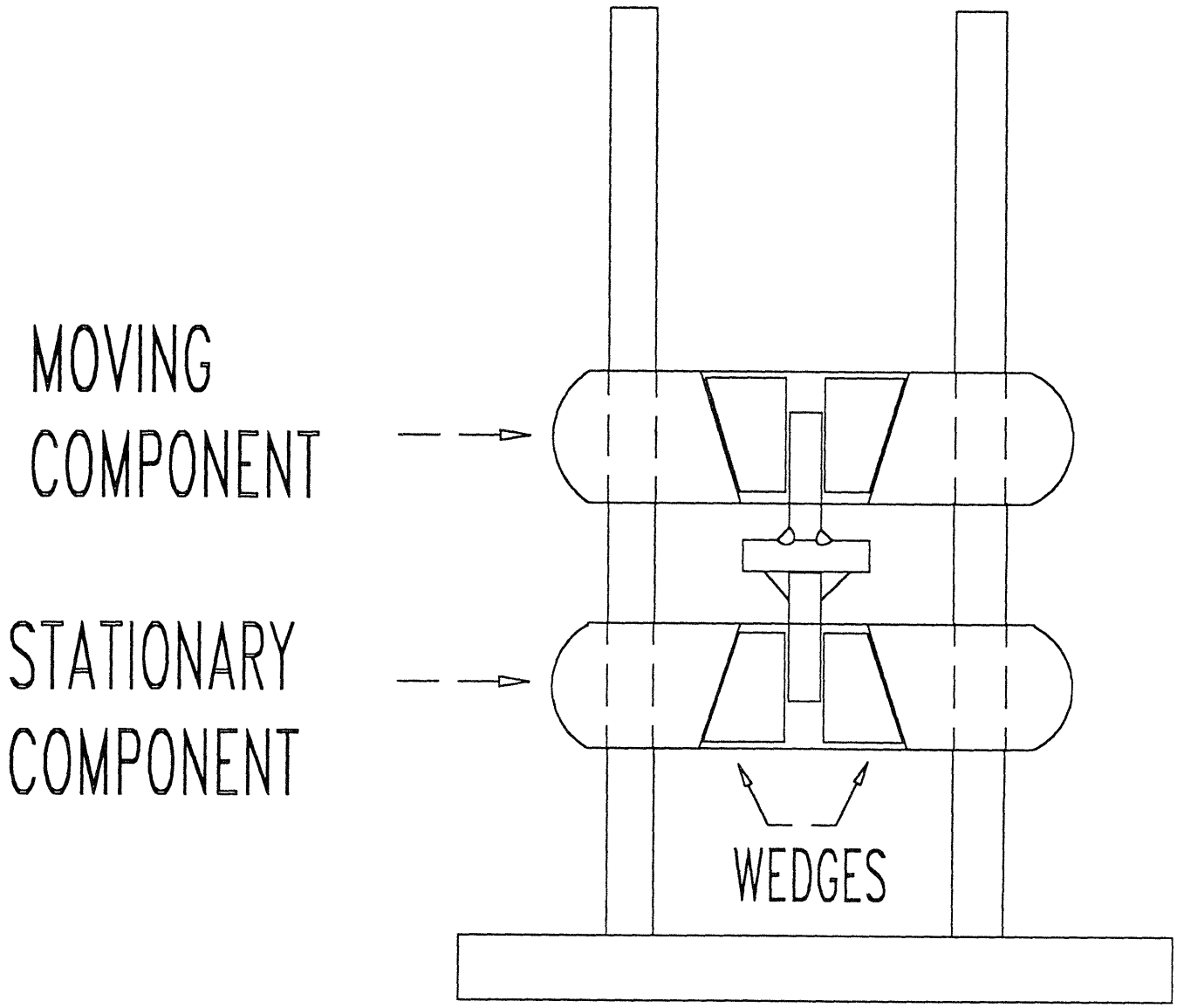

FIGURE 5.4 Specimen Setup in Testing Machine

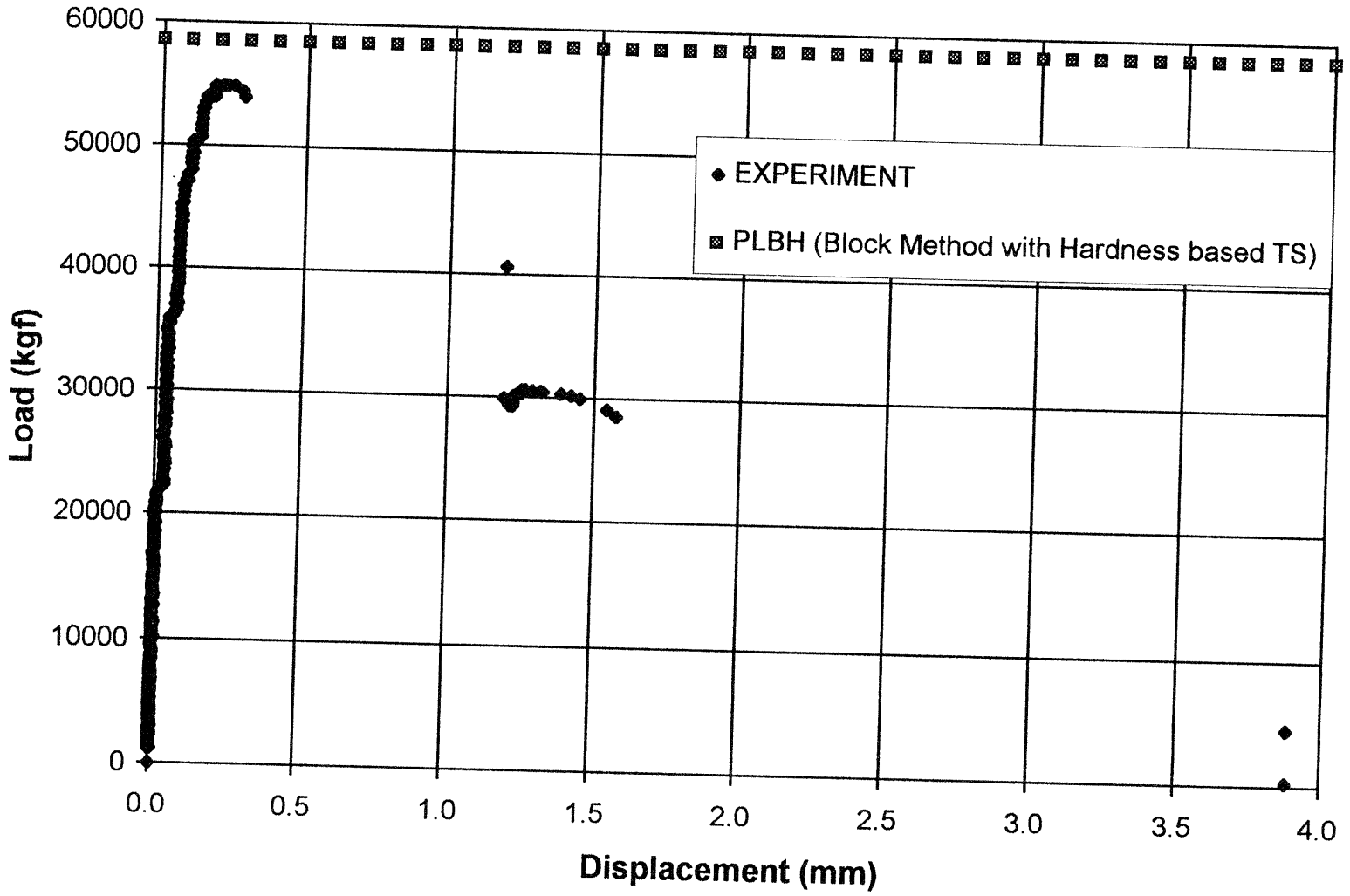

FIGURE 5.5 Loads for Test 1 (Penetration = 0 mm)

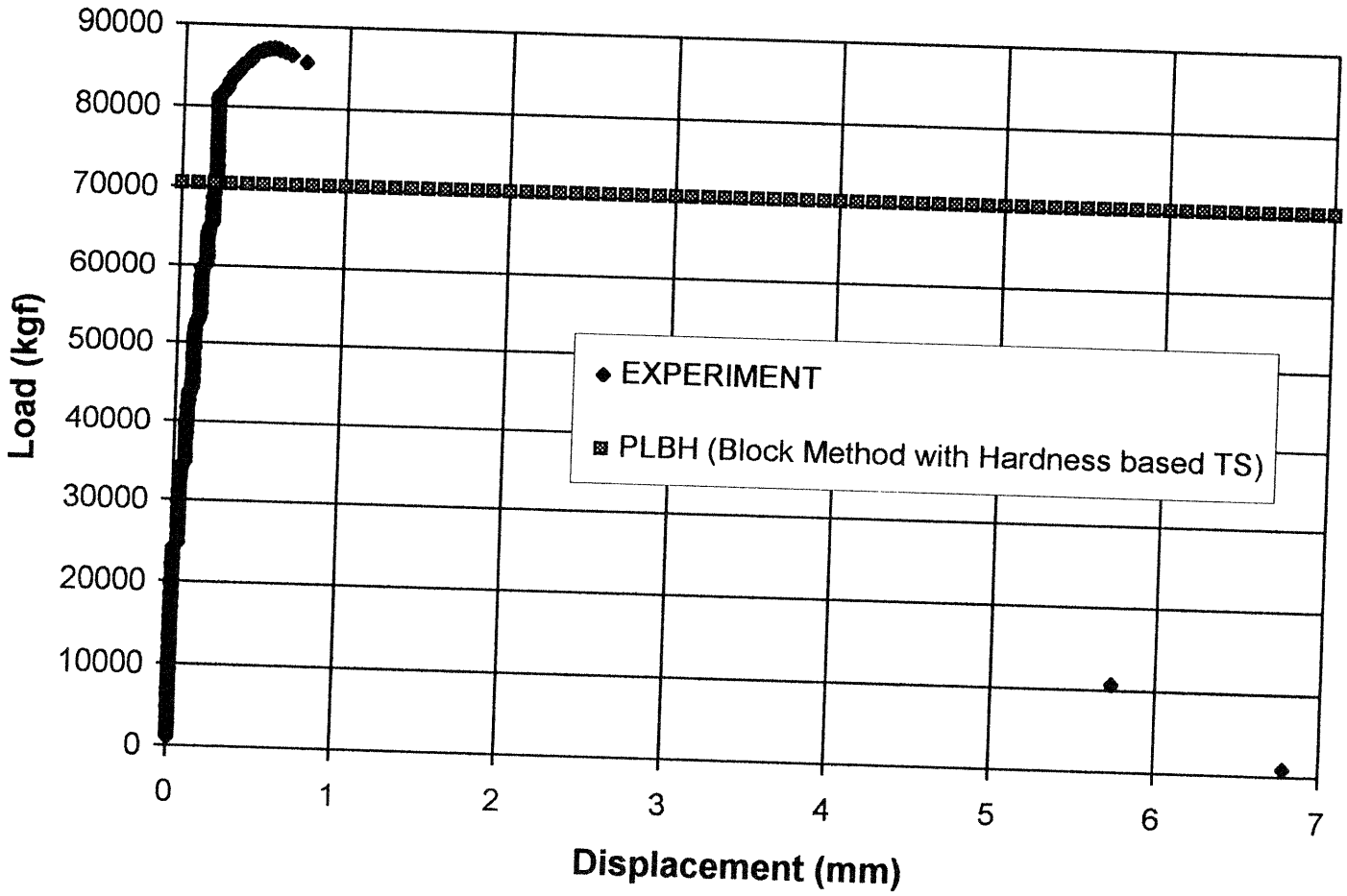

FIGURE 5.6 Loads for Test 2 (Penetration = 0 mm)

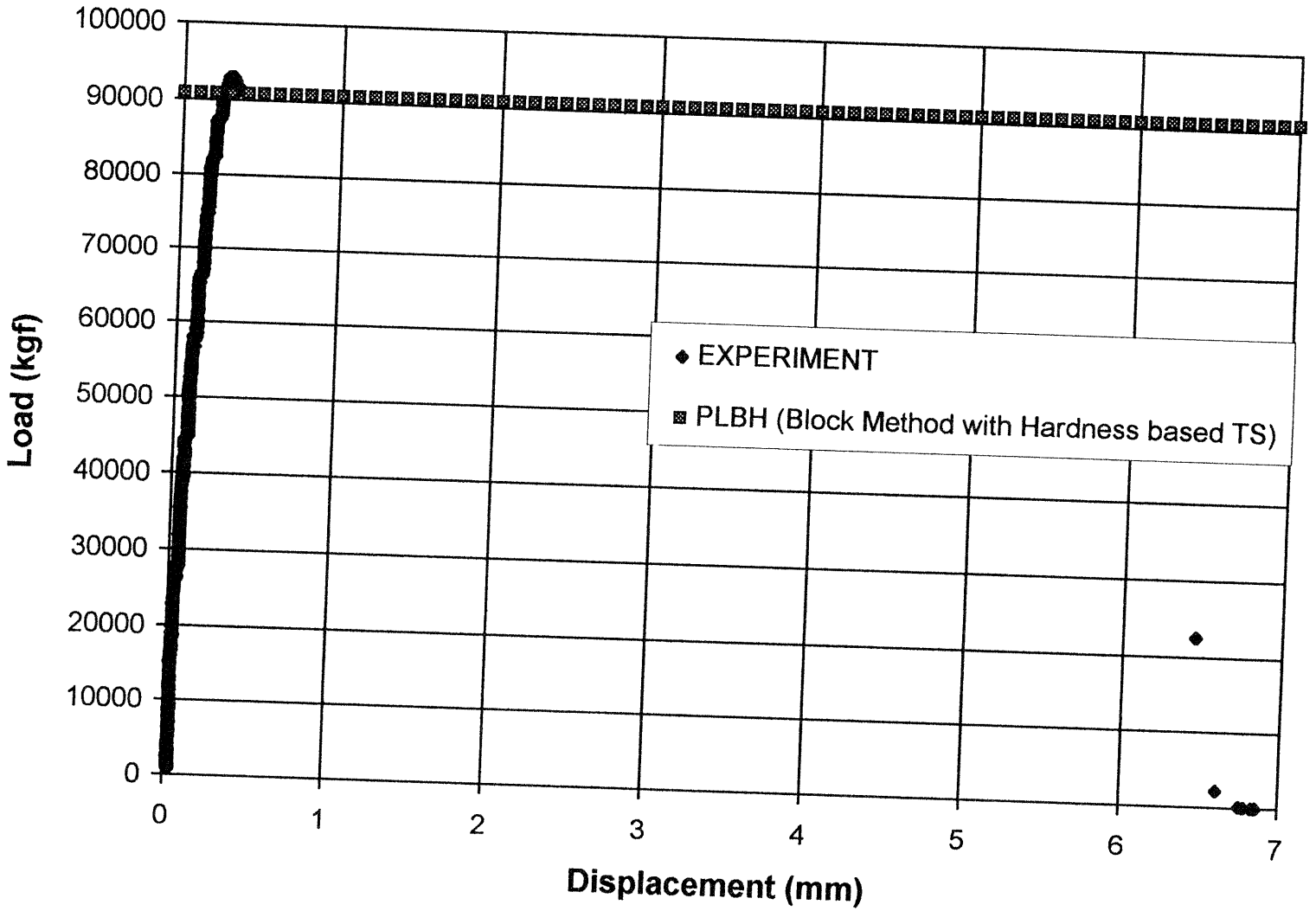

FIGURE 5.7 Loads for Test 3 (Penetration = 1.1 mm)

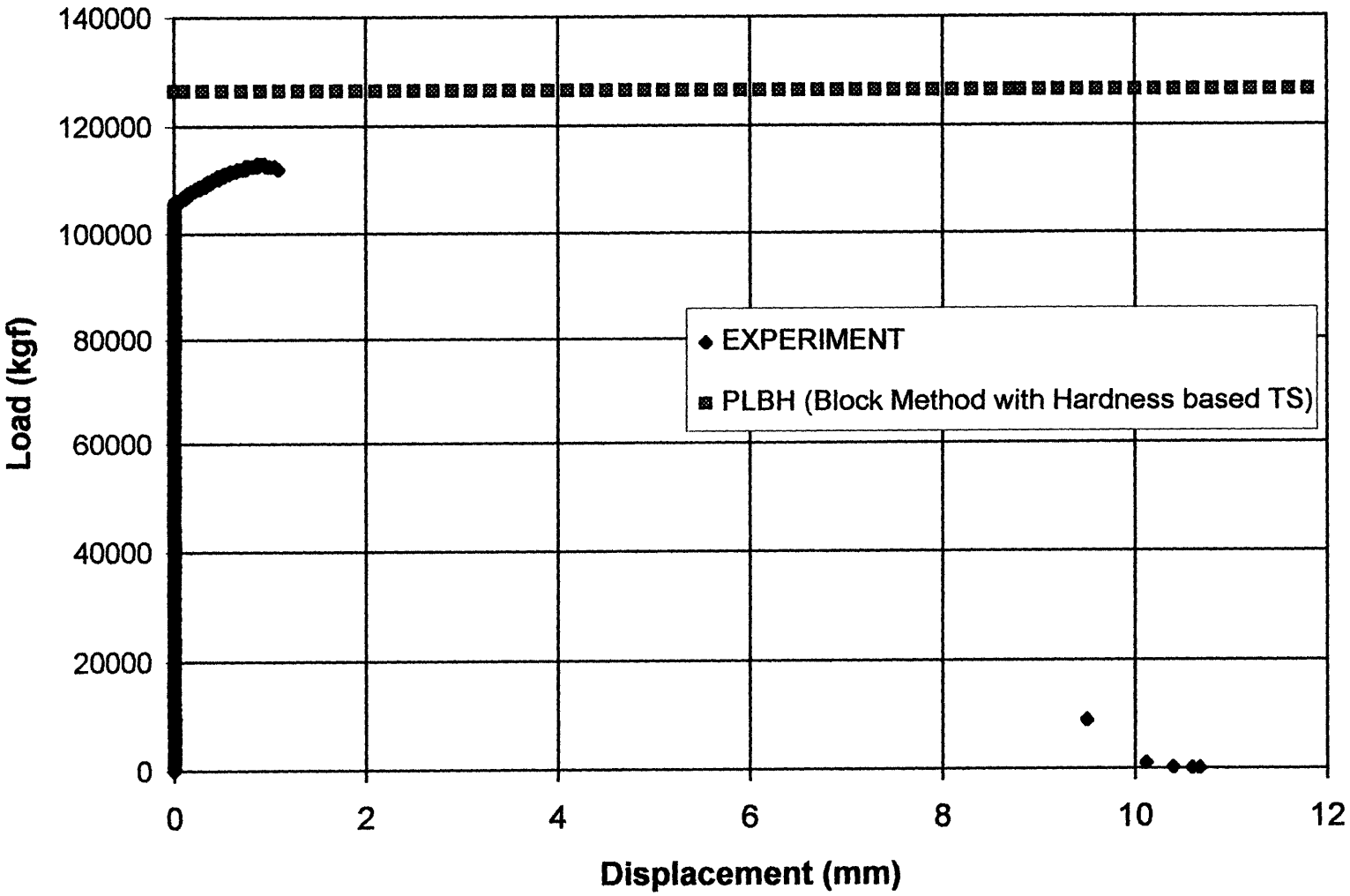

FIGURE 5.8 Loads for Test 4 (Penetration = 2.2 mm)

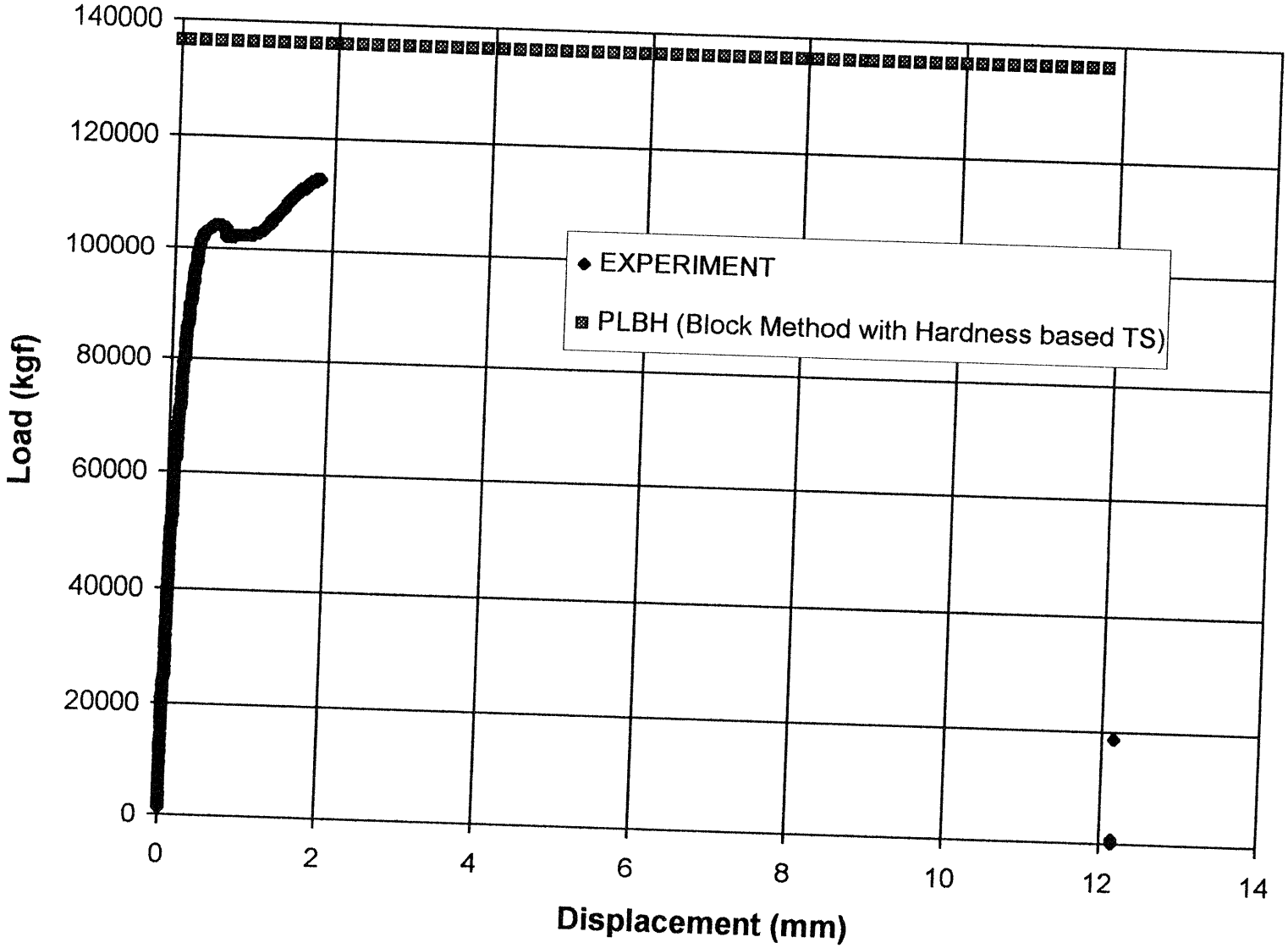

FIGURE 5.9 Loads for Test 5 (Penetration = 2.7 mm)

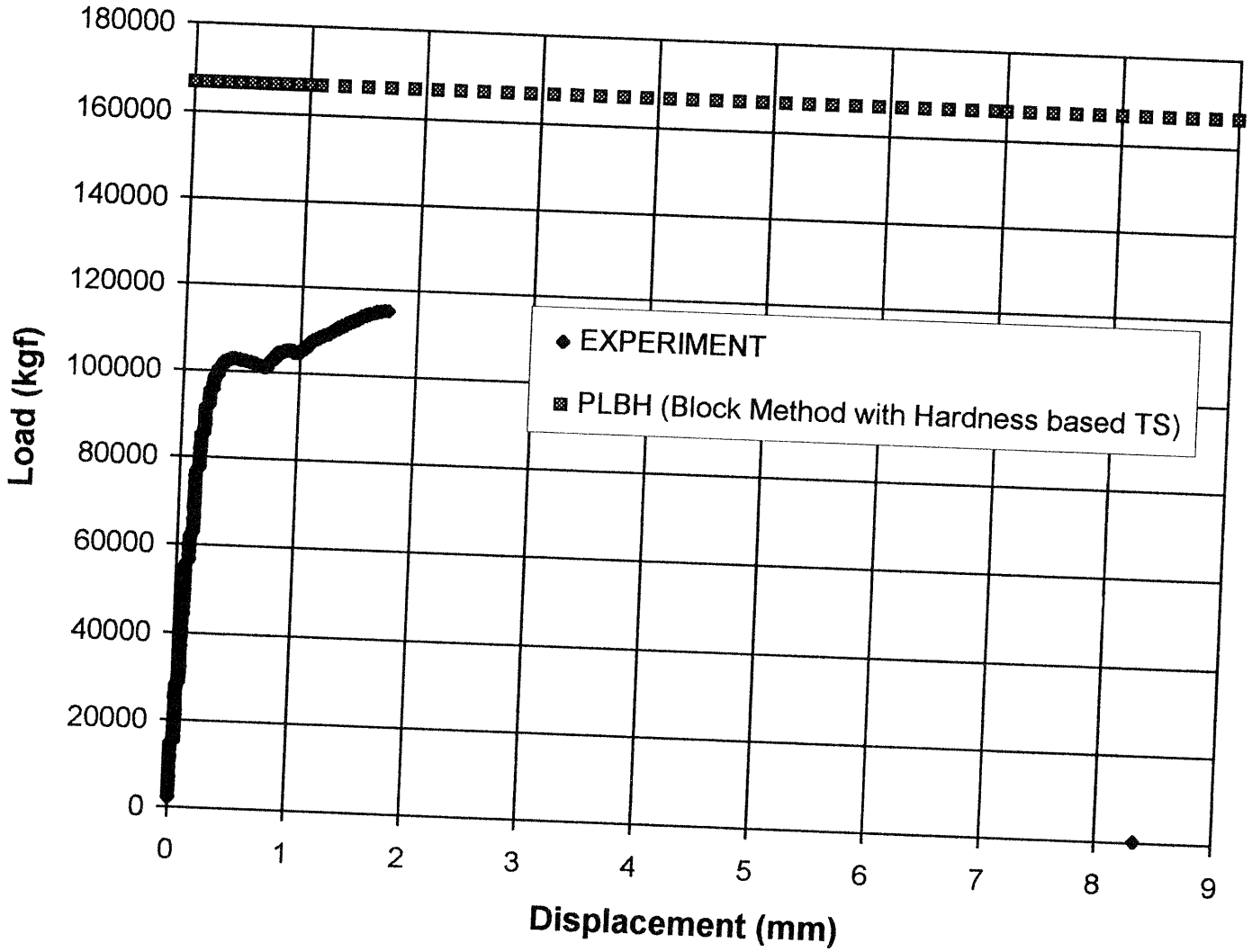

FIGURE 5.10 Loads for Test 6 (Penetration = 3.2 mm)

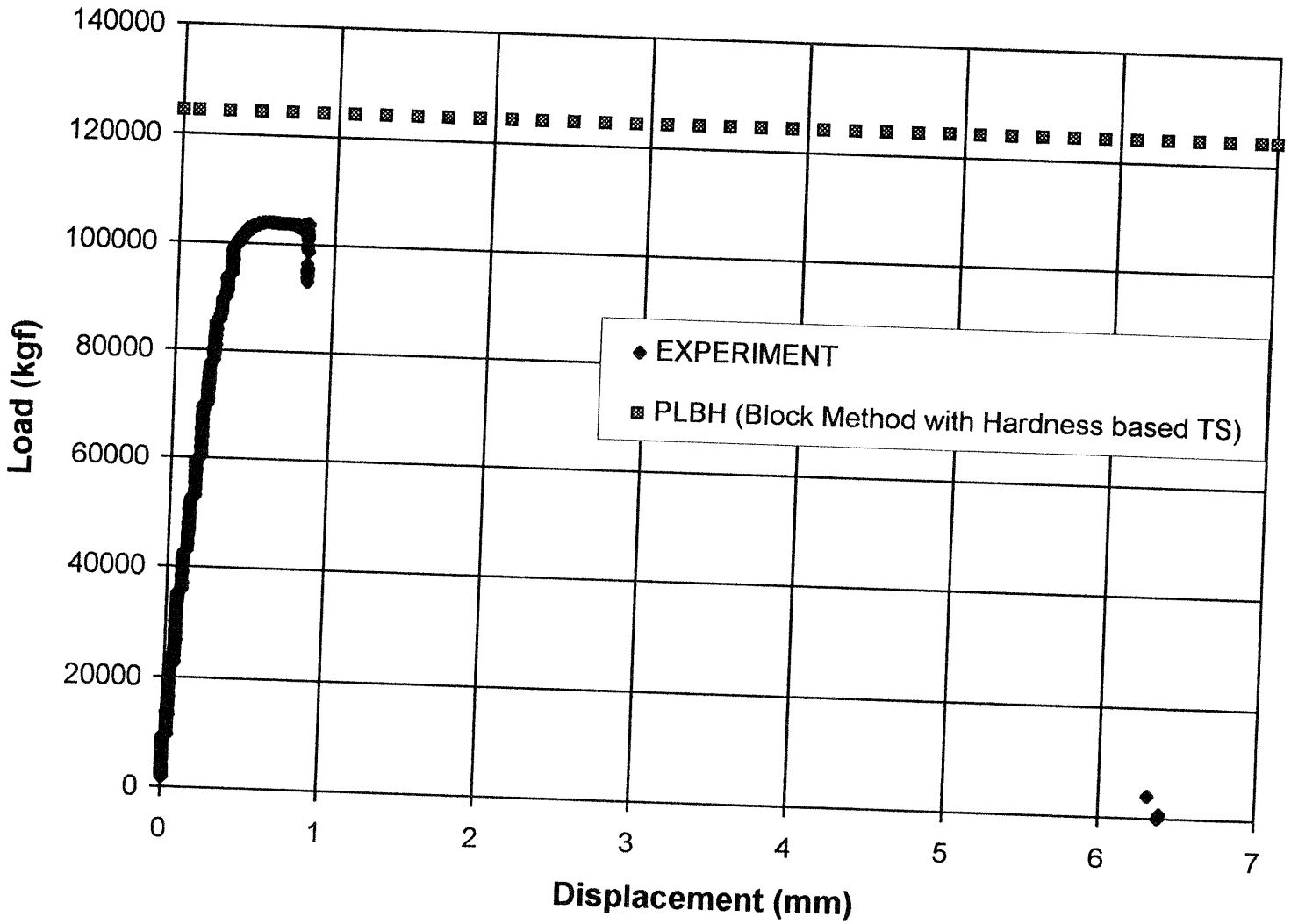

FIGURE 5.11 Loads for Test 7 (Penetration = 2.1 mm)

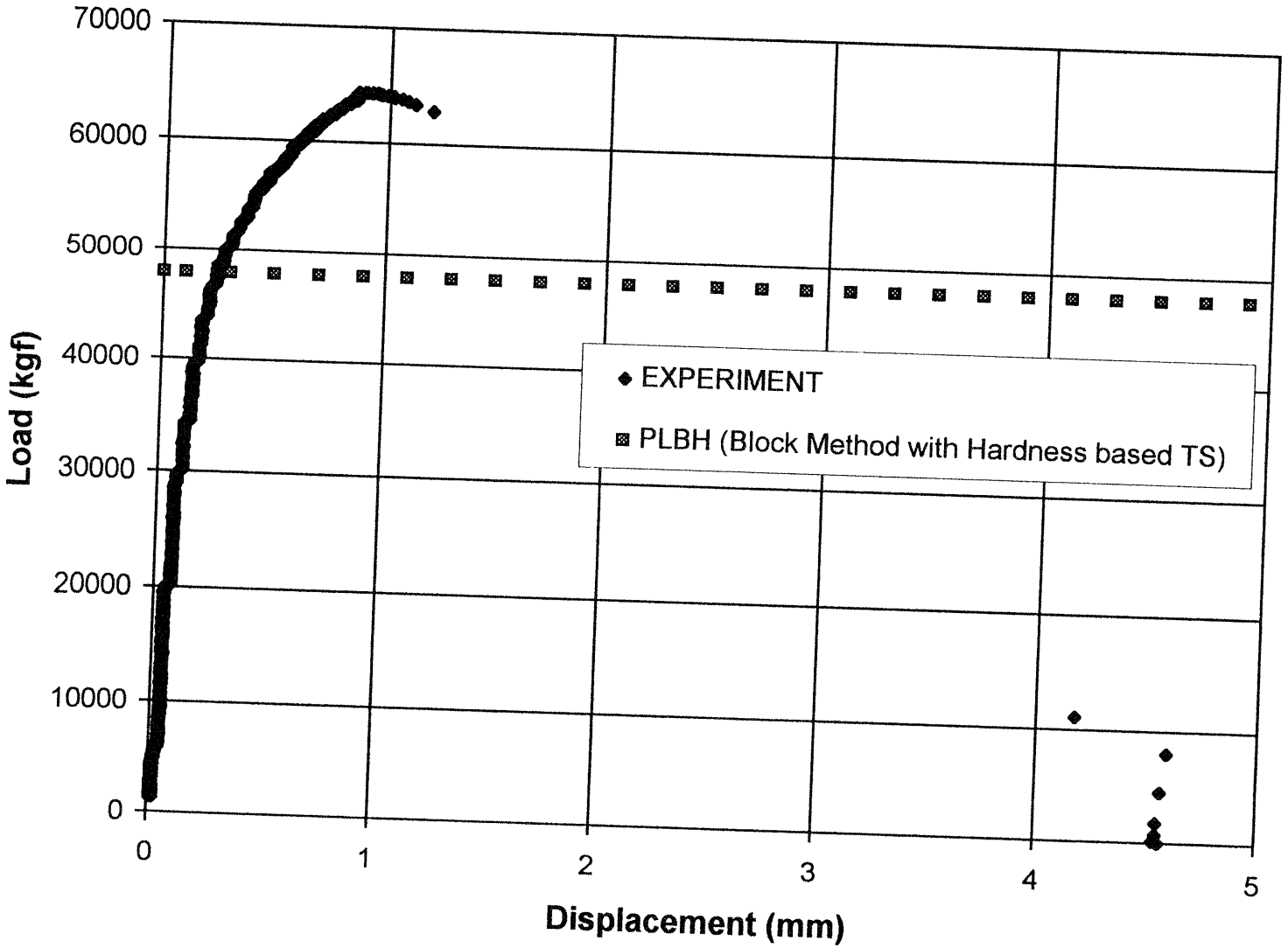

FIGURE 5.12 Loads for Test 8 (Penetration = 0 mm)

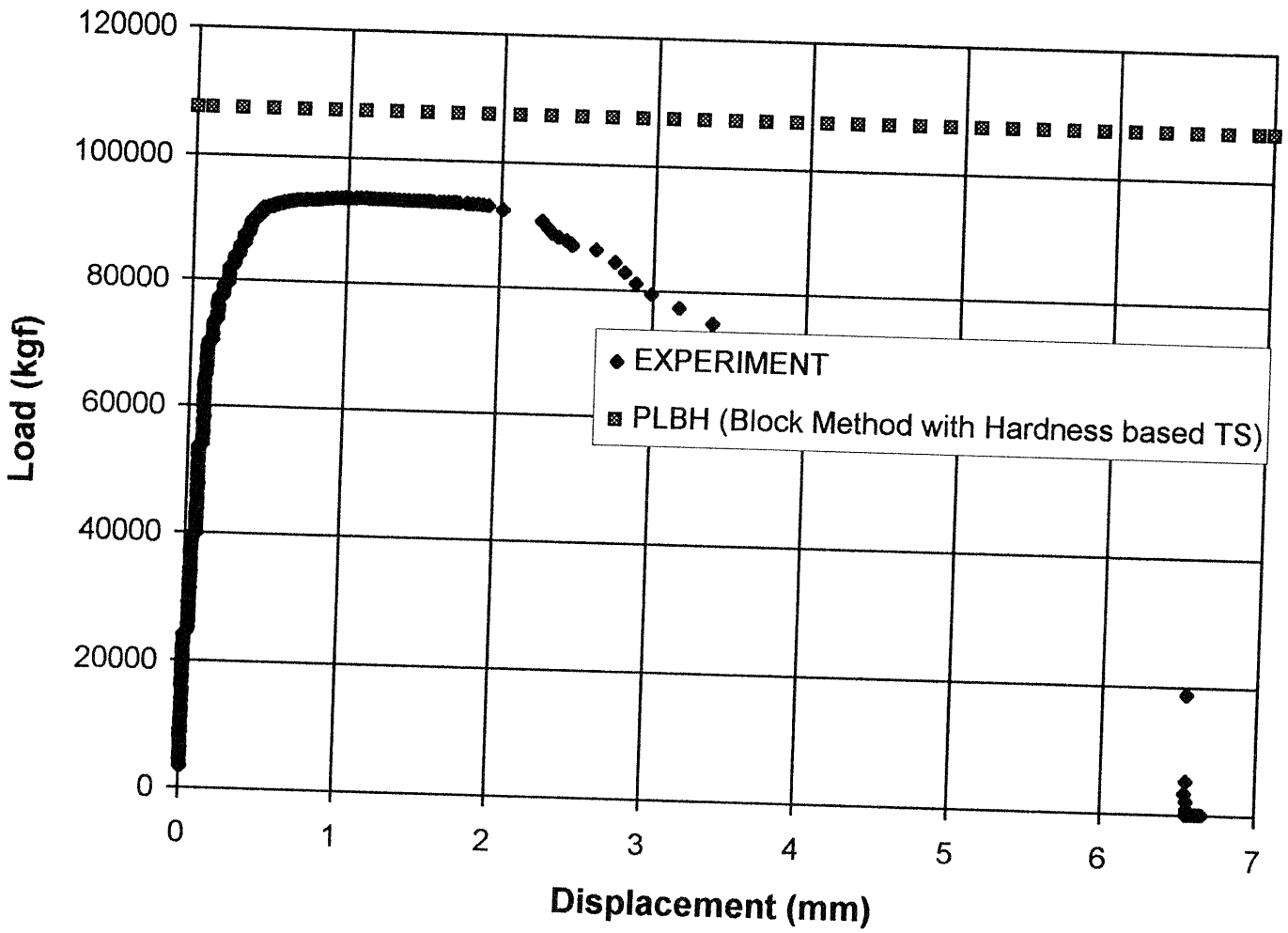

FIGURE 5.13 Loads for Test 9 (Penetration = 2.2 mm)

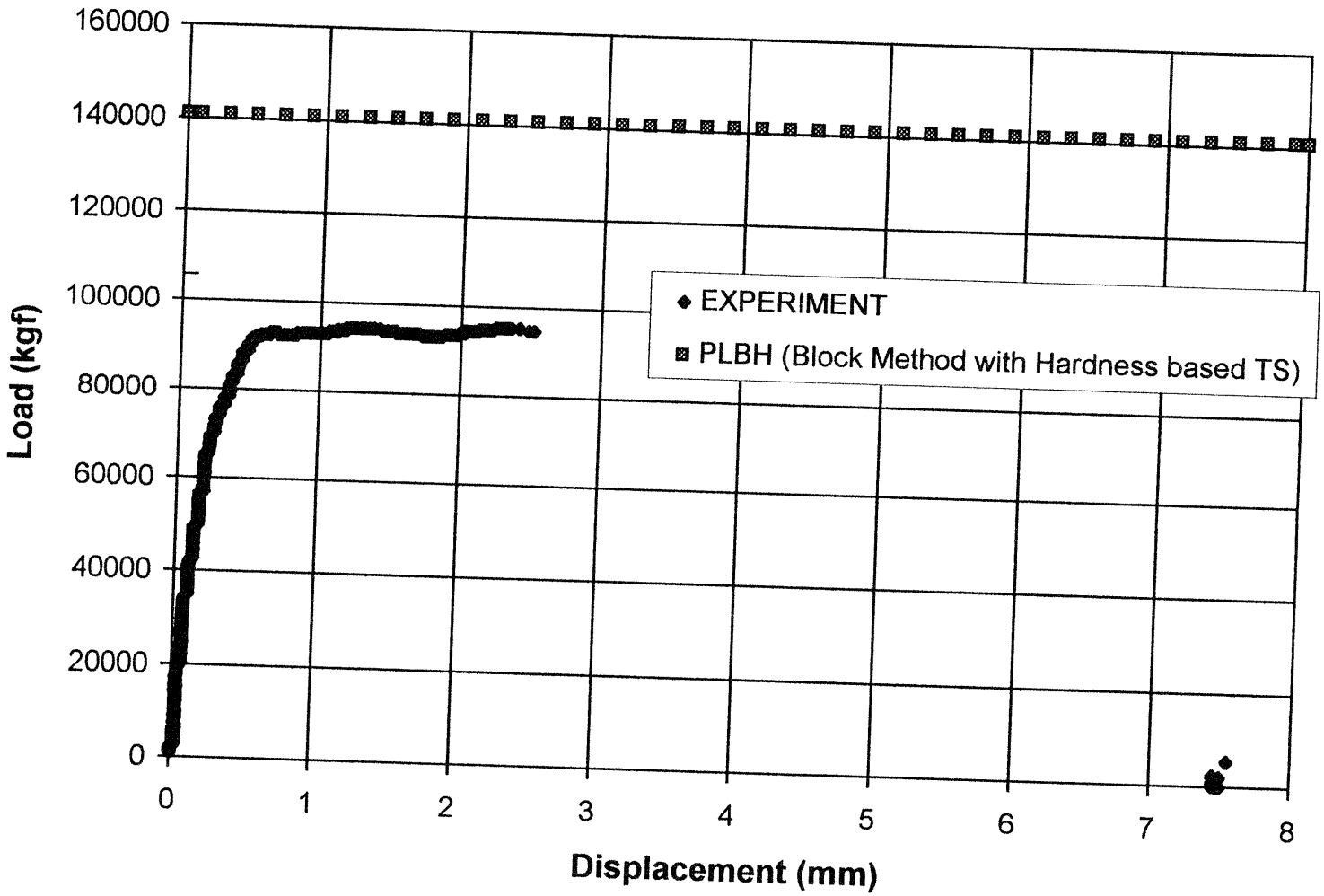

FIGURE 5.14 Loads for Test 10 (Penetration = 3.3 mm)

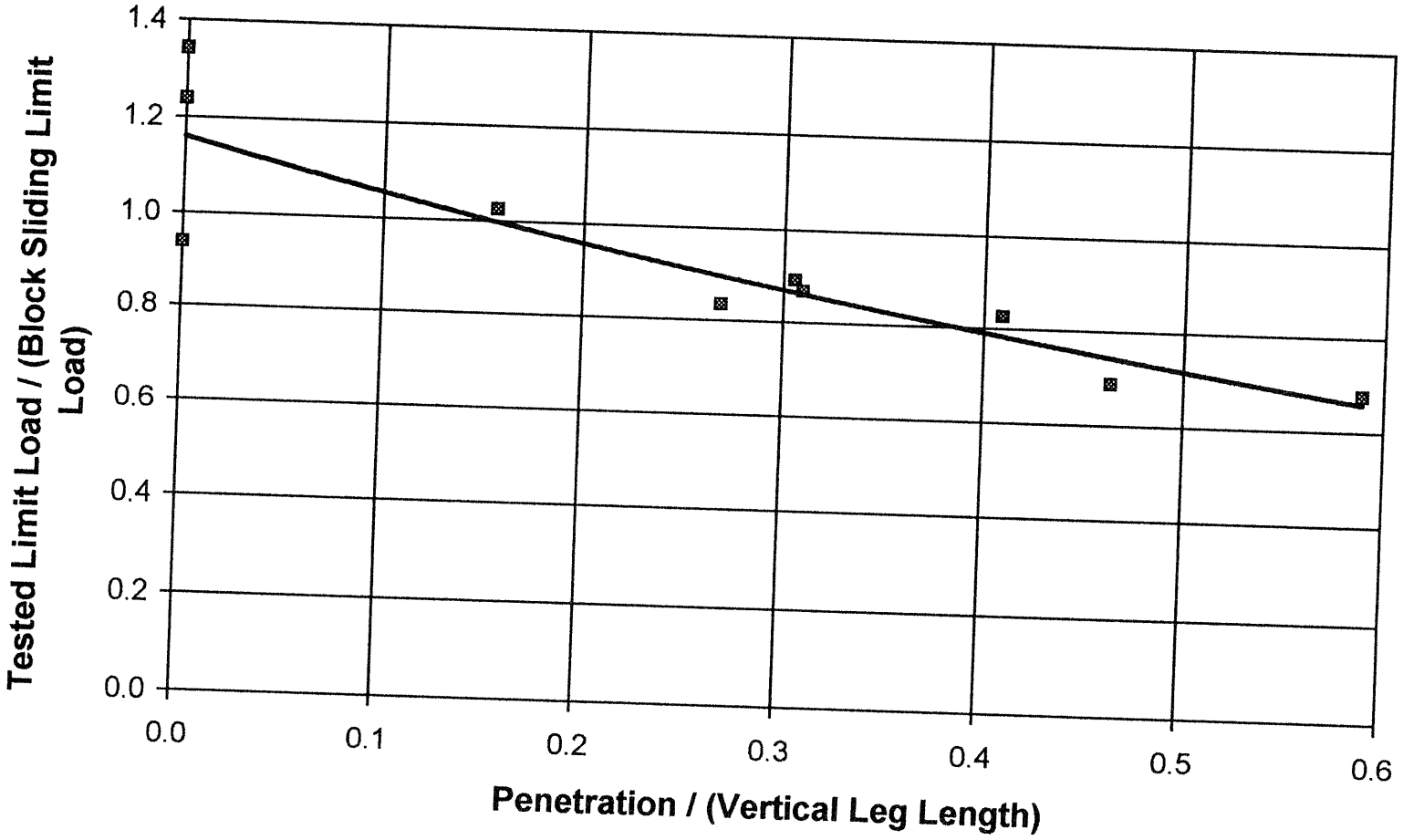

FIGURE 5.15 Ratio of Tested Limit Load to Block Sliding Estimate (with Hardness TS) vs. Normalized Penetration

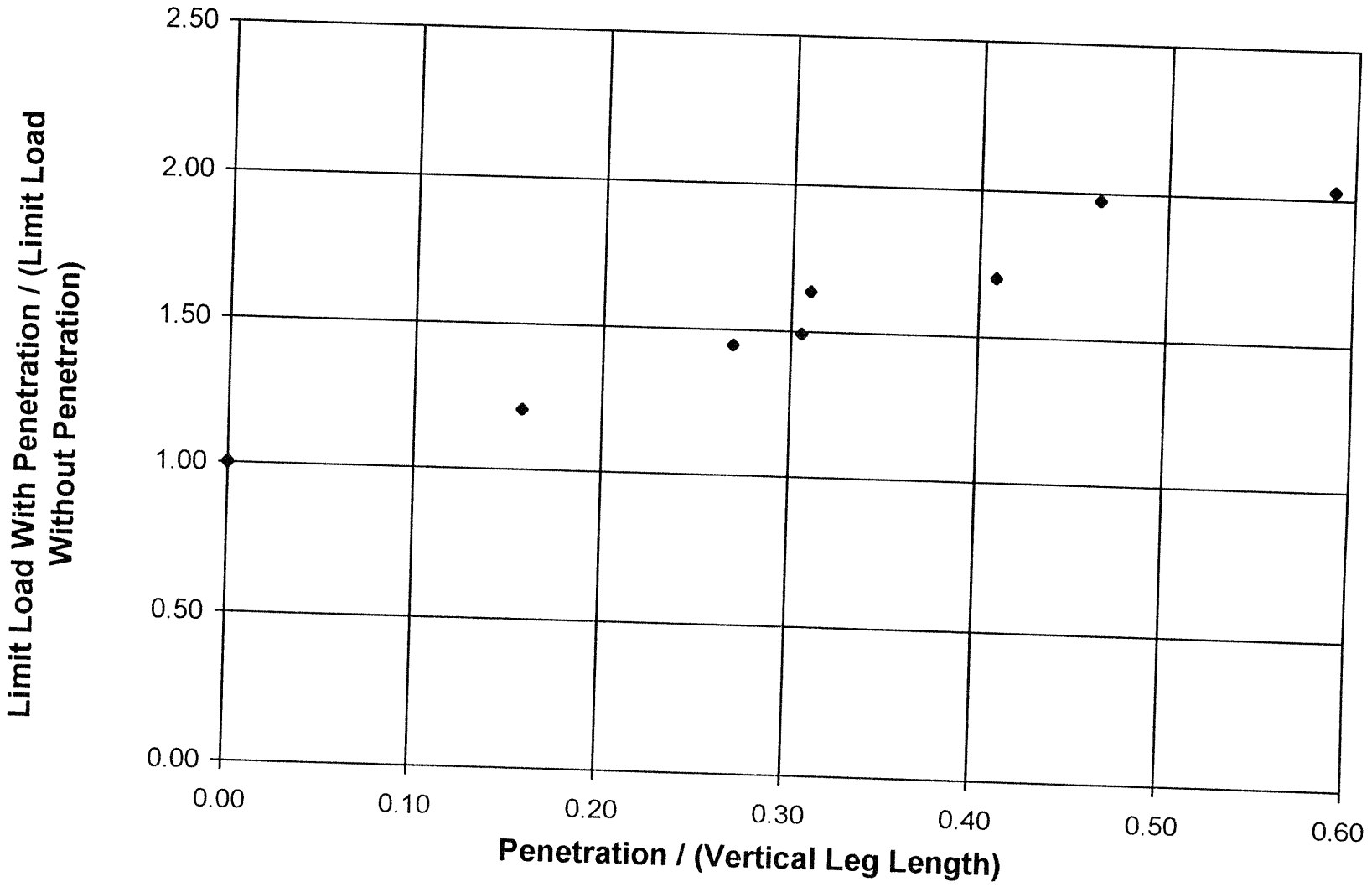

FIGURE 5.16 Weld Penetration Geometrical Benefit using Block Sliding Theory for Test Geometries (Leg Ratios 0.9-1.1)

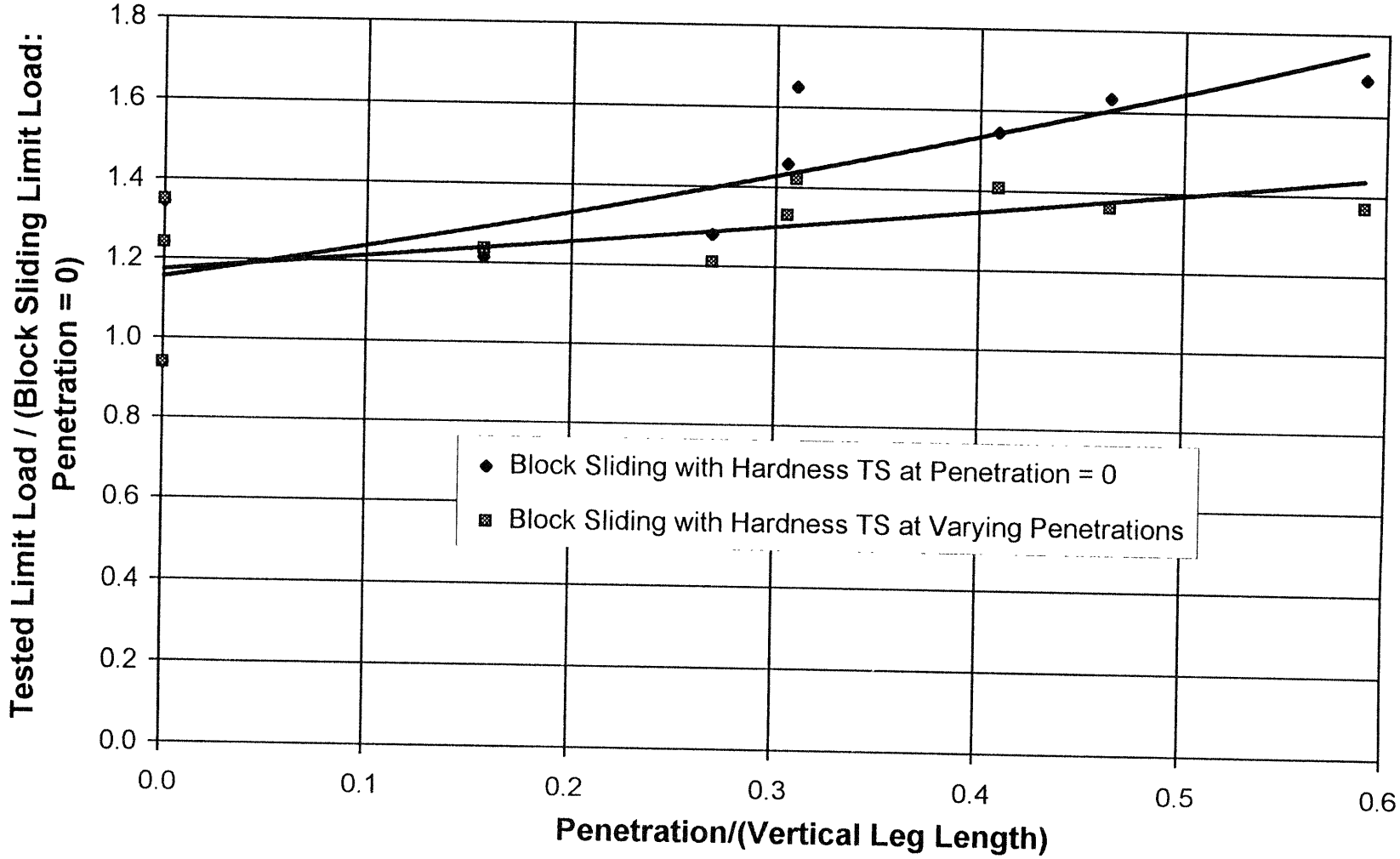

FIGURE 5.17 Ratio of Tested Limit Load to Block Sliding Estimate (Without Penetration) vs. Normalized Penetration

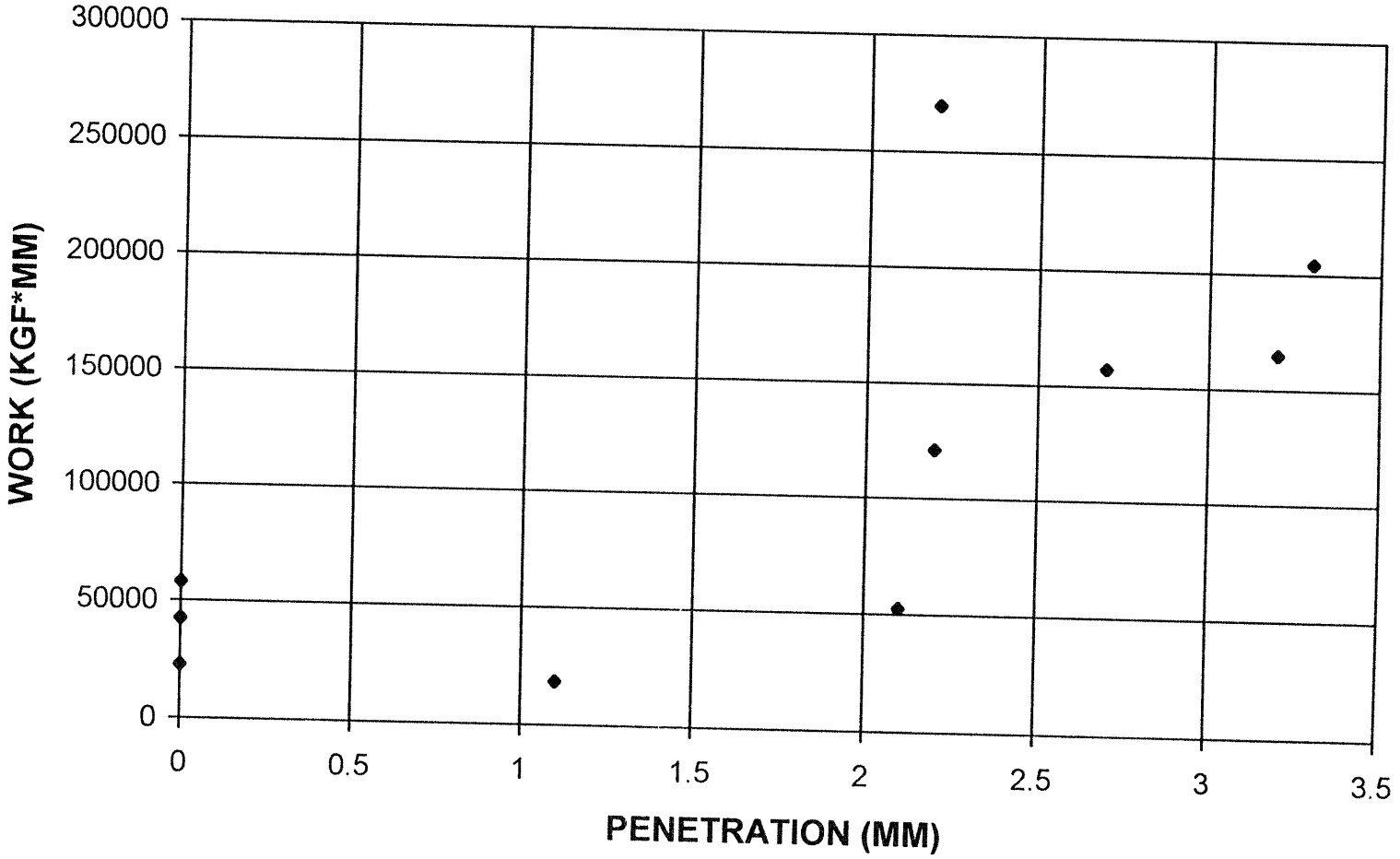

FIGURE 5.18 Work to Deform Test Specimens

TABLE 5.1 Comparison of Test Results to Predicted Theory

Pla	Actual Limit Load (kg\mm)
Plbho	Limit Load from Block Sliding Theory Assuming no Penetration (Shear Stress from Hardness Tests at Varying Penetrations)
Plbh	Limit Load from Block Sliding Theory (Shear Stress from Hardness Tests)
Plbhoo	Limit Load from Block Sliding Theory Assuming No Penetration (Shear Stress from Hardness Tests at Penetration = 0)
Plbm	Limit Load from Block Sliding Theory (Shear Stress from Recommendations by the Manufacturer)
Kh	Shear Stress for Weld Converted from Rockwell A Hardness Values
Km	Shear Stress for Weld Based Upon TS by Manufacturer
K	Shear Stress by Either Manufacturer or Hardness Tests (Value Cancels Out)

Excel-Arc 71	Fabco 802
Km (kg\mm^2)	Km (kg/mm^2)
35.48	33 16

Test	Penetration (mm)	Kh(hardness) (kg/mm^2)	dx (horiz. leg length) (mm)	dy (vert leg length) (mm)	Leg Length Ratio (horiz./vert.)	Limit Load (Pla) (Actual) (kg/mm)	Limit Load (Plbh) (Block Sliding) (kg/mm)	Limit Load (Plbm) (Block Sliding) (kg/mm)
1	0.0	40.59	5.7	5.7	1 00	434.23	462.75	404.44
2	0 0	46.68	5.9	5 9	1.00	683.22	550.83	418.63
3	1.1	42.22	7.0	7.0	1.00	730.73	713.08	599.26
4	2.2	47.09	7.2	7.2	1.00	903.19	1012.00	762.37
5	2.7	47.21	6.6	6.8	0.97	903.56	1092.00	820.57
6	3 2	51.55	6.9	6 6	1.05	927.30	1345.00	925.85
7	2.1	45.46	7 8	7.5	1.04	825.47	987.45	770.56
8	0.0	35.72	4.9	5.4	0.91	518.34	385.78	358 17
9	2.2	41.40	7 1	6.3	1.13	741.95	854 23	684.22
10	3 3	44 25	5.6	6.3	0.89	759.72	1123.00	841.72

Test	Penetration (mm)	Penetration/(leg length)	Plbho (kg/mm)	Plbhoo (kgf/mm)	Pla/Plbh	Pla/Plbhoo Block Sliding wi	Plbh/Plbho	Pla/Plbho Block Sliding with Hardness TS
1	0 0	0.00	462.75	462.75	0.94	0.94	1.00	0.94
2	0 0	0.00	550.83	550.83	1.24	1.24	1.00	1.24
3	1.1	0.16	591.02	601.93	1.02	1.21	1.21	1.24
4	2.2	0 31	678.04	619.15	0.89	1.46	1.49	1.33
5	2.7	0.41	641.77	584.78	0.83	1.55	1.70	1 41
6	3.2	0.46	680.48	567 62	0.69	1.63	1.98	1.36
7	2 1	0.27	681.94	645.04	0.84	1.28	1.45	1.21
8	0.0	0.00	384 02	385.78	1.34	1.34	1.00	1.35
9	2 2	0.31	521.69	449.86	0.87	1.65	1.64	1.42
10	3.3	0.59	553.84	449.77	0.68	1.69	2.03	1.37

TABLE 5.2 Hardness to Tensile Strength Conversion
(ASTM, 1993)

Rockwell A Scale	Tensile Strength (ksi)	Rockwell A Scale	Tensile Strength (ksi)
72	201	58.3	100
71.5	194	57.6	98
70.9	188	57	94
70.4	182	56.4	92
69.9	177	55.8	90
69.4	171	55.2	89
68.9	166	54.6	88
68.4	161	54	86
67.9	156	53.4	84
67.4	152	52.8	83
66.8	149	52.3	82
66.3	146	51.7	81
65.8	141	51.1	80
65.3	138	50.6	77
64.6	135	50	73
64.3	131	49.5	72
63.8	128	48.9	70
63.3	125	48.4	69
62.8	123	47.9	68
62.4	119	47.3	67
62	117	46.8	66
61.5	115	46.3	65
61	112	45.8	64
60.5	110	45.3	63
61.5	116	44.8	62
60.9	114	44.3	61
60.2	109	43.8	60
59.5	104	43.3	59
58.9	102		

CHAPTER 6
EFFECT OF DEEPER PENETRATION WELDS ON PRODUCTION COSTS

An important consideration for the use of deeper penetration fillet welds is the cost. By a comparison of the trends in the parameters used to make penetrating welds, an estimate of the relative costs for production can be estimated. Parameters used to compare relative fillet weld expenses were: amperage, voltage, penetration, leg lengths, weld feed speed, and travel speed of the electrode arc. Data for the welded test specimens is shown in Table 6.1.

To recognize a benefit with penetration, it was necessary to compare the deepest penetrating weld settings to parameters recommended by the welding manufacturer. Test 3 corresponds closest to parameters recommended by the electrode manufacurer. In addition, welding parameters for Test 3 are closest to the average weld parameters used in shipbuilding today at Ingalls Shipbuilding and Newport News Shipbuilding as shown in Table 4.2. Higher voltage and amperage values used at Mitsubishi Heavy Industries corresponds closer to the parameters used in Test 4 or Test 5.

Deeper penetrating welds have a higher deposition rate as shown in Figure 6.1. Comparison of Test 6 (penetration = 3.2 mm) to Test 3 (penetration = 1.1 mm) shows that the deeper penetrating weld of Test 6 increases the deposition rate by 70%. Higher amperages were needed to create deeper penetrating welds. FCAW accounts for the higher amperages by raising the wire feed speed increasing the deposition rate. The product of weld cross sectional area and the travel speed gives the deposition rate of the weld. The use of wire feed speed and welding electrode size were not used in the determination of the deposition rate because weld spatter was experienced.

Figure 6.2 displays a decrease in specific energy required for deeper penetrating welds. The amount of electrical energy per unit length of weld material (specific energy) is determined from the voltage times the amperage divided by the travel speed.

A comparison of specific energy for Test 6 and Test 3 shows that there was a 5% decrease in the amount of energy required to perform a standard length of weld. Therefore, the test results show deeper penetrating welds require less electrical energy. This may result from the high current densities of the deep penetrating weld parameters and faster travel speeds. Higher concentration of heat may melt more depth of base plate and allow for less heat loss by conduction through the plate.

Another benefit of the high penetrating welds is the increased travel speed of the welding machine. Increasing welding current and electrode feed speed increases the deposition rate of the weld. In order to keep the leg length constant the travel speed of the machine must be increased. Figure 6.3 shows a 70 % increase in the machine travel speed from Test 3 (1.1 mm) to Test 6 (3.2 mm). Less labor and machine time could lead to 60% savings with the deep penetrating welds.

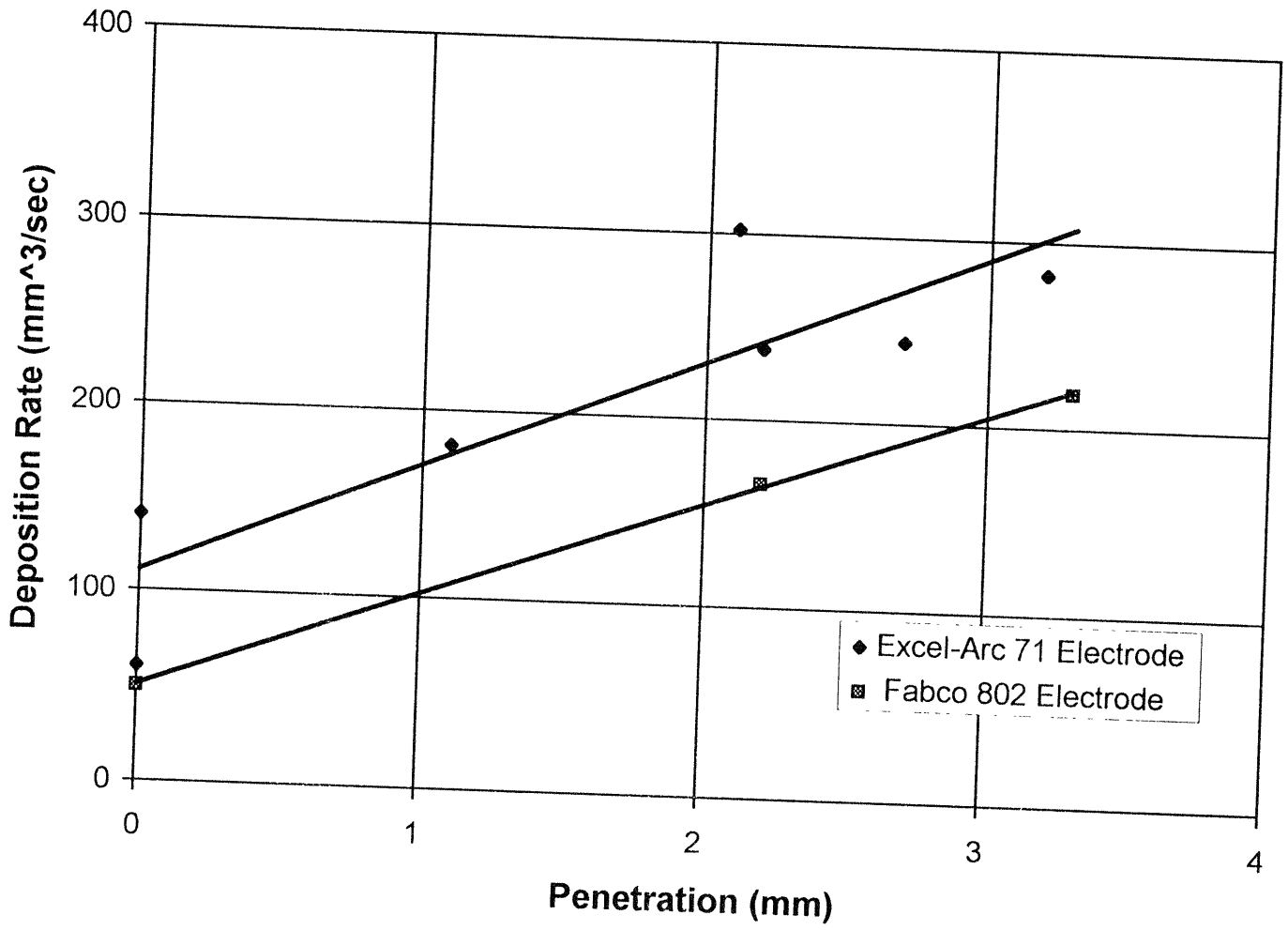

FIGURE 6.1 Deposition Rate vs. Weld Penetration

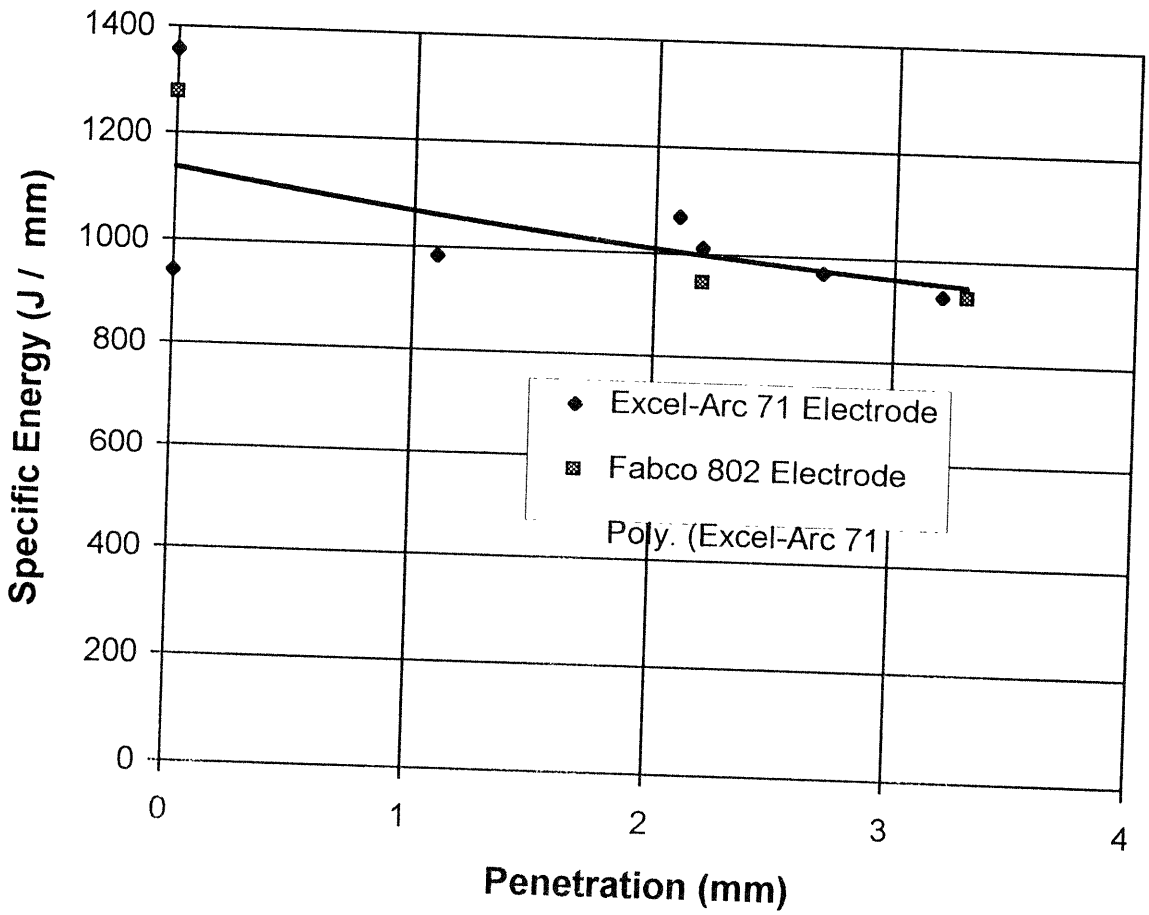

FIGURE 6.2 Specific Energy vs. Weld Penetration

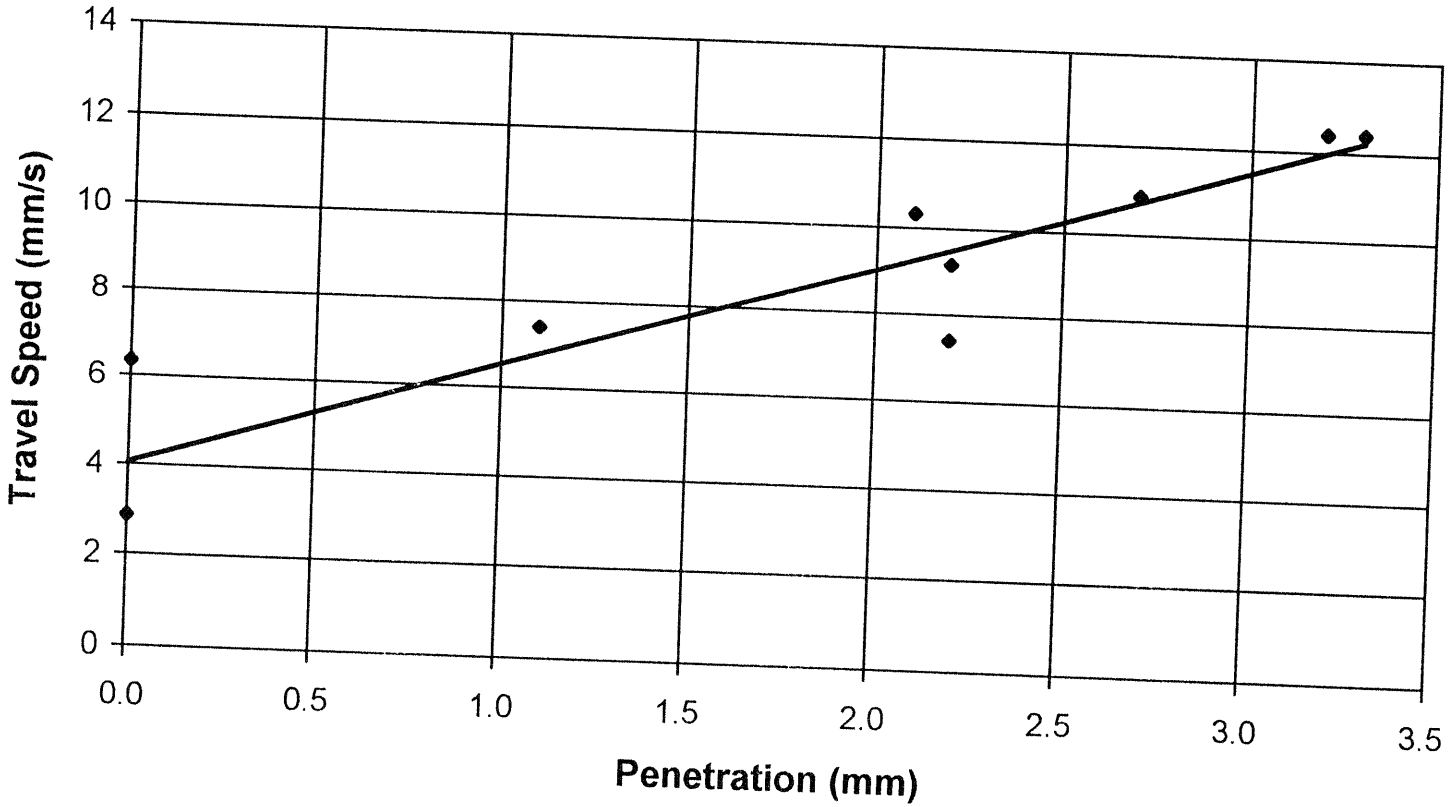

FIGURE 6.3 Welding Machine Travel Speed vs. Weld Penetration

Table 6.1 Weld Parameter Data Showing Effect of Deeper Penetration on Deposition Rate and Specific Energy

TEST	Steel	FCAW	AMP	Volt	PEN (mm)	LEG (mm)	Feed (mm/s)	TRAVEL (mm/s)	Deposition Rate (mm^3/s)	Specific Energy (Joule/mm)
1	EH36	Excel-Arc 71	170	23.0	0	6.5*6.5	84.67	2.88	60.81	1358.27
2			230	26.0	0	6.6*6.7	169.33	6.35	140.40	941.73
3			270	27.0	1.1	7.0*7.0	211.67	7.41	181.50	984.03
4			300	31.0	2.2	7.2*7.2	254.00	9.19	238.11	1012.37
5			330	32.0	2.7	6.6*6.8	296.33	10.88	244.14	970.62
6			350	33.0	3.2	6.9*6.6	338.67	12.40	282.43	931.18
7*			330	33.5	2.1	7.8*7.5	296.33	10.33	302.13	1070.25
8	DH36	Fabco 802	160	23.0	0	5.8*6.0	84.67	2.88	50.09	1278.37
9			260	27.0	2.2	7.1*6.3	211.67	7.41	165.69	947.58
10			350	33.0	3.3	5.6*6.3	338.67	12.40	218.80	931.18

Note: Penetration is based on the depth of permeation regardless of porosity/slag inclusions.
Leg Length is based on the total leg length including porosity/slag inclusions.
* Test 7 had the welding electrode positioned 2.5 mm above the joint.

CHAPTER 7

CONCLUSIONS & RECOMMENDATIONS

7.1 Conclusions

1. The main conclusion is that deeper penetrating fillet welds experimentally developed could be made stronger, tougher, faster, and with less specific energy than welds without penetration.

2. A survey of ship manufacturers determined that automated welding of fillet welds is predominantly Flux Cored Arc Welding (FCAW).

3. Changing fillet weld parameters without beveling can achieve deeper penetrations than are currently being used for fillet welds in ships. With 6 mm leg lengths, fillet weld penetrations of 4 mm can be achieved by varying weld parameters; current having the largest effect. Tests with weld parameters recommended by the electrode manufacturer gave a penetration of 1.1 mm.

4. Weld penetration significantly increases the strength of fillet welds loaded in tension. Tension and peeling failure do occur in grounding of ships built with existing design standards. Fillet welds of stiffeners must have a T-joint strength equivalent to the web in order to prevent failure of welds in tension loading. In the peeling mode of failure the weld tearing work must be larger than the complementary work required to fold the hull plate in order to prevent weld failure. Testing on 6 mm leg length welds (Excel-Arc 71) showed an increase of 63% in the tensile strength with penetrations increasing from 0 to 3.2 mm. The weld strength increased 50% from the 1.1 mm penetration with the parameters recommended by the manufacturer to the 3.2 mm penetration achieved by altering weld parameters. Fabco 802 electrode showed an increase in weld tensile strength of 37% with a 3.3 mm increase in penetration.

5. The fillet weld tensile strength for the deepest penetrating weld of 3.2 mm (Excel-Arc 71) matches a 14 mm web thickness strength for the EH36 plate.

6. Theoretical predictions of the limit load based on measured hardness values showed an overprediction of tensile strength with deeper penetrations by up to 40% to 50%. This shows that the upper bounds for welds with deeper penetration need to be improved, perhaps by admitting yielding to the base or web material.

7. The manufacturers' tensile strengths from multi-pass welds differed from those estimated from the hardnesses of single pass welds used in testing. This was especially so for deeper penetrating welds; perhaps due to cooling rate. Deeper penetrating welds showed an increase in the hardness of the welds by 30% to 40%. Results of hardness tests showed that the weld material is not homogeneous.

8. Deeper penetration welds appear to be an inexpensive way to increase fillet weld joint strength. Penetration increases the joint strength without adding weld material and avoids the cost of beveling the plate. Deposition rate increases for deep penetrating welds due to the higher feed speeds in FCAW. Welding for 3.2 mm penetration gave a 70% increase in the deposition rate as compared to manufacturer recommended welding parameters producing 1.1 mm penetrations. The energy per unit length needed to weld a 3.2 mm penetration decreased by 5% as compared to that for the 1.1 mm penetration.

7.2 Recommendations

1. A finite element analysis should be performed on welds with inhomogeneous weld material properties. Inhomogeneous welds and overmatched weld material may be shifting the plastic deformation zone away from the paths assumed by the upper bound and slip line theoretical solutions shown in this thesis. FEA would lead to better understanding of the limit load in tension loading for inhomogeneous welds.

2. The determination of the yield strength of a weld in shear needs to be better approximated. A more detailed use of Vickers Hardness testing of the weld material and heat affected zone would lead to a better approximation of the yield strength of the material. A combination of machined tension test specimens and hardness test samples may lead to a better understanding of the strength properties of the weld material.

3. In the design of tension test specimens with 6 mm leg lengths, at least 50 mm should be removed from the weld ends in order to give a uniform penetration for test specimens.

4. Welding electrode manufacturers should give estimates for the depth of penetration possible for electrodes at specified welding parameters for some appropriate steels.

5. The effect of root gap on weld penetration and strength should be examined. Ship design standards do not require stiffeners to fit tightly against the hull without a gap. Increasing the root gap may lead to deeper penetrations as well as stronger and tougher joints.

6. Implementation of deeper penetrating weld parameters should be considered by the classification societies and ship builders. The potential reduction in welding cost and increase in joint strength should give incentive to build ships with deeper penetration. The use of automated welding systems allows for good reproduction of welds using specified parameter settings.

References

American Bureau of Shipping, Rules for the Approval of Electrodes for Manual Arc Welding in Hull Construction, 1965, p. 11.

American Bureau of Shipping, Rules for Building and Classing Steel Vessels, 1993, Parts 2 & 3.

Annual Book of ASTM Standards, Metals-Mechanical Testing; Elevated and Low-Temperature Tests; Metallography, 1992, v 3.01, p. 469.

Annual Book of ASTM Standards, Steel-Bars Forgings, Bearing, Chain, Springs, 1993, v 1.05, pp. 175-193.

Askeland, D., The Science and Engineering of Materials, Boston, Massachusetts: PWS-Kent Publishing Company, 1984, pp. 129, 144, 382.

Blodgett, O., Design of Welded Structures, Cleveland, Ohio: The James F. Lincoln Arc Welding Foundation, 1975, p. 1.1-3.

Brooks, C., Weld Strength and Crack Growth Ductility from the Lazy-L Test, M.Sc. Thesis, Department of Mechanical Engineering, M.I.T., 1995.

Bureau Veritas, Rules and Regulations, 1980, p. 9-15.

Chakrabarty, J. , Theory of Plasticity, McGraw Hill Book Company, 1987, pp. 407-453.

Davies, A., The Science and Practice of Welding: Volume 1, Tenth Edition, Cambridge, England: Cambridge University Press, 1992, pp. 275-279.

Debbink, M., Newport News Shipbuilding, correspondence, 1995.

Eftring, N., Leeide, N., Ronn, L. and C. Rosendahl, High Tensile Steel in Shipbuilding III, Sweden: The Swedish Ship Research Foundation, 1973, pp. 15-20.

Extreme Loads Response Symposium: Sponsored by The Ship Structure Committee and The Society of Naval Architects and Marine Engineers, 1981, pp 125-131

Gaines, E., "Designing Partial-Penetration Tee Joints for Naval Ships", Journal of Ship Production, Vol. 6, No. 1, Feb. 1990, pp. 27-34.

Guerra, A. and F. A. McClintock, Joint MIT-Industry Program on Tanker Safety Upper Bounds to the Tensile Limit Loads of Cracked Welded T-Joints, 1994.

Hicks, J., Welded Joint Design, New York, New York: Halsted Press, 1979, ch.7.

Johnson, W., Sowerby, R. and R. Venter, Plane Strain Slip Line Fields for Metal Deformation Processes, New York, New York: Pergamon Press, 1982, ch 6.

Kato, B., and K. Morita, "Strength of Transverse Fillet Welded Joints", *Welding Journal*, 1974, v53, pp.59-64.

Kirkov, K. D., Tearing Resistance for Fillet Welds in Ships Exposed to Grounding - A Full Scale Test and Cost Implications, M.Sc. Thesis, Department of Ocean Engineering, M.I.T., 1994.

Koga, S., Kawasaki Heavy Industries, correspondence, 1995.

Koo, J., Welding Metallurgy of Structural Steels, Annandale, New Jersey: The Metallurgical Society, 1987, pp. 383 & 483.

Krumpen, R. P. and C. R. Jordan. "Updating of Fillet Weld Strength Parameters for Commercial Shipbuilding", SSC-323, 1984.

Leide, N., Rosendahl, C. and L. Rohn, High Tensile Steel in Shipbuilding, Sweden: The Swedish Ship Research Foundation, 1975, ch 4.

Lloyd, G., Rules for the Classification and Construction of Seagoing Steel Ships, Germany: Germanischer Lloyd, 1983, pp. 7-7, 9-8, 9-9.

Lloyd's Register, Rules and Regulations for the Classification and Construction of Ships, 1992.

Llyod's Register of Shipping, Rules for the Manufacture, Testing and Certification of Materials, 1984, ch. 11: pp.11-13.

Marks' Standard Handbook for Mechanical Engineers, 1987, Ninth Edition, pp. 5-13, 6-27.

Masubuchi, K., Design and Fabrication of Welded Ships, Columbus, Ohio: Batelle Memorial Institute, 1968.

Masubuchi, K., Koga, S., and McDonald, H., "Present Status of V.L.C.C. Welding Procedures in Japan", Welding Systems Laboratory, M.I.T., 1993.

McClellan, R., Ingalls Shipyard, correspondence, 1994.

McClintock, F., Fully Plastic Mechanics for Welded T-Joints, Joint MIT-Industry Program on Tanker Safety, Report 26, 1994.

MIL-STD-1628A, Military Standard Fabrication, Welding, and Inspection of Ships Structures.

MIL-STD-1689A, Military Standard Fillet Weld Size, Strength, and Efficiency Determination.

Nippon Kaiji Kyokai, Rules and Regulations for the Classification and Construction of Ships, 1986.

Ship Structure Committee, "Review of Fillet Weld Strength Parameters for Shipbuilding", SSC-296, 1980.

Ship Structure Committee, "Survey of Structural Tolerances in the United States Commercial Shipbuilding Industry", SSC-273, 1978.

Sueoka, H., Mitsubishi, Heavy Industries, LTD., correspondence, 1995.

Taggart, R., Ship Design and Construction, New York, New York: The Society of Naval Architects and Marine Engineers, 1980, pp. 341-367.

Taylor, D, Merchant Ship Construction, Second Edition. England: Butterworth & Co., Ltd., pp. 67-71.

Technical and Research Bulletin No. 2-19, "Higher-Strength Steels in Hull Structures", New York, New York: The Society of Naval Architects and Marine Engineers, 1971.

Technical & Research Bulletin 2-20, "Guide for High Strength and Special Application Steels for Marine Use", New York, New York: The Society of Naval Architects and Marine Engineers, 1976, pp. 7-9.

Terai, K., Present Status of Welding in Shipbuilding, 1970, pp. 46-50.

Welding & Fabrication Data Book, Penton Publishing, 1988/1989.

Welding Handbook, Volume 1, Eighth Edition, Miami, Florida: American Welding Society, 1987.

Welding Handbook, Volume 2, Eighth Edition, Miami, Florida: American Welding Society, 1987.

Young, W., Roark's Formulas for Stress & Strain: Sixth Edition, New York, New York: McGraw-Hill, Inc., 1989.

APPENDIX A

Navy Design of Fillet Welds

APPENDIX A
NAVY DESIGN OF FILLET WELDS

Although the Navy does not design VLCC ships, the considerations and theory used in the weld design are the same. MIL-STD-1628A (Ships) provides guidelines for fillet weld size, strength, and efficiency determination. The standard is approved for use by all agencies in the Department of Defense. The Navy has recently changed its design standards for fillets welds without penetration to meet the design presented by Krumpen and Jordan (1984). An extension of the design considerations for bevel-edged tee joints (deeper penetration) has been researched and is pending approval for a military standard (Gaines, 1994).

For welds without penetration the following design equations are used based on fracture in the weld, fracture in the heat affected zone (HAZ) of the intercostal (web) member, and fracture in the HAZ of the continuous member. The joint strength determination depends on the loading direction, weld failure region, and the comparison of weld strength to either the strength of the continuous or intercostal (web) member. For stiffeners the intercostal will typically be weaker than continuous member (hull) when loaded in tension (transversely). The formulas for determining weld size for the relevant conditions of matching weld strength to intercostal strength (100% efficiency) in transverse loading are:

S = leg length of fillet weld

R_1 = tensile strength of intercostal member

T_1 = thickness of intercostal plate

R_4 = transverse shear strength of weld = 1.44 X (longitudinal shear strength of weld)

R_3 = shear strength of intercostal member

R_5 = tensile strength of continuous member

Failure Region	Leg Length Required
Weld throat (45 degree plane)	$S = \frac{R_1 \times T_1}{1.414 \times R_4}$
HAZB (Intercostal Member)	$S = \frac{R_1 \times T_1}{2.2 \times R_3}$
HAZB (Continuous Member)	$S = \frac{R_1 \times T_1}{2.0 \times R_5}$

For symmetric fillet welds with penetration the MIL-STD-1628A approximates the strength based on an equivalent throat thickness determination of the weld joint. The standard is used for the construction of partial penetration welds from beveled plate. The design of the welds are based on equating the tensile strength of the weaker joint member to the longitudinal shear strength of the fillet weld. This results in conservative designs since the strength of welds transversely has been determined to be larger than the longitudinal strength as shown by Krumpen and Jordan (1984). The current standard design equations from MIL-STD-1628A are as follows:

D = effective width of the weld in shear

e = joint efficiency required

R_1 = tensile strength of intercostal member (if the weaker member)

T_1 = thickness of intercostal plate

R_2 = longitudinal strength of fillet weld

Z = land width

S = size of reinforcing fillet (must be at least .25 in)

$$D = \frac{e \times T_1 \times R_1}{2 \times R_2} \qquad \text{(A.1)}$$

$$B = \frac{D}{1.414} \qquad (\text{if } D < .707 \text{ in}) \qquad \text{(A.2)}$$

$$B = \sqrt{D^2 - .25} \qquad (\text{if } D > .707 \text{ in}) \qquad \text{(A.3)}$$

The existing criterion for beveled welds has been shown to be conservative and a proposal for a new design method has been introduced by Gaines (1990). The proposal by Gaines builds upon the alternate design method shown in Krumpen and Jordan (1984) to include fillet welds that are deeper penetrating due to beveling the intercostal plate under both longitudinal and transverse loading. The design for failure in the heat affected zone of the continuous plate (transverse loading) is based on the continuous member tensile strength times the total length of the heat affected zone boundary. For failure across the weld throat the strength of the weld is the transverse shear strength times the total throat failure length. Crack failure of the weld along the heat affected zone of the intercostal plate is calculated from Mohr's circle to find when the maximum shear strength of the weld is less than the shear strength of the intercostal member. Weld joint strength calculated for different locations in the weld and heat affected zone area are calculated as follows:

R_1 = tensile strength of intercostal member

T_1 = thickness of intercostal plate

R_4 = transverse shear strength of weld = 1.44 X (longitudinal shear strength of weld)

R_3 = shear strength of intercostal member

R_5 = tensile strength of continuous member

efficiency = weld joint efficiency required

HAZB = approximated length of the heat affected zone boundary

Failure Region	Leg Length Required
Weld throat (45 degree plane)	$T_1 < \frac{(R_4 \times \text{throat length})}{(R_1 \times \text{efficiency})}$
HAZB (Intercostal Member)	$T_1 < \frac{(\text{HAZB length} \times R_3)}{\text{efficiency} \times \sqrt{(\text{Cos}(\theta_{AH})/2)^2 + (\sin(\theta_{AH})^2}}$
HAZB (Continuous Member)	$T_1 < \frac{(\text{HAZB length} \times R_5)}{(R_1 \times \text{efficiency})}$

APPENDIX B

Solving for Slip-Line Fields

Chapter 3 Rate Independent Plasticity, cont.

3.4 Stress and Deformation Analysis in Plasticity, cont.

Art. 5 Slip-Line Fields

1. Introduction. Practically important and exact solutions to the plasticity equations can be found by considering plane strain ($\epsilon_{zz} = 0$ and no gradients, $\partial(\ )/\partial z = 0$) and by neglecting both the elastic part of the strain and strain-hardening. Such solutions, satisfying all the principles of continuum mechanics throughout a plastically deforming region, may still not be correct. Why? Because the remaining material, assumed non-yielding, may in fact be unable to remain so. After all, a lower bound has not been shown there. Therefore, plane strain slip-line fields in general give only upper bounds to the limit load.

2. Stress Fields. With this background, turn to pp. 375-378 of McClintock and Argon and pp. 67-70 and p. 130 in McClintock (1971) "Plasticity Aspects of Fracture" in Fracture, V.3, H. Liebowitz, ed., pp. 147-225. Methods of solving these equations are summarized below.
ALSO REFERENCE: CHAKRABARTY, J., THEORY OF PLASTICITY, 1987, pp. 407-453.

a) Steps for solving for stress in a given plane strain, plastic slip-line field. Inventing a slip-line field for a given problem is a matter of experience, guided by some of the mathematical characteristics of slip-line fields, and by experiments with etched high-nitrogen steel or finite-element programs Here, we assume that a proposed slip-line field is given, and apply the above equations of plasticity to verify that the field is valid and to find the resulting fields, first of stress and later of displacement and strain. The stress analysis of a given slip-line field can be codified in the following steps.

1) Sketch the slip-line field on a large enough sheet of paper so

that in each region you can sketch and label: i) stresses on elements of various orientations. ii) Mohr's circles. iii) mean normal stress σ, iv) slip-line coordinates α, β and orientations ϕ, and later v) velocities u, v relative to slip-lines.

2) Start at a point on a presumably deforming free boundary.

3) For an element at that point, having one face as the free boundary ($\sigma_{nn} = 0$), guess a stress σ_{ss} that is tension or compression parallel to the boundary.

4) Sketch the stress on that element. Calculate the mean in-plane normal stress σ.

5) Sketch Mohr's circle for that element.

6) Find on Mohr's circle the α, β axes (of maximum shear stress with the algebraically maximum principal stress 45^0 (90^0 on Mohr's circle) CCW from α toward β). Find the n, s axes (normal and tangential to boundary), and the x, y axes. Find the counter-clockwise angle 2ϕ from the x axis to the α direction. Sketch elements aligned with the α, β, the x, y, and the principal stress directions.

7) From this Mohr's circle, find the α, β and the principal stress axes on the physical plane.

8) Repeat at other points on presumably deforming free boundaries until all slip-lines are identified as either α or β lines, and σ and ϕ are calculated for all boundary regions. Note regions of constant state (having the same σ and ϕ along a boundary).

9) Having identified the α and β lines, integrate the Hencky equations for the stresses along them ($d\sigma = 2k d\phi$ along an α line, $d\sigma = -2k d\phi$ along a β line), using the values of σ and ϕ on each boundary as initial conditions. Constant state regions along the boundary integrate inward as constant state triangular regions in the interior.

10) If at any stage you think the guess of tension or compression is wrong, (e.g. because some fact you know to be true is contradicted), change the guess and start over. That is mostly just changing signs. Don't try to follow both guesses at the same time.

3. Displacement and strain fields. The slip-line field for stress in plane-strain, non-hardening plasticity satisfies the yield criterion and equilibrium equations. This provides three equations for the three in-plane components of stress. If the only boundary conditions were to consist of applied tractions, the stress would be uniquely defined in any deforming region. The magnitude of the deformation would be indeterminate, however. Physically, this can be seen in the tensile test. Too high a load will cause an accelerating extension of the specimen, whereas an applied extension, controlled in a testing machine by the lead screws or by the flow of oil to the cylinder, can give stable extension even with falling load. Therefore, for stability, at least some displacement boundary conditions must be specified. Displacement conditions are also applied by the surroundings to parts of a redundant, fail-safe structure. The strains derived from the corresponding displacements must be consistent with the stress-strain relations and the postulated stress field. Thus it may be necessary to find displacements to confirm a stress field (see also Hill, 1950, p. 131). Furthermore, displacements and strains are often of importance in their own right, for example in fracture by hole growth, in crack growth in fatigue, or in metal working processes. It must be remembered, however, that the strain distribution may not be unique in a low-hardening material. For example, at incipient necking, a specimen can neck anywhere along its length.

a) Fundamental equations. As with the stress distribution, in plane-strain, rigid-plastic non-hardening plasticity it is easiest to use coordinate axes of maximum shear for strain and displacements. To assure compatibility, we work with the displacements. It then remains to find displacement fields that give incompressible strains.

The conditions of incompressibility, expressed in terms of the displacements referred to the curvilinear coordinates giving maximum shear, are known as the Geiringer equations (e.g. Hill, 1950, pp. 128-136; McClintock and Argon, 1966, pp. 375-378; McClintock, 1971, pp. 67-70; Mendelson, 1970, pp. 260-268). The notation is shown in Fig. 1. The coordinates of maximum shear stress, α, β, are chosen so that the direction of maximum principal stress and strain lies between them. The

angle ϕ is positive counterclockwise from the x to the α direction. Displacement increments or "velocities" in the α, β directions are denoted by u and v, respectively. The Geiringer equations of incompressibility are then

$$\text{along an } \alpha \text{ line}, \quad du = v\,d\phi \quad , \tag{1a}$$

$$\text{along a } \beta \text{ line}, \quad dv = -u\,d\phi \quad . \tag{1b}$$

Solution of the Geiringer equations is generally started at some point in the body where rigid regions or boundary conditions provide information on u and v along each of two intersecting slip-lines. Integration proceeds outward from that point, as will be summarized below.

Once the displacements are known, the strains can be found from the strain-displacement relations. For the curvilinear α, β coordinates, the expression involves the radii of curvature R,S along the α, β slip-lines, respectively, as shown in Fig. 2:

$$\frac{1}{R} = \frac{\partial \phi}{\partial s_\alpha} \quad , \quad \frac{1}{S} = -\frac{\partial \phi}{\partial s_\beta} \quad . \tag{2a,b}$$

It is an indication of the relative youth of plasticity as a branch of mechanics that the strain-displacement equation was only stated by Green in 1953 (see also McClintock, 1971, p. 130). It is

$$\gamma_{\alpha\beta} = \frac{\partial v}{\partial s_\alpha} + \frac{u}{R} + \frac{\partial u}{\partial s_\beta} + \frac{v}{S} \quad . \tag{3}$$

As R and S increase, the form for Cartesian coordinates can be recognized.

The strain in x, y coordinates can be obtained from Mohr's circle:

$$\gamma_{xy} = \gamma_{\alpha\beta} \cos 2\phi \quad ,$$

$$\epsilon_{xx} = -(\gamma_{\alpha\beta}/2) \sin 2\phi = -\epsilon_{yy} \quad . \tag{4}$$

b) Summary of procedure.

1) Look for any slip-lines with no displacement components specified on either end. If there are any such lines, remove the resulting non-uniqueness by assigning displacements at some point along them, often keeping the strain relatively uniform by assuming uniform displacement gradients across bands of lines with such non-unique displacements.

2) Look for a point where both components of displacement are known, either from adjoining rigid material on two sides, or from the assumptions of Step 1.

3) Starting from the point of Step 2, integrate Eq. 1a or 1b, as appropriate, on the slip-lines along any rigid-plastic boundaries. It may be convenient to fix local coordinates in the rigid region, and later to add in the displacements of these local coordinates relative to the global ones.

4) Integrate the Geiringer equations (1a, 1b) along lines normal to any rigid-plastic boundary.

5) Find the radii from Eqs. 2 and the strain from Eq 3.

c) Numerical integration. For numerical intergration, the corners of the element are denoted by pairs of subscripts, as shown in Fig. 3. With displacements known along two intersecting sides (three nodes) of the element, those at the fourth node, u_{22}, v_{22}, are found by simultaneously solving the Geiringer equations (1a, b) in the form

$$\text{along an } \alpha \text{ line}, \quad u_{22}-u_{12} = .5(v_{22}+v_{12})(\phi_{22}-\phi_{12}) \quad , \qquad (1c)$$

$$\text{along a } \beta \text{ line}, \quad v_{22}-v_{21} = -.5(u_{22}+u_{21})(\phi_{22}-\phi_{21}) \quad . \qquad (1d)$$

For the radii of curvature, a trigonometric function is retained for improved accuracy with large angular increments and chordal measurement of

ΔS_α , ΔS_β :

$$\frac{1}{R} = \frac{\partial \phi}{\partial s_\alpha} \approx \frac{\sin((\phi_{21} - \phi_{11})/2)}{\Delta s_\alpha/2} \quad , \tag{2c}$$

$$\frac{1}{S} = -\frac{\partial \phi}{\partial s_\beta} \approx -\frac{\sin((\phi_{12} - \phi_{11})/2)}{\Delta s_\beta/2} \quad . \tag{2d}$$

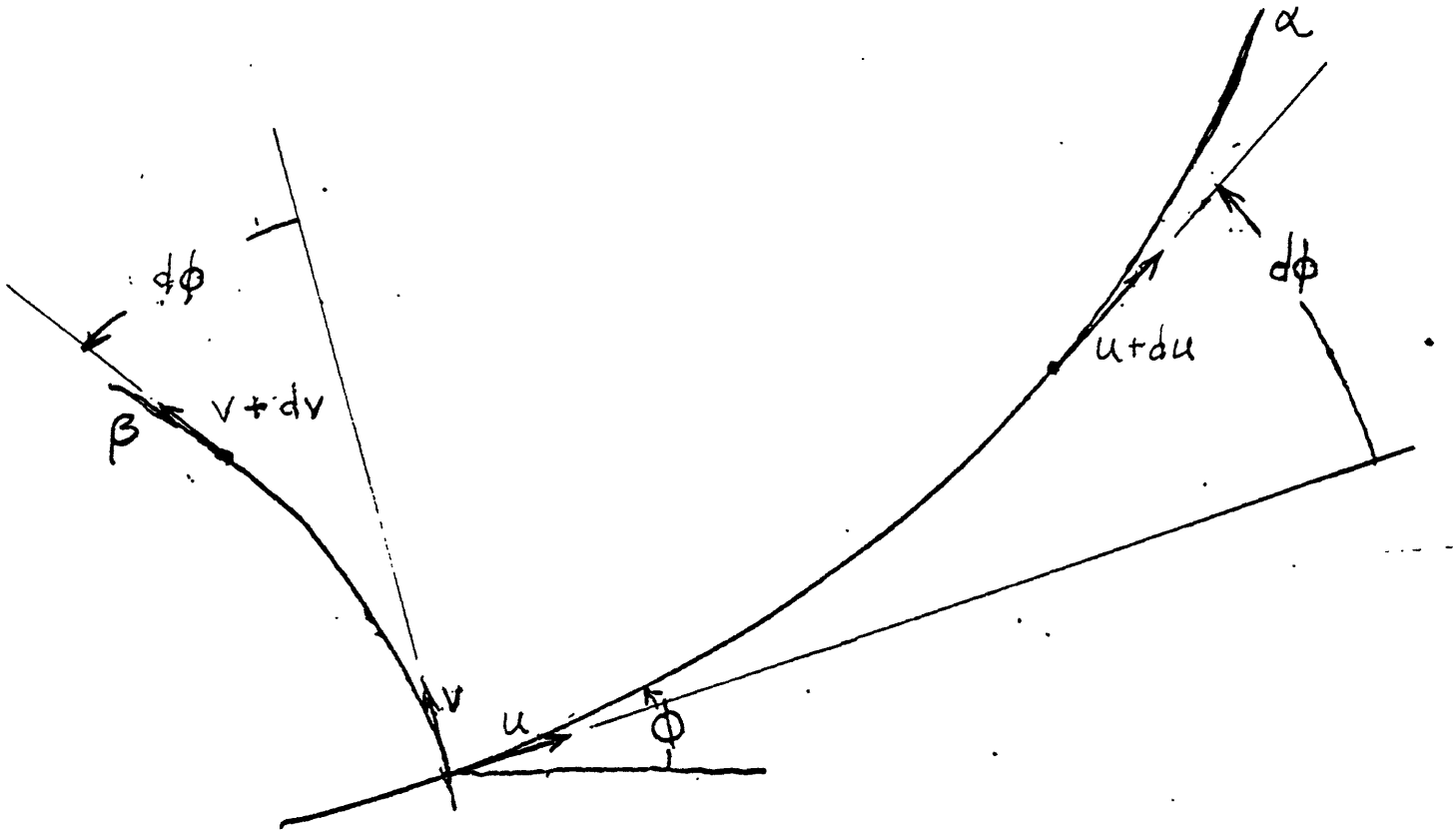

Fig. 1 Notation for the Geringer equations: along α , $du = v d\phi$; along β , $dv = - u d\phi$

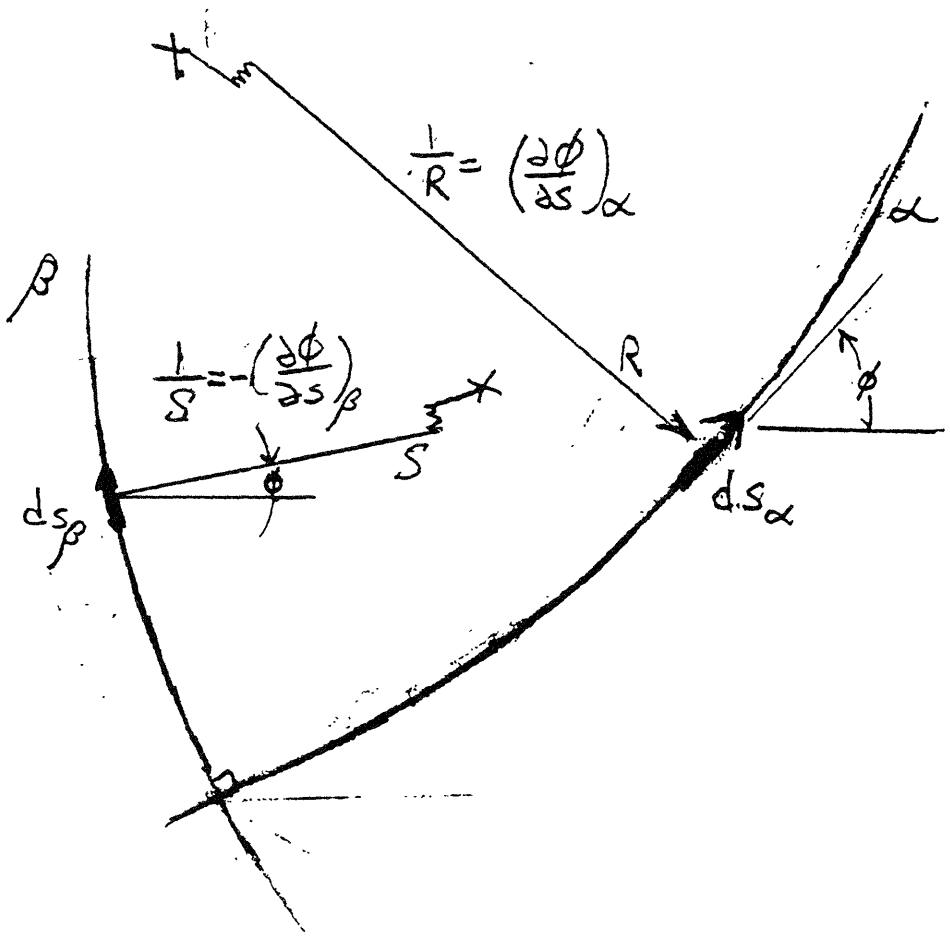

Fig. 2 Curvatures 1/R and 1/S of α and β slip-lines.

Probs. for Sec. 3.4, Stress and Deformation Analysis in Plasticity, cont.

Art. 5 Slip-Line Fields

1. Rigid-plastic, plane strain plasticity.

Determine the stress, displacement, and strain fields for the grooved plate shown in Fig. (a), with one non-zero flank angle.

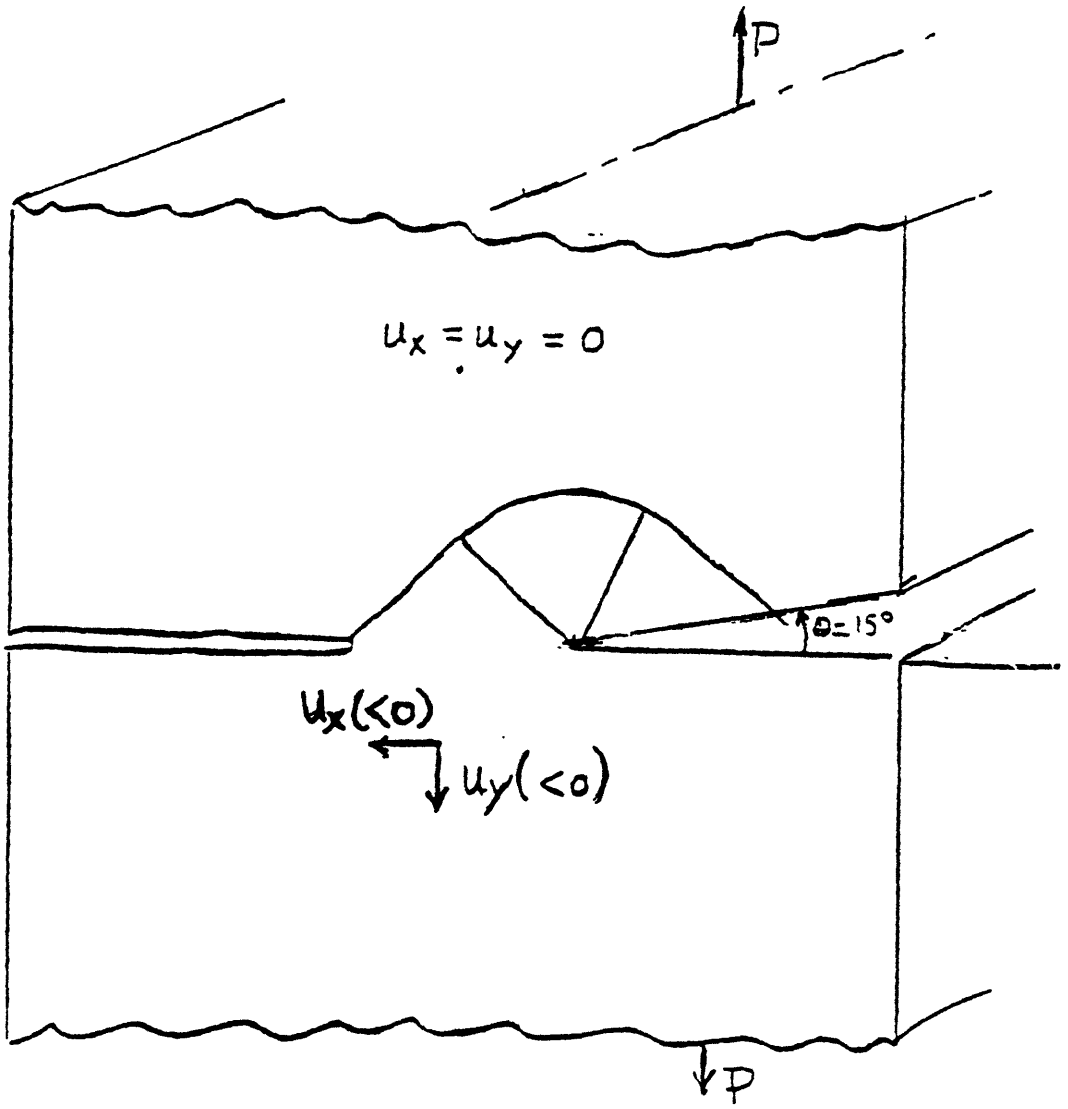

Fig a) Asymmetrically grooved plate. (The angle θ causes the asymmetry)

2. Slip-line fields for allowable specimen hardness for wedge grips. In using wedge grips for tension tests it is important that the hardness of the test specimen, say the diamond pyramid hardness HDP_s in kgf/mm^2, be enough lower than that of the teeth of the wedge grips, HDP_t, so that even if the teeth have become somewhat dulled, the specimen, but not the teeth, will deform. Consider the slip-line field of Fig. (a).

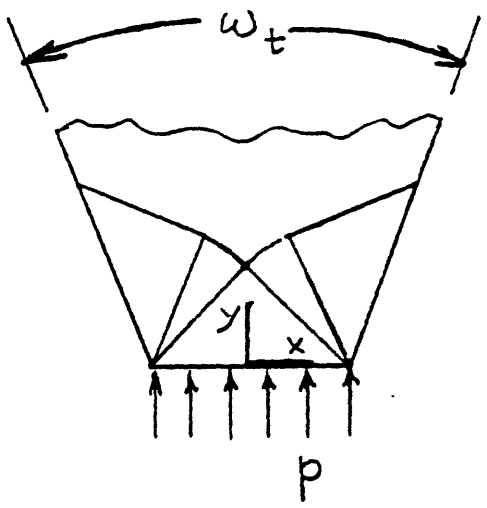

Fig. a) Slip-line field for blunting of a tooth of wedge grips.

a) Derive an upper limit to HDP_s/HDP_t in terms of ω_t

b) Evaluate your expression for $\omega_t = 45^\circ$.

3. Slip-line field for a micro-junction in frictional contact.

a) Show that the slip-line field shown in Fig. a), for a junction under combined shear and normal force, satisfies the equilibrium and compatibility equations within the deforming region.

b) How would you show that this stress field is exact for a non-strainhardening material?

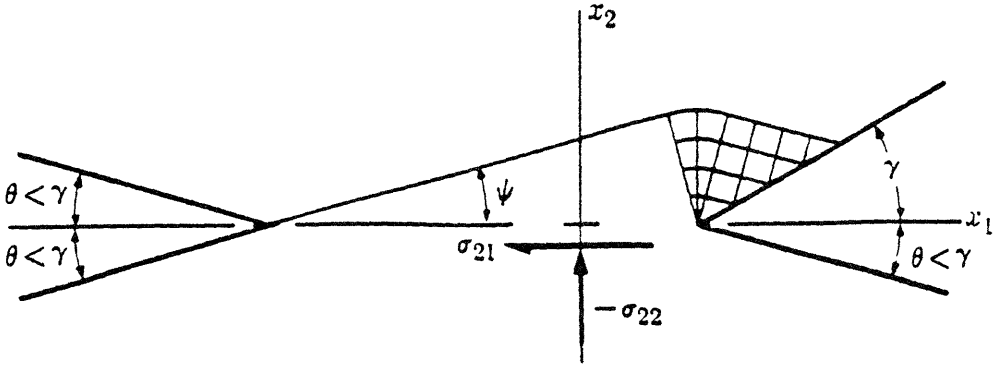

Fig. a) Slip-line field for a junction under combined shear and normal forces.

APPENDIX C

Slip-Line Method for Determining Weld Limit Loads in Tension

APPENDIX C

SLIP LINE METHOD FOR DETERMINING WELD LIMIT LOADS IN TENSION

The following calculations are used to interpolate the slip line field solution solved by Chakrabarty (1987) and shown in Table 3.1. The slip line solution is described in Chapter 3.3.

$i := 0..3$

β=10 DEG

α1= The α value in degrees when β=10 degrees.
X1= The x/a value for a given α and β value.
Y1= The y/a value for a given α and β value.
P1= The P/2ka value for the given condition of α and β intersection .
Q1= The Q/2ka value for the given condition of α and β intersection.

$$\alpha 1 = \begin{bmatrix} 0 \\ 10 \\ 20 \\ 30 \end{bmatrix} \quad X1 := \begin{bmatrix} 1.15846 \\ 1.38332 \\ 1.57730 \\ 1.73236 \end{bmatrix} \quad Y1 = \begin{bmatrix} .18884 \\ 0 \\ -.23137 \\ -.50019 \end{bmatrix} \quad P1 = \begin{bmatrix} .437652 \\ .5 \\ .49545 \\ .40827 \end{bmatrix} \quad Q1 = \begin{bmatrix} .60777 \\ .76067 \\ .96049 \\ 1.189 \end{bmatrix}$$

$$F(\alpha) = \begin{bmatrix} 1 \\ \alpha \\ \alpha^2 \end{bmatrix}$$

F(α) expresses the functions that are combined linearly to give the best curve fit to the data.

$Sx = \text{linfit}(\alpha 1, X1, F)$

$$Sx = \begin{bmatrix} 1.15806 \\ 0.02439 \\ -1.745 \cdot 10^{-4} \end{bmatrix}$$

The set Sx is the coefficients for the functions expressed above for the curve fit data X(α).

$Sy = \text{linfit}(\alpha 1, Y1, F)$

$$Sy = \begin{bmatrix} 0.18909 \\ -0.01699 \\ -1.9995 \cdot 10^{-4} \end{bmatrix}$$

The set Sy is the coefficients for the functions expressed above for the curve fit data Y(α).

To find the intersection of the equations X(α), Y(α), and Y=X-A:

Guess values: $X1 = 1$
$Y1 = 1$
$\alpha = 2$
Starting points for computer iteration.

Given

$Sy_0 + Sy_1 \cdot \alpha + Sy_2 \cdot \alpha^2 = Y1$ Eqn 1: Y(α)

$Sx_0 + Sx_1 \cdot \alpha + Sx_2 \cdot \alpha^2 = X1$ Eqn2: X(α)

$X1 - 1 = Y1$ Eqn 3: Y(X)

$$\begin{pmatrix} X1val \\ Y1val \\ \alpha val \end{pmatrix} = Find(X1, Y1, \alpha)$$ Solve for three unknowns.

Results for β=10 deg:

$X1val = 1.17625$
$Y1val = 0.17625$
$\alpha val = 0.74972$
Solutions for three unknowns.
Relation of X,Y,α,β, along penet. line.

To interpolate the values for P and Q:

$vp = lspline(\alpha 1, P1)$
$vq = lspline(\alpha 1, Q1)$
Gives a curve fit for P(α) and Q(α)

$interp(vp, \alpha 1, P1, \alpha val) = 0.44325$ P1/2ka=.44325 Along β=10 deg.

$interp(vq, \alpha 1, Q1, \alpha val) = 0.61844$ Q1/2ka=.61844

Adding in the uniform pressure for the weld case:

$Qw = interp(vq, \alpha 1, Q1, \alpha val) + .5 \cdot X1val$

$Pw = interp(vp, \alpha 1, P1, \alpha val) - (.5 - .5 \cdot Y1val)$

$Qw = 1.20657$ Q/2ka
$Pw = 0.03137$ P/2ka

To determine the equivalent depth of penetration:

$$xg1 := \sqrt{2}\cdot(X1val - 1)$$

$$xg1 = 0.24925$$

xg = XG(penetration)/a.

The force along the slipline in the Plimit direction:

$$P1limit := Pw\cdot\cos\left(\frac{\pi}{4}\right) + Qw\cdot\cos\left(\frac{\pi}{4}\right)$$

$$P1limit = 0.87535$$

Plimit= Pl(weld strength)/2ka

β=20 DEG

α2= The α value in degrees when β=20 degrees.
X2= The x/a value for a given α and β value.
Y2= The y/a value for a given α and β value.
P2= The P/2ka value for the given condition of α and β intersection .
Q2= The Q/2ka value for the given condition of α and β intersection.

$$\alpha 2 = \begin{bmatrix} 0 \\ 10 \\ 20 \\ 30 \end{bmatrix} \quad X2 = \begin{bmatrix} 1.28171 \\ 1.57730 \\ 1.85262 \\ 2.09558 \end{bmatrix} \quad Y2 = \begin{bmatrix} .40233 \\ .23173 \\ 0.00 \\ -.28998 \end{bmatrix} \quad P2 = \begin{bmatrix} .43223 \\ .50455 \\ .5 \\ .3929 \end{bmatrix} \quad Q2 = \begin{bmatrix} .746238 \\ .96049 \\ 1.24397 \\ 1.57921 \end{bmatrix}$$

$$F(\alpha) := \begin{bmatrix} 1 \\ \alpha \\ \alpha^2 \end{bmatrix}$$

F(α) expresses the functions that are combined linearly to give the best curve fit to the data.

$$Sx := linfit(\alpha 2, X2, F)$$

$$Sx = \begin{bmatrix} 1.28111 \\ 0.03112 \\ -1.31575\cdot 10^{-4} \end{bmatrix}$$

Sx is the coefficients for the functions expressed above for the curve fit data X(α).

$$Sy := linfit(\alpha 2, Y2, F)$$

$$Sy = \begin{bmatrix} 0.40247 \\ -0.01413 \\ -2.9845\cdot 10^{-4} \end{bmatrix}$$

Sy is the coefficients for the functions expressed above for the curve fit data Y(α).

To find the intersection of the equations X(α), Y(α), and Y=X-A:

Guess values: $X2 := 1$ $Y2 := 1$ $\alpha := 2$ Starting points for computer iteration.

Given

$Sy_0 + Sy_1 \cdot \alpha + Sy_2 \cdot \alpha^2 = Y2$ Eqn 1: Y(α)

$Sx_0 + Sx_1 \alpha - Sx_2 \cdot \alpha^2 = X2$ Eqn2: X(α)

$X2 - 1 = Y2$ Eqn 3: Y(X)

$$\begin{pmatrix} X2val \\ Y2val \\ \alpha 2val \end{pmatrix} := \text{Find}(X2, Y2, \alpha)$$ Solve for three unknowns.

Results for β=20 deg:

$X2val = 1.36344$

$Y2val = 0.36344$ Solutions for three unknowns.

$\alpha 2val = 2.61711$ Relation of X,Y,α,β, along penet. line.

To interpolate the values for P and Q:

$vp := \text{lspline}(\alpha 2, P2)$

$vq := \text{lspline}(\alpha 2, Q2)$ Gives a curve fit for P(α) and Q(α)

$\text{interp}(vp, \alpha 2, P2, \alpha 2val) = 0.45449$ P2/2ka=.45449 Along β=20 deg.

$\text{interp}(vq, \alpha 2, Q2, \alpha 2val) = 0.79865$ Q2/2ka=.79865

Adding in the uniform pressure for the weld case:

$Qw := \text{interp}(vq, \alpha 2, Q2, \alpha 2val) + .5 \cdot X2val$

$Pw := \text{interp}(vp, \alpha 2, P2, \alpha 2val) - (.5 - .5 \cdot Y2val)$

$Qw = 1.48037$ Q/2ka

$Pw = 0.13621$ P/2ka

To determine the equivalent depth of penetration:

$$xg2 := \sqrt{2 \cdot (X2val - 1)}$$

$$xg2 = 0.51398$$

xg = XG(penetration)/a.

The force along the slipline in the Plimit direction:

$$P2limit := Pw \cdot \cos\left(\frac{\pi}{4}\right) + Qw \cdot \cos\left(\frac{\pi}{4}\right)$$

$$P2limit = 1.14309$$

Plimit= Pl(weld strength)/2ka

β=30 DEG

α3= The α value in degrees when β=30 degrees.
X3= The x/a value for a given α and β value.
Y3= The y/a value for a given α and β value.
P3= The P/2ka value for the given condition of α and β intersection .
Q3= The Q/2ka value for the given condition of α and β intersection.

$$\alpha 3 := \begin{bmatrix} 0 \\ 10 \\ 20 \\ 30 \end{bmatrix} \quad X3 := \begin{bmatrix} 1.36603 \\ 1.73236 \\ 2.09558 \\ 2.44045 \end{bmatrix} \quad Y3 := \begin{bmatrix} .63397 \\ .50019 \\ .28998 \\ 0.00 \end{bmatrix} \quad P3 := \begin{bmatrix} .49136 \\ .59173 \\ .60710 \\ .5 \end{bmatrix} \quad Q3 := \begin{bmatrix} .898259 \\ 1.189 \\ 1.57921 \\ 2.05487 \end{bmatrix}$$

$$F(\alpha) := \begin{bmatrix} 1 \\ \alpha \\ \alpha^2 \end{bmatrix}$$

F(α) expresses the functions that are combined linearly to give the best curve fit to the data.

$$Sx := linfit(\alpha 3, X3, F)$$

$$Sx = \begin{bmatrix} 1.36527 \\ 0.03747 \\ -5.365 \cdot 10^{-5} \end{bmatrix}$$

Sx is the coefficients for the functions expressed above for the curve fit data X(α).

$$Sy := linfit(\alpha 3, Y3, F)$$

$$Sy = \begin{bmatrix} 0.6338 \\ -0.00941 \\ -3.905 \cdot 10^{-4} \end{bmatrix}$$

Sy is the coefficients for the functions expressed above for the curve fit data Y(α).

To find the intersection of the equations X(α), Y(α), and Y=X-A:

Guess values: $X3 = 1$, $Y3 = 1$, $\alpha = 2$ — Starting points for computer iteration.

Given

$Sy_0 + Sy_1 \cdot \alpha + Sy_2 \cdot \alpha^2 = Y3$ — Eqn 1: Y(α)

$Sx_0 + Sx_1 \cdot \alpha - Sx_2 \cdot \alpha^2 = X3$ — Eqn2: X(α)

$X3 - 1 = Y3$ — Eqn 3: Y(X)

$$\begin{pmatrix} X3val \\ Y3val \\ \alpha 3val \end{pmatrix} = Find(X3, Y3, \alpha)$$ — Solve for three unknowns.

Results for β=30 deg:

$X3val = 1.57098$

$Y3val = 0.57098$ — Solutions for three unknowns.

$\alpha 3val = 5.44698$ — Relation of X,Y,α,β, along penet. line.

To interpolate the values for P and Q:

$vp = lspline(\alpha 3, P3)$

$vq = lspline(\alpha 3, Q3)$ — Gives a curve fit for P(α) and Q(α)

$interp(vp, \alpha 3, P3, \alpha 3val) = 0.55159$ — P3/2ka=.55159

$interp(vq, \alpha 3, Q3, \alpha 3val) = 1.04865$ — Q3/2ka=1.04865

Along β=30 deg.

Adding in the uniform pressure for the weld case:

$Qw = interp(vq, \alpha 3, Q3, \alpha 3val) + .5 \cdot X3val$

$Pw = interp(vp, \alpha 3, P3, \alpha 3val) - (.5 - .5 \cdot Y3val)$

$Qw = 1.83414$ — Q/2ka

$Pw = 0.33708$ — P/2ka

To determine the equivalent depth of penetration:

$$xg3 := \sqrt{2}\cdot(X3val - 1)$$

$$xg3 = 0.80749$$

xg = XG(penetration)/a.

The force along the slipline in the Plimit direction:

$$P3limit := Pw\cdot\cos\left(\frac{\pi}{4}\right) + Qw\cdot\cos\left(\frac{\pi}{4}\right)$$

$$P3limit = 1.53528$$

Plimit= Pl(weld strength)/2ka

β=0 and α=0

x/a=1
y/a=0
p/2ka= .5
q/2ka= .5

$$P0limit := (.5 - .5)\cdot\cos\left(\frac{\pi}{4}\right) + (.5 + .5)\cdot\cos\left(\frac{\pi}{4}\right)$$

Uniform pressure added.

$$P0limit = 0.70711$$

Summary of the Results: (Normalized loads and penetrations)

P0limit = 0.70711	xg0 = 0.0	Plimit =Limit load/2ka
		xg= Pentration/a
P1limit = 0.87535	xg1 = 0.24925	
P2limit = 1.14309	xg2 = 0.51398	
P3limit = 1.53528	xg3 = 0.80749	

Calculation of the Limit Load

$a := \frac{6.0}{\sqrt{2}} \cdot mm$

The calculation for a is the throat thickness of the fillet weld based ona leg length of 6 mm.

$a = 4.24264 \cdot mm$

$k := 35.48 \cdot \frac{kgf}{mm^2}$

Effective shear strength is based on the approximation of (Tensile Strength)/sqrt(3) for the manufacturers tested TS value of 87400 psi for the Excel Arc 71 electrode.

Limit Load (double fillet)

$PL0 := 4 \cdot k \cdot a \cdot P0limit$

$PL1 := 4 \cdot k \cdot a \cdot P1limit$

$PL2 := 4 \cdot k \cdot a \cdot P2limit$

$PL3 := 4 \cdot k \cdot a \cdot P3limit$

Penetration

$XG0 := xg0 \cdot a$

$XG1 := xg1 \cdot a$

$XG2 := xg2 \cdot a$

$XG3 := xg3 \cdot a$

Limit Load	Penetration
$PL0 = 425.76 \cdot \frac{kgf}{mm}$	$XG0 = 0.0$
$PL1 = 527.06339 \cdot \frac{kgf}{mm}$	$XG1 = 1.05748 \cdot mm$
$PL2 = 688.27523 \cdot \frac{kgf}{mm}$	$XG2 = 2.18065 \cdot mm$
$PL3 = 924.41629 \cdot \frac{kgf}{mm}$	$XG3 = 3.42589 \cdot mm$

APPENDIX D

Upper Bound from Block Sliding to Estimate the Fillet Weld Limit Load in Tension

APPENDIX D

UPPER BOUND METHOD FROM BLOCK SLIDING TO ESTIMATE THE FILLET WELD LIMIT LOAD IN TENSION

This method is from calculations included in Report 26 by McClintock (1994).
These calculations support the method described in Chapter 3.4.

A . Assigned Variables

Variable Definition
θw= weld angle
dx= weld leg length along the x-axis (mm)
Hv= average Vickers hardness (Kg/mm^2)
k= yield strength in shear (N/mm^2)
x_c= x-coordinte of the crack tip (mm)
y_c= y-coordinate of the crack tip
θ_{AB}= angle to the upper slip line from the x-axis (radians)
θ_{BC}= angle to the lower slip line from the x-axis (radians)
θ_{ABt}= angle from the crack tip to the upper toe (radians)
θ_{BCt}= angle from the crack tip to the lower toe (radians)
l_{AB}= length of the upper slip plane (mm)
l_{BC}= length of the lower slip plane (mm)
b= length of the tested specimen
a= throat thickness of the weld without penetration

Assigned Variable Values:

$x_c := 0 \cdot mm, 1 \cdot mm .. 6 \cdot mm$

$y_c := 0 \cdot mm$

$\theta_w := \frac{\pi}{4} \cdot rad$

$d_x := 6 \cdot mm$

Solution:

$$\theta_{ABt}(x_c) := \frac{\pi}{2} + \operatorname{atan}\left(\frac{-x_c}{d_x \cdot \tan(\theta_w) - y_c}\right)$$

$$\theta_{BCt}(x_c) := -\operatorname{atan}\left(\frac{y_c}{d_x + x_c}\right)$$

$$\theta_{ABo}(x_c) := \theta_{ABt}(x_c)$$

$$\theta_{BCo}(x_c) := \theta_{BCt}(x_c)$$

$$l_{BCo}(x_c) := \frac{\left(d_x + x_c - \frac{y_c}{\tan(\theta_w)}\right) \cdot \sin(\theta_w)}{\sin(\theta_w + \theta_{BCo}(x_c))}$$

$$l_{ABo}(x_c) := l_{BCo}(x_c) \cdot \frac{\sin(\theta_w + \theta_{BCo}(x_c))}{\sin(\theta_w + \theta_{ABo}(x_c))}$$

If the upper slip line breaks through to the weld surface.

B. Calculation of Yield Stress of Weld in Pure Shear

$TSw := 61.448 \cdot \frac{kgf}{mm^2}$ TSw is the tensile strength of the weld material based on manufacturer testing. (EXCEL-ARC 71 Electrode)

$ko := \frac{TSw}{\sqrt{3}}$ Ko is the yield stress of the material in pure shear. Assuming nonhardening material.

$ko = 35.477 \cdot \frac{kgf}{mm^2}$

C. Calculation of the Limit Load of the Web

$t := 15 \cdot mm$ Thickness of the web.

$TSb := 57.716 \cdot \frac{kgf}{mm^2}$ Tsb is the tensile strength of the base plate from tests by the manufacturer.

$PL_{bp} := t \cdot \frac{2}{\sqrt{3}} \cdot TSb$ The 2/sqrt(3) accounts for the plane strain condition.

PLbp is the limit load of the web plate.

$PL_{bp} = 999.67 \cdot \frac{kgf}{mm}$

D. Calculation of the Limit Load of the Weld in Transverse Loading

Upper Bound Limit Load (Load/Length) [Double fillet]

$$P_{ubo}(x_c) := \frac{2 \cdot ko}{\sin\left(\theta_{ABo}(x_c) - \theta_{BCo}(x_c)\right)} \cdot \left(l_{ABo}(x_c) \cdot \left|\cos\left(\theta_{BCo}(x_c)\right)\right| + l_{BCo}(x_c) \cdot \left|\cos\left(\theta_{ABo}(x_c)\right)\right|\right)$$

Upper Bound Limit Load (Load/2ka) [Single fillet, for comparison to Slip Line Solution)

$$a := \frac{6}{\sqrt{2}} \cdot mm$$

Throat thickness is based on a 6 mm leg length.

$$P_{ubn}(x_c) := \frac{1}{2 \cdot a \cdot \sin\left(\theta_{ABo}(x_c) - \theta_{BCo}(x_c)\right)} \cdot \left(l_{ABo}(x_c) \cdot \left|\cos\left(\theta_{BCo}(x_c)\right)\right| + l_{BCo}(x_c) \cdot \left|\cos\left(\theta_{ABo}(x_c)\right)\right|\right)$$

Comparison of Upper Bound to the Slip Line Solution (for EXCEL-ARC 71 electrode)

Upper Bound Method (Double Fillet) (Limit Load kgf/mm)	Slip Line Solution (Double Fillet) (Limit load kgf/mm)
$P_{ubo}(0.0 \cdot mm) = 425.724 \cdot \frac{kgf}{mm}$	PL0= 425.76 kgf/mm
$P_{ubo}(1.05748 \cdot mm) = 527.205 \cdot \frac{kgf}{mm}$	PL1= 527.063 kgf/mm
$P_{ubo}(2.18065 \cdot mm) = 692.918 \cdot \frac{kgf}{mm}$	PL2= 688.275 kgf/mm
$P_{ubo}(3.42589 \cdot mm) = 946.394 \cdot \frac{kgf}{mm}$	PL3= 924.416 kgf/mm

Comparison of Upper Bound to the Slip Line Solution (Normalized limit load and penetration)

Upper Bound Method (Limit Load/2ka)	Slip Line Solution (Limit Load/2ka)
$P_{ubn}(0\cdot mm) = 0.707$	.707
$P_{ubn}(.5\cdot mm) = 0.776$	.780
$P_{ubn}(1.0\cdot mm) = 0.864$	.865
$P_{ubn}(1.5\cdot mm) = 0.972$	.968
$P_{ubn}(2.0\cdot mm) = 1.1$	1.093
$P_{ubn}(2.5\cdot mm) = 1.247$	1.237
$P_{ubn}(3.0\cdot mm) = 1.414$	1.395
$P_{ubn}(3.5\cdot mm) = 1.601$	1.560
$P_{ubn}(4.0\cdot mm) = 1.807$	1.723

APPENDIX E

Information on Tested Welding Electrodes and Steel Plate

EXCEL-ARC 71

AWS E71T-1

NWSA 636-Y

INDEX: 940502

DESCRIPTION:

EXCEL-ARC 71 is designed for general purpose, all-position fabrication with either CO_2 or a 75%Ar/25% CO_2 gas mixture. EXCEL-ARC 71 offers a spray type transfer of weld metal and produces a low hydrogen weld deposit with deep penetration at a high deposition rate. Clean up time is kept to a minimum because of the low spatter levels and the ease at which the slag is removed. EXCEL-ARC 71 also meets 20 ft. lb impact strength at both -20° F. and -40° F.

APPLICATIONS:

EXCEL-ARC 71 is designed for all- position welding of mild and low alloy steels in single and multi-pass applications.

FEATURES AND BENEFITS:

- Low fume
- Low spatter
- Excellent operator appeal
- Easy slag removal
- Resists worm tracking under normal conditions
- X-ray quality welds
- Bridges poor fit-up
- Low hydrogen weld deposit

SHIELDING GAS:

100% carbon dioxide (CO_2) 75/25 (75%Ar/25%CO_2)

TYPICAL *WELD METAL PROPERTIES: (Chem Pad)

Weld Metal Analysis:	CO_2	75%Ar/25%CO_2
Carbon	.015	.017
Manganese	1.11	1.29
Silicon	.58	.76
Sulphur	.017	.017
Phosphorus	.011	.011

TYPICAL * DIFFUSIBLE HYDROGEN: (Gas Chromotography)

6.1ml/100 gr.

RECOMMENDED WELDING DATA:

Diameter Inches	M.M.		Weld Position	Approx. Amperage	Voltage	Wire Feed Speed	Dep. Rate Lb/Hr	Shielding Gas	Gas Flow cfh	Current	Stickout ± 1/4"
CO_2											
.045	0.9	Optimum	Vertical -Up	170	23	260	4.4	CO_2	35	DCEP	1/2"
.045	0.9		Vertical-Up	185	24	310	6.1	CO_2	35	DCEP	1/2"
.045	0.9		Vertical-Up	220	25	383	7.5	CO_2	35	DCEP	1/2"
.045	0.9		Horizontal	260	27	500	8.9	CO_2	35	DCEP	1/2"
75/25											
.045	0.9		Vertical -Up	170	22	260	4.5	75/25	35	DCEP	1/2"
.045	0.9	Optimum	Vertical -Up	185	23	310	6.2	75/25	35	DCEP	1/2"
.045	0.9		Vertical -Up	220	24	383	7.8	75/25	35	DCEP	1/2"
.035	0.9		Horizontal	250	26	500	9.0	75/25	35	DCEP	1/2"

WELDING RANGE:

	Minimum			Maximum		
Diameters	Amps	Volts	Wire Feed Speed	Amps	Volts	Wire Feed Speed
.035	110	20	240	250	28	750
.045	120	21	168	300	30	625
.052	160	21	175	320	30	490
1/16	170	22	110	400	31	400
5/64	200	26	95	450	33	270
3/32	300	26	95	600	36	255

TYPICAL * MECHANICAL PROPERTIES: (AW) (EXCEL-ARC 71)

	CO_2	75%Ar/25%CO_2
Tensile Strength.....	87,400 psi	98,300 psi
Yield Srength.....	80,300 psi	89,500 psi
Elongation % in 2".....	26.8%	25.8
Reduction of Area.....	63%	61%

TYPICAL * CHARPY V-NOTCH IMPACT VALUES: (AW)

Avg. at 0 * F.	50 ft. lbs.	47 ft. lbs.
Avg. at -20* F.	40 ft. lbs.	41 ft. lbs.
Avg. at -40* F.	25 ft. lbs.	22 ft. lbs.

CONFORMANCES AND APPROVALS:

AWS A5.20, Class E71T-1	ASME SFA5.20, Class E71T-1	BV 3Y SA	DNV 3Y SA
American Bureau of Shipping	Lloyds Registry of Shipping 3Y SA	Mil-E-24403A type 71T-1C	

HOBART BROTHERS COMPANY
TROY, OHIO 45373. U.S.A.
PHONE 513-332-4000 FAX # 513-332-4090

HOBART
WELDING PRODUCTS

FabCO® 802

AWS E71T-1

NWSA 636-J

INDEX: 910901

DESCRIPTION:

FabCO 802 is an all-position, flux cored wire designed for optimum performance when used with 100% CO_2 shielding gas. The extremely smooth and stable arc transfer coupled with the quick freezing slag make this wire well suited for welding in all positions. FabCO 802 produces a quality, x-ray clear weld deposit with excellent mechanical properties. The bead contour is flat to slightly convex and the bead wets in nicely with the sidewalls. Clean-up time is kept to a minimum due to low spatter levels and easy slag removal. FabCO 802 is available in .035", .045", .052" and 1/16" diameters.

APPLICATIONS:

FabCO 802 is designed for all position welding of mild and low alloy steels in single and multi-pass applications. Pre-cleaning of steel is not always necessary as FabCO 802 can be used over average rust and mill scale. FabCO 802 is widely used in the fabrication of ships, storage vessels, structures, earth moving equipment and piping.

FEATURES AND BENEFITS:

- Low fume
- Low spatter
- Excellent operator appeal
- Easy slag removal
- Resists worm tracking under normal conditions
- X-ray quality welds
- Bridges poor fit-up
- Low hydrogen weld deposit

SHIELDING GAS:

100% carbon dioxide (CO_2)

RECOMMENDED WELDING DATA:

Diameter Inches	M.M.		Weld Position	Approx. Amperage	Voltage	Wire Feed Speed	Dep. Rate Lb/Hr	Shielding Gas	Gas Flow cfh	Current	Stickout ± 1/4"
.035	0.9		Flat-Vert up	110	20	240	2.8	CO_2	30	DCEP	1/2"
.035	0.9	Optimum	Flat-Horiz.	190	25	500	5.9	CO_2	30	DCEP	1/2"
.035	0.9		Flat-Horiz.	220	28	700	8.5	CO_2	35	DCEP	1/2"
.035	0.9		Vert-up-Ovhd.	190	24	500	5.2	CO_2	30	DCEP	1/2"
.045	1.1		Flat-Horiz.	170	22	268	5.0	CO_2	35	DCEP	3/4"
.045	1.1	Optimum	Flat-Horiz.	200	22	335	6.0	CO_2	35	DCEP	3/4"
.045	1.1	Optimum	V-Up & Ovhd.	200	23	335	6.0	CO_2	35	DCEP	3/4"
.045	1.1		Flat-Horiz.	270	27	500	9.2	CO_2	35	DCEP	3/4"
.045	1.1		Flat-Horiz.	300	30	625	12.4	CO_2	40	DCEP	3/4"

WELDING RANGE:

Diameters	Minimum			Maximum		
	Amps	Volts	Wire Feed Speed	Amps	Volts	Wire Feed Speed
.035	110	20	240	250	28	750
.045	120	21	168	300	30	625
.052	160	21	175	320	30	490
1/16	170	21	110	400	31	400

TYPICAL *WELD METAL PROPERTIES: (Chem Pad) (FABCO 802)

Weld Metal Analysis:

Carbon	.04
Manganese	1.20
Silicon	.60
Phosphorus	.014
Sulphur	.014

TYPICAL * MECHANICAL PROPERTIES: (AW)

		SR@ 1150° F. (8hrs.)
Tensile Strength	81,700 psi	79,000 psi
Yield Strength	72,600 psi	65,900 psi
Elongation % in 2"	28.5%	31.5%
Reduction of Area	65%	65%

TYPICAL * CHARPY V-NOTCH IMPACT VALUES: (AW)

Avg. at 0 ° F.	40 ft. lbs.	45 ft. lbs.
Ave. at -20° F.	35 ft. lbs.	35 ft. lbs.

CONFORMANCES AND APPROVALS:

AWS A5.20, Class E71T-1
ABS to Grade 2YSA
Bureau Veritas SA 2YM HH

ASME SFA5.20, Class E71T-1
ABS to Grade 2SA

Federal Bureau of Roads, Class E71T-1
MIL-E- 24403/1 71T-1C

*The information contained or otherwise referenced herein is presented only as "typical" without guarantee or warranty and Hobart Brothers Company expressly disclaims any liability incurred from any reliance thereon. Typical data are those obtained when welded and tested in accordance with AWS 5.20 specification. Other tests and procedures may produce different results. No data is to be construed as a recommendation for any welding condition or technique not controlled by Hobart Brothers Company."

*Material Safety Data Sheets on any Hobart Brothers Company products may be obtained from Hobart Customer Service.

**Because Hobart Brothers Company is constantly improving products, Hobart reserves the right to change design and/or specifications without notice.

HOBART BROTHERS COMPANY
TROY, OHIO 45373. U.S.A.
PHONE 513-332-4000 FAX # 513-332-4090

HOBART
WELDING PRODUCTS

(EH 36)

계약번호 CONTRACT : SPPA12AB

주문번호 ORDER NO : STOCK

품명 COMMODITY : PLATE

제품규격 SPECIFICATION : LR-EH36

품질검사 증명서 MILL TEST CERTIFICATE

수요가 CUSTOMER : H.M.D LTD.CO.

주문자 SUPPLIER : H.M.D LTD.CO.

포항종합제철
POHANG IRON & STEEL CO.
(POHANG WORKS)

증명서번호 CERTIFICATE NO : 92-PP-0504-03

발행일자 DATE OF ISSUE : MAY. 04. 1992

C.GOOD

제품치수 DIMENSIONS	수량 Quantity	중량 WEIGHT (KG)	장입번호 CHARGE NO	제품번호 PRODUCT NO	인장시험 TENSILE TEST			충격시험 IMPACT (V) NOTCH			비고	화학성분 CHEMICAL COMPOSITION (%)													H X100 H X1000 . X10000 [X10000
					YP KG/MM²	TS		ENERGY - 40 C KG-M		SA	HEAT TREATMENT	C	Si	Mn	P	S	SAL	CU	NB	V	NI	MO	CR		
												3	2	2		3	3	2	3	3	2	2	2	
1X2400X12000	1	4,746	Y80050	59493402	TCA 40.6	57.4	23	TA	7.9		N	1	170	38	140	16	7	45	30	3	5	20	TR	2
** SPECIMEN NO : TENSION ==>		5949361		IMPACT ==>	5949341																			
*** SUB TOTAL (020)*		1			4,746 (KG)																			
** HEAT TREATMENT **																								
NORMALIZING ===>		890 DEG C X 37MIN																						
*** GRADE TOTAL ***		1			4,746 (KG)																			
*** GRAND TOTAL ***		1			4,746 (KG)																			

=== LAST ITEM ===

ORIGINAL

NOTE: POSITION T:TOP, M:MIDDLE, B:BOTTOM DIRECTION L:LONGITUDINAL, C:CROSSWISE, Z:THICKNESS GL(GAUGE LENGTH) RECTANGULAR (A:200mm, B:
C:180mm, D:80mm, R:56.5(%) ROUND (F:50mm, G:40mm, H:56.5(%) IMPACT SUB-SIZE 1:2.5mm, 2:3.3mm, 3:5.0mm, 4:7.5mm SA SHEAR AREA
UST ULTRASONIC TEST HEAT TREATMENT N:NORMALIZED, Q:QUENCHED, T:TEMPERED PILAC:POSCO IN LINE ACCELERATED COOLING, DQ:DIRECT QU
CR:CONTROLLED ROLLED DIVISION C:CHECK ANALYSIS, T:LADLE ANALYSIS SAI Sol-Al TAI Total-Al

(DH 36)

LUKENS STEEL
A LUKENS COMPANY

TEST CERTIFICATE

(ATTN: Rob Walnut)

PAGE NO. 01 OF 01
FILE NO: 6942-01-29
DATE: 05/04/93
MILL ORDER NO: 64583-001

CUSTOMER P.O.: 1A62266
DESCRIPTION:
1 - RECTANGLE .75 -X- 96 -X- 240

SOLD TO:
J.T. RYERSON & SON, INC.
2621 WEST 15TH PLACE
CHICAGO, IL 60608

SEND TO: 03-C
J.T. RYERSON & SON, INC.
8301 S. STEWART ST.E
ATTN: MS. MARTHA GOMEZ
CHICAGO, IL 60620

SHIP TO:
J. T. RYERSON & SON, INC.
83RD & STEWART STREET
66945
CHICAGO, IL 60620

THIS MATERIAL HAS BEEN MANUFACTURED AND TESTED IN ACCORDANCE WITH PURCHASE ORDER REQUIREMENTS AND SPECIFICATIONS

RYER 3477-B YR 90
NORM., ASME SA537 CO CL. 1 ABS. CL. 1, NORM., ABS
BM36.

ASTM A131-89, GR. AH36 & DH36. ASTM A537-86, CL. 1
CHAPTER 43, AH36 & DH36. MIL-S-22698C AMD1 AH36 &

CHEMICAL ANALYSIS

HEAT SCOPE	C	MN	P	S	CU	SI	NI	CR	MO	V	TI	B	CB				
C109% /3GB																	65 7-8
C109%	.14	1.29	.010	.003	.19	.22	.16	.13	.01				.035				

TENSILES / CHARPY V IMPACTS / FULL / OTHER TESTS PERFORMED

TYP	YLD (PSI X 100)	TENS (PSI X 100)	% ELONG 8"	% RA	TYPE	TEMP	FT LAS			MILS LATERAL EXPANSION			% SHEAR			OTHER TESTS PERFORMED
BX	542	752	23.0		BL	-50F	160	189	208							

INFORMATION

WEIGHT PER PIECE = 4901 LBS. 2228 KG.
ALL STEEL HAS BEEN MELTED AND MANUFACTURED IN U.S.A.
TYPE: PLATE
REPORT NO. CC#343836
COIL #23197 CR 577559

HEAT TREAT CYCLES / TESTS PERFORMED

MATL	TEST	NOM TEMP	MIN TEMP	MAX TEMP	HOLD MINS.	COOL METHOD	FAIR EM TEM
X	X	1660			0037	AC	

HEAT TREAT CYCLES / TESTS ONLY / DEG

START END TEMP	NOM TEMP	MIN TEMP	MAX TEMP	HOLD MINS.	HEAT RATE MAX	FAIR COO RAT MA

WE HEREBY CERTIFY THE ABOVE INFORMATION IS CORRECT:

Quality Assurance Laboratory

Scott C. Weaver

JUN 04 REVISION

APPENDIX F

Photographs of Weld Profiles

VOLT	STEEL = A-36	AMPERAGE = 300	VOLT
	WELD = E71T-1 \ Excel-Arc 71 \ C25	TRAVEL = 23.5 (ipm)	
24	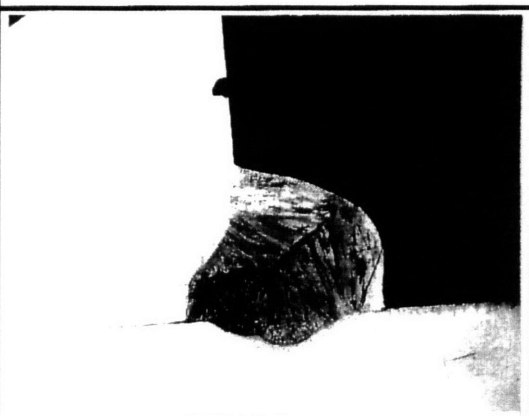 TRIAL 2	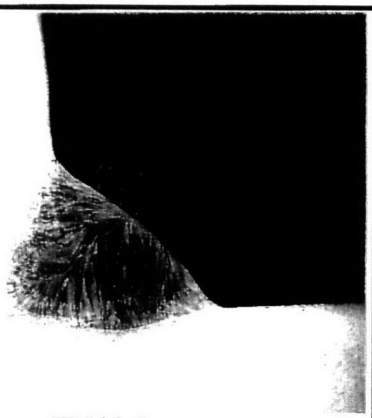 TRIAL 3	28
26	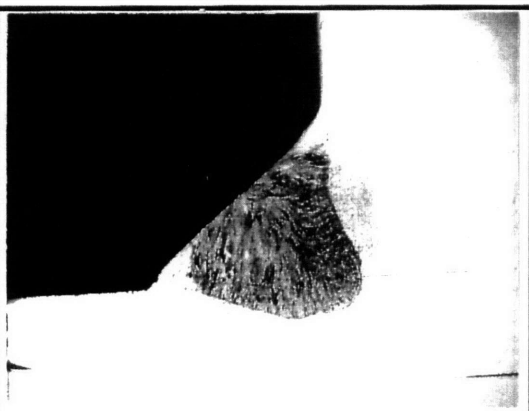 TRIAL 1	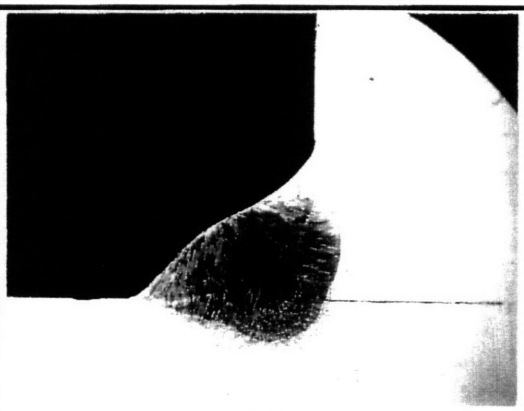 TRIAL 4	30

SCALE (MM)

0 1 2 3 4 5

VOLT	STEEL = A-36	AMPERAGE = 265	VOLT
	WELD = E71T-1 \ Excel-Arc 71 \ CO2	TRAVEL = 19 (ipm) (ipo	
26	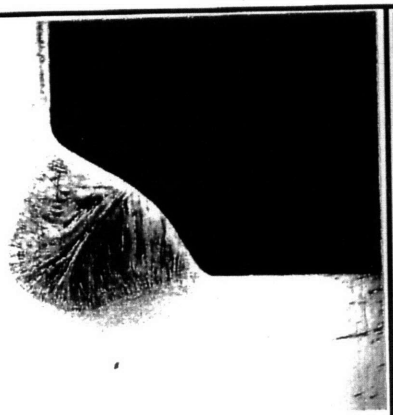 TRIAL 5	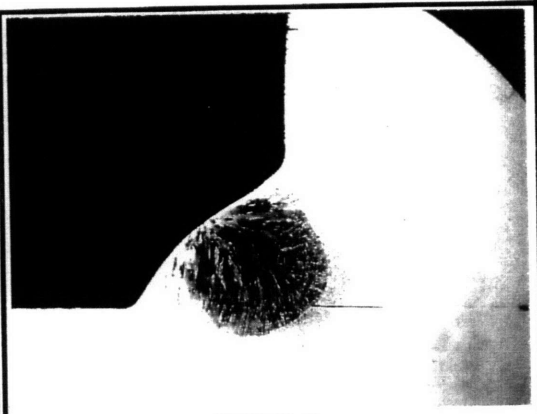 TRIAL 6	27

SCALE (MM)

0 1 2 3 4 5

VOLT / WK ANG	STEEL = A-36 WELD = E71T-1\Excel-Arc 71\CO2 TRAVEL = 23.5 (ipm)		VOLT / WK ANG
	AMPS = 300	AMPS = 340	
27 / 45°	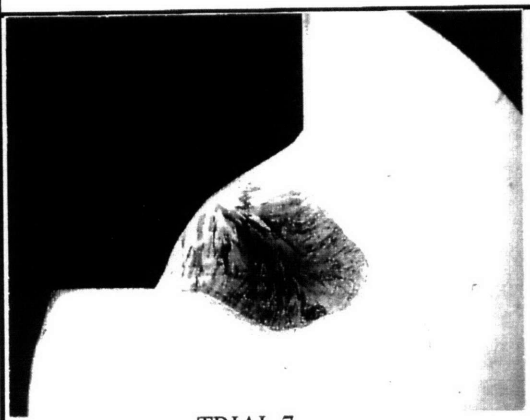 TRIAL 7	 TRIAL 18	33 / 45°
27 / 45°	 TRIAL 17	 TRIAL 19	30 / 50°
30 / 50°	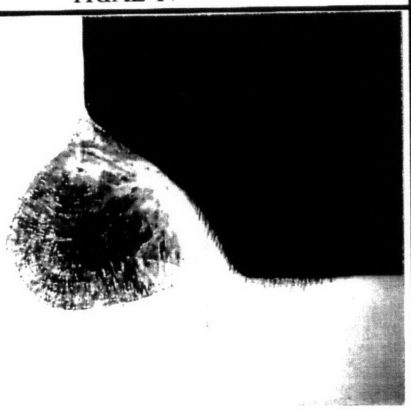 TRIAL 20		

SCALE (MM)

0 1 2 3 4 5

AMPS	STEEL = A-36	VOLTAGE = 30	AMPS
	WELD = E71T-1 \ Excel-Arc 71 \ C02	TRAVEL = 23.5 (ipm)	
300	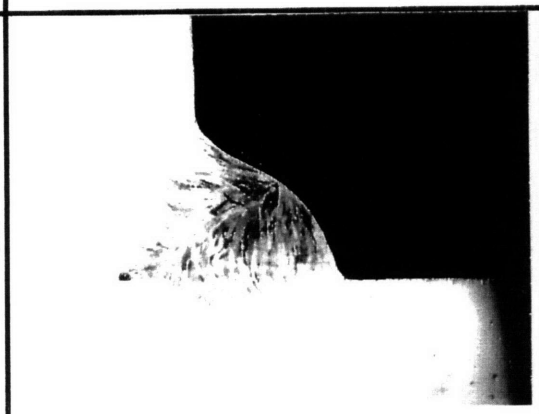 TRIAL 8	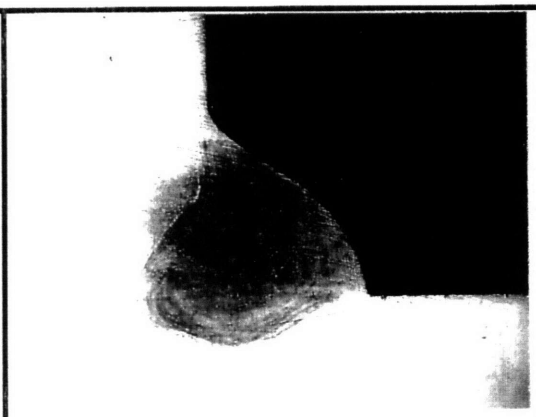 TRIAL 11	315
310	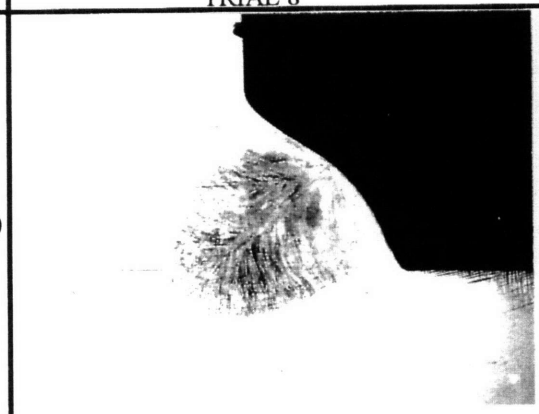 TRIAL 9	 TRIAL 12	320
315	 TRIAL 10	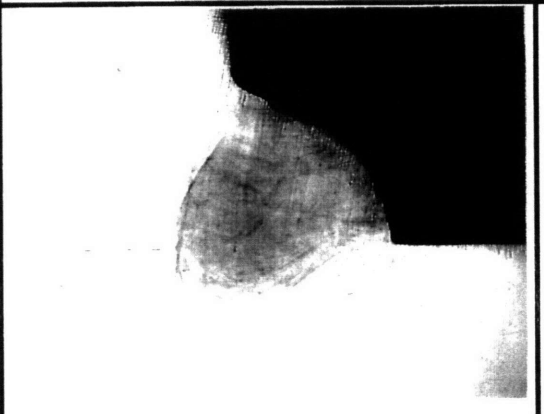 TRIAL 13	325

SCALE (MM)

0 1 2 3 4 5

VOLT	STEEL = A-36	AMPERAGE = 340	VOLT
	WELD = E71T-1 \ Excel-Arc 71 \ C02	TRAVEL = 23.5 (ipm)	
30	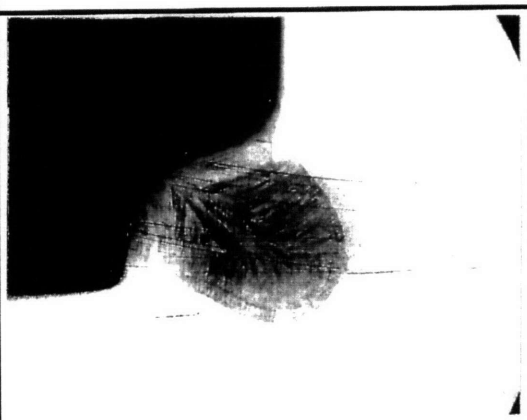 TRIAL 14		
32	 TRIAL 15		
33	 TRIAL 16		

SCALE (MM)

0 1 2 3 4 5

VOLTS	STEEL = EH-36	WELD = E71T-1 \ Excel-Arc 71 \ CO2	VOLTS
	AMPS = 150 TRAVEL = 7.25 (ipm)	AMPS = 200 TRAVEL = 10.5 (ipm)	
20	 TRIAL 25	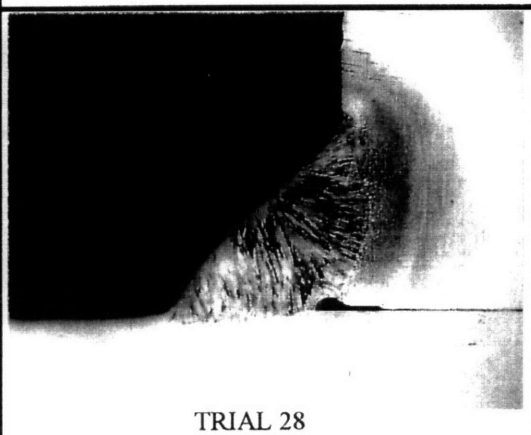 TRIAL 28	22
21.5	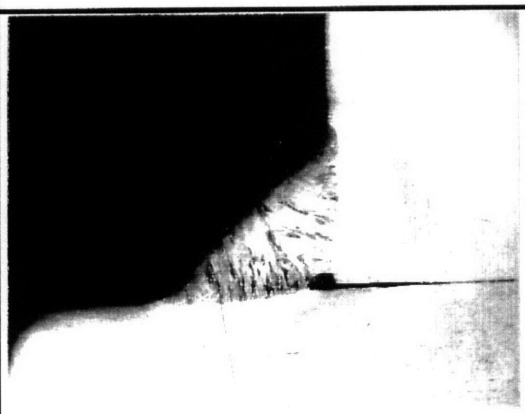 TRIAL 26	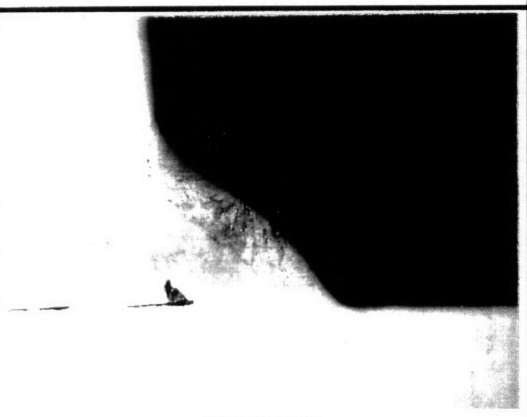 TRIAL 29	23.5
23	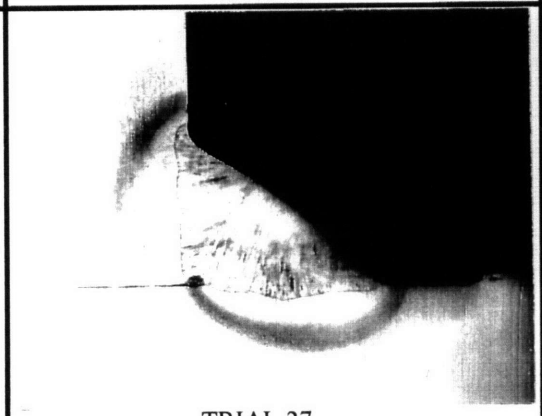 TRIAL 27	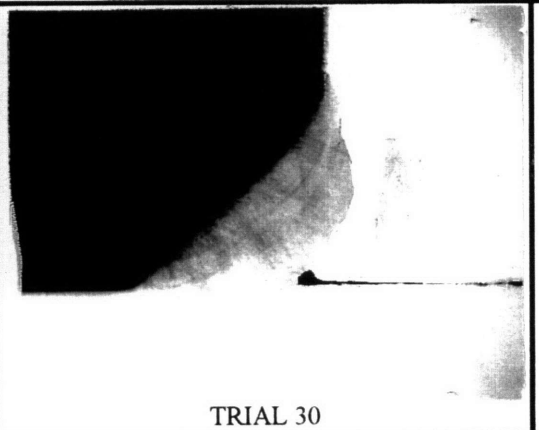 TRIAL 30	25

SCALE (MM)

0 1 2 3 4 5

VOLTS	STEEL = EH-36	WELD = E71T-1 \ Excel-Arc 71 \ CO2	VOLTS
	AMPS = 235 TRAVEL = 15 (ipm)	AMPS = 280 TRAVEL = 17.5 (ipm)	
23.5	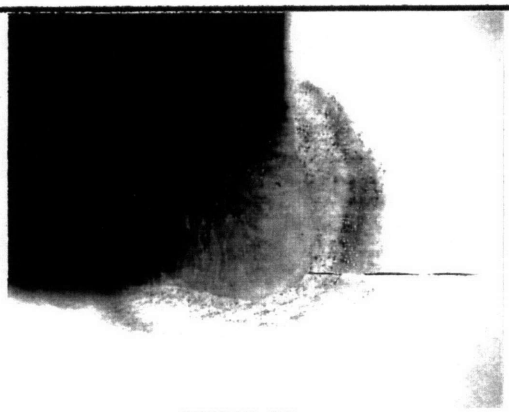 TRIAL 31	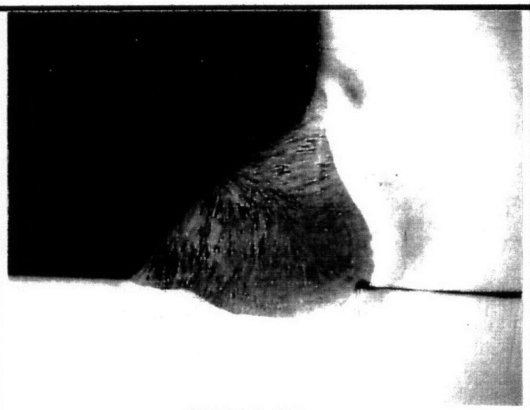 TRIAL 34	25.5
25	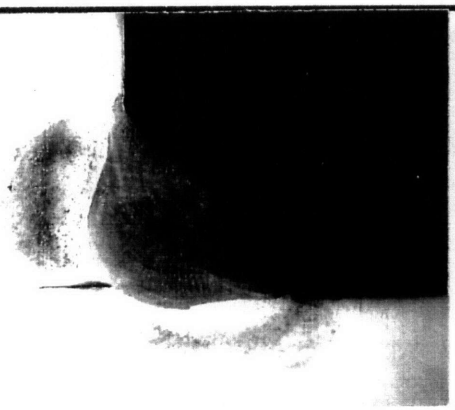 TRIAL 32	 TRIAL 35	27
26.5	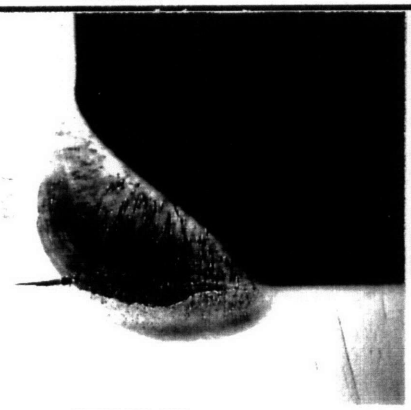 TRIAL 33	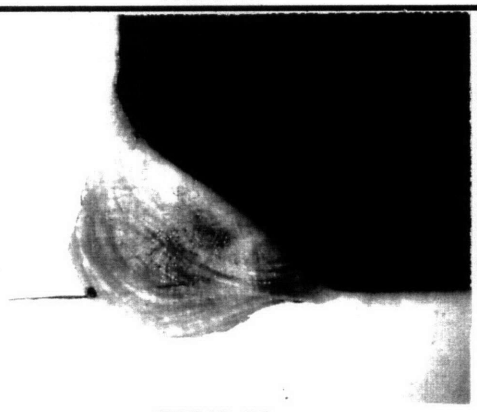 TRIAL 36	29.5

SCALE (MM)

0 1 2 3 4 5

VOLTS	STEEL = EH-36	WELD = E71T-1 \ Excel-Arc 71 \ CO2	VOLTS
	AMPS = 300 TRAVEL = 21.7 (ipm)	AMPS = 330 TRAVEL = 24.5 (ipm)	
28	 TRIAL 37	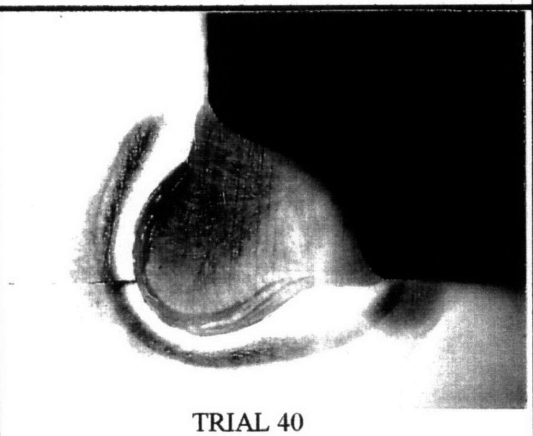 TRIAL 40	29.5
29.5	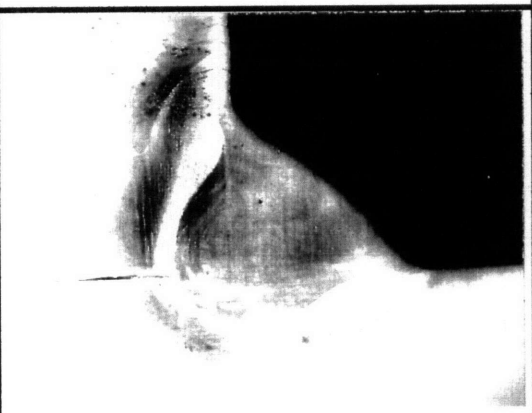 TRIAL 38	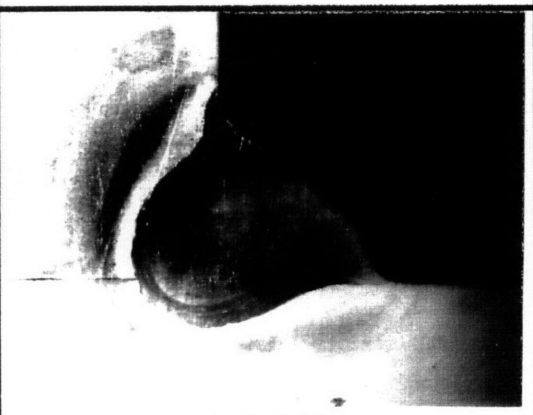 TRIAL 41	31
31	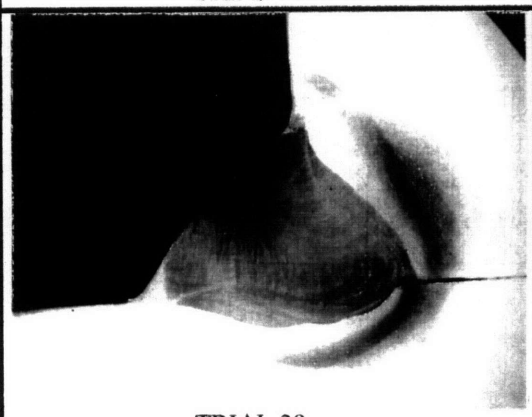 TRIAL 39	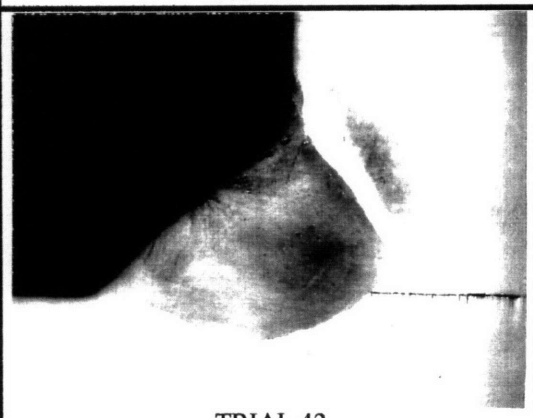 TRIAL 42	33.5

SCALE (MM)

0 1 2 3 4 5

VOLTS	STEEL=EH-36 WELD=E71T-1\Excel-Arc 71\CO2 TRAVEL = 29.25 (ipm)		VOLTS
	AMPS = 365	AMPS = 365	
31	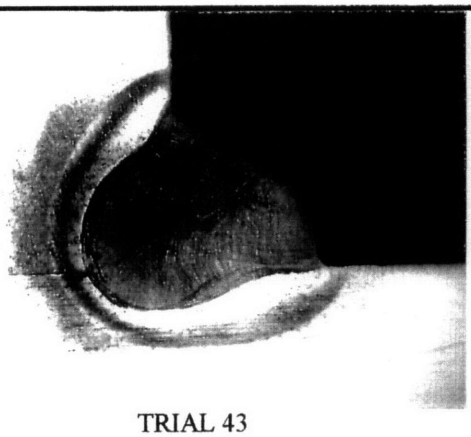 TRIAL 43	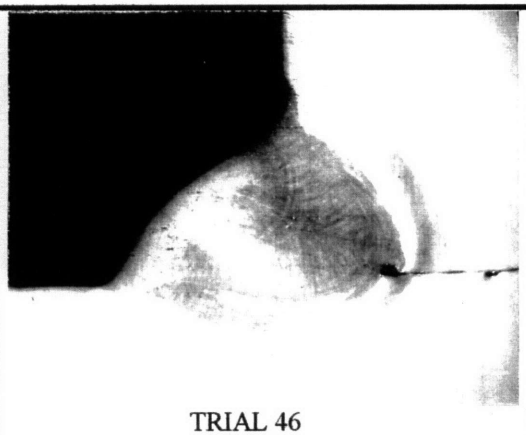 TRIAL 46	35.5
32.5	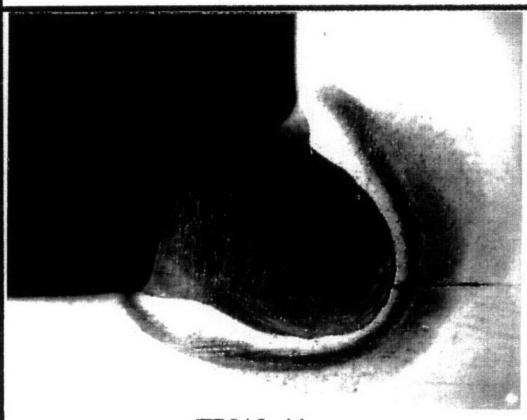 TRIAL 44	 TRIAL 52	34
34	 TRIAL 45	Trial 52 had the welding electrode located 3mm above the weld joint intersection. The other welds shown had the welding electrode located directly at the joint interface.	

SCALE (MM)

0 1 2 3 4 5

VOLTS	STEEL=EH-36 WELD=E71T-1\Excel-Arc 71\CO2 TRAVEL = 24.5 (ipm)		VOLTS
	AMPS = 330	AMPS = 330	
35	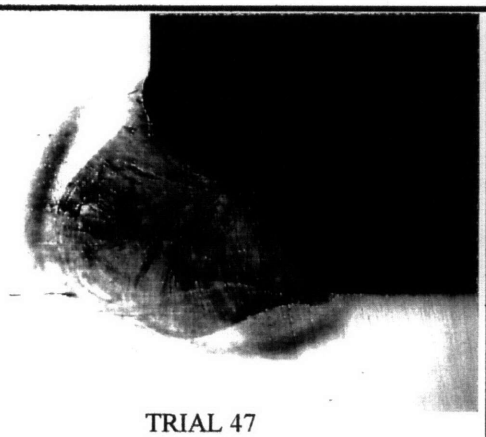 TRIAL 47	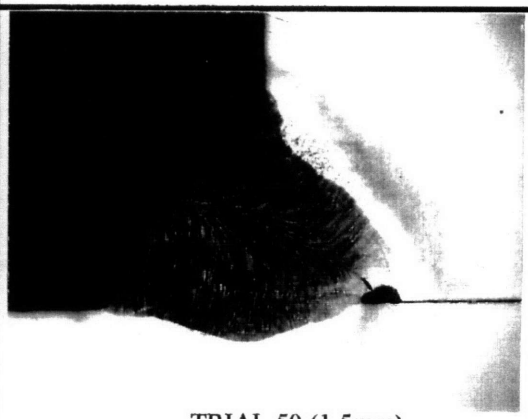 TRIAL 50 (1.5mm)	33.5
29.5	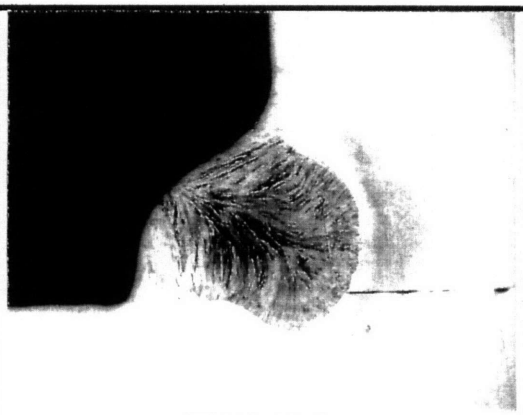 TRIAL 48 (3mm)	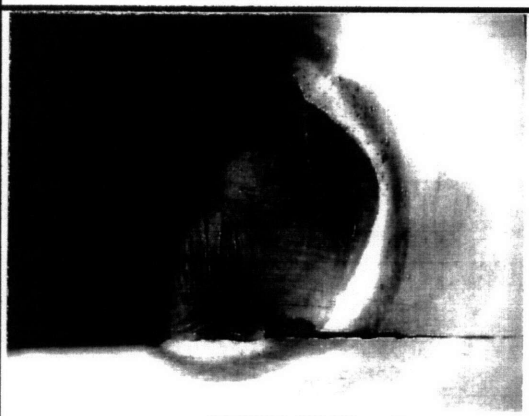 TRIAL 51 (5mm)	33.5
33.5	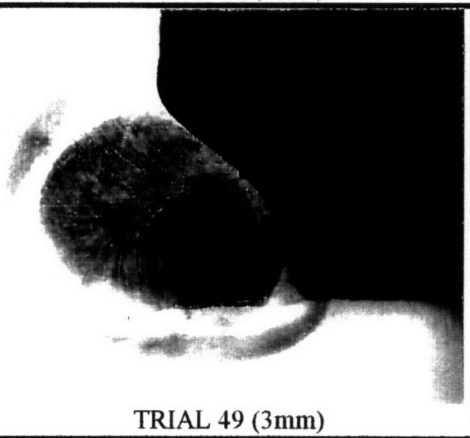 TRIAL 49 (3mm)	Trials 48 thru 51 had the welding electrode located above the weld joint intersection by the amount indicated in brackets. Trial 47 had the welding electrode located directly at the joint interface.	

SCALE (MM)

0 1 2 3 4 5

VOLTS	AMPS	TRAVEL	STEEL=EH-36 WELD=E71T-1 \ Excel-Arc 71 \ CO2	HARDNESS VALUES (ROCKWELL A)
23	170	6.8 ipm	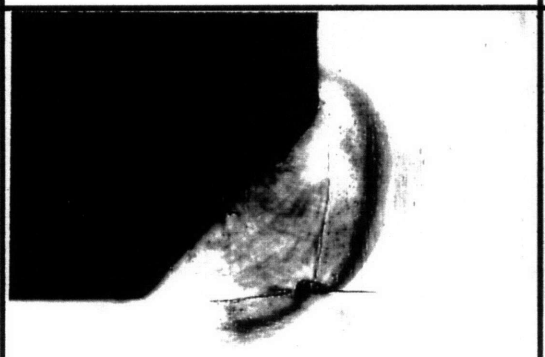 TEST 1	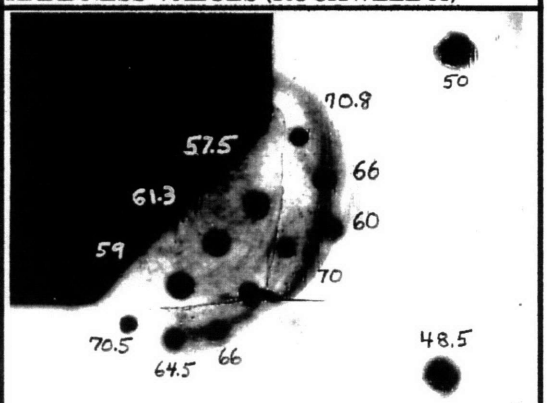 TEST 1
26	230	15 ipm	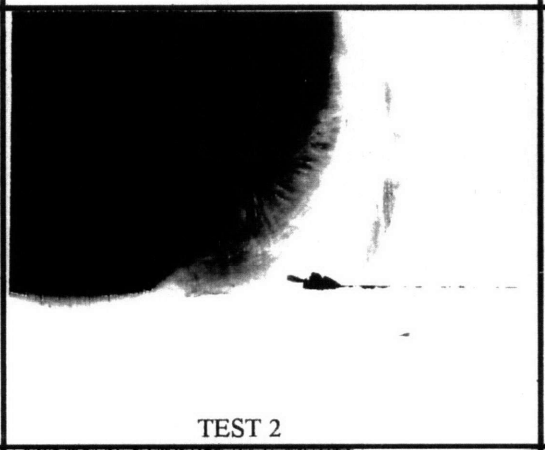 TEST 2	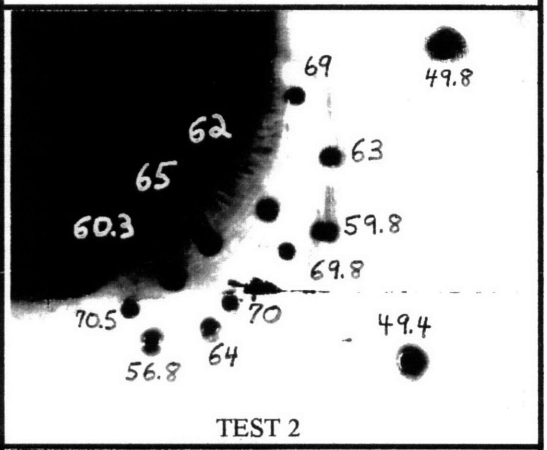 TEST 2
27	270	17.5 ipm	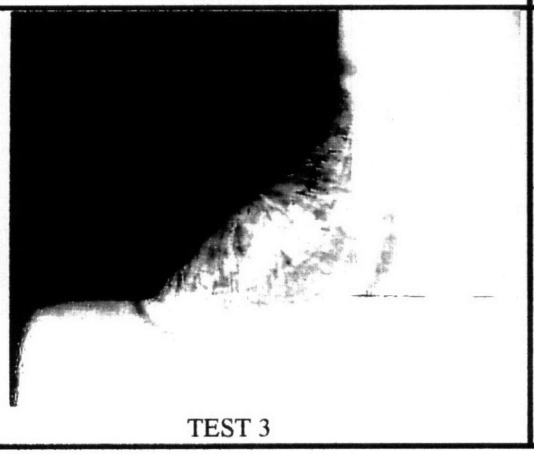 TEST 3	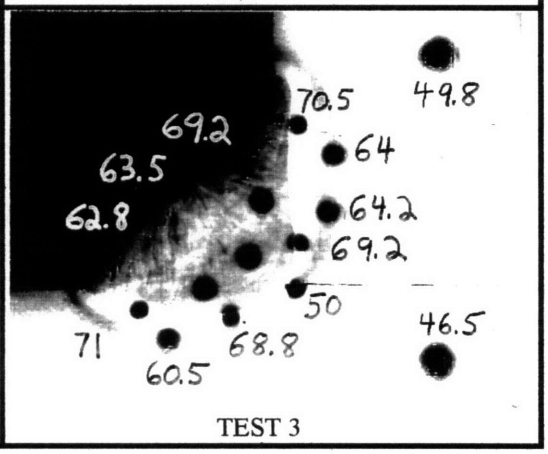 TEST 3

SCALE (MM)

0 1 2 3 4 5

VOLTS	AMPS	TRAVEL	STEEL=EH-36 WELD=E71T-1 \ Excel-Arc 71 \ CO2	HARDNESS VALUES (ROCKWELL A)
31	300	21.7 ipm	 TEST 4	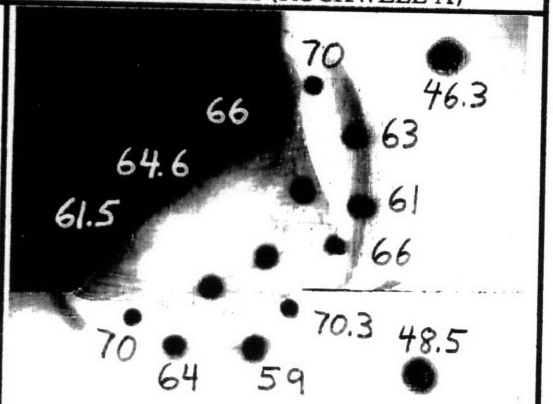 TEST 4
32	330	25.7 ipm	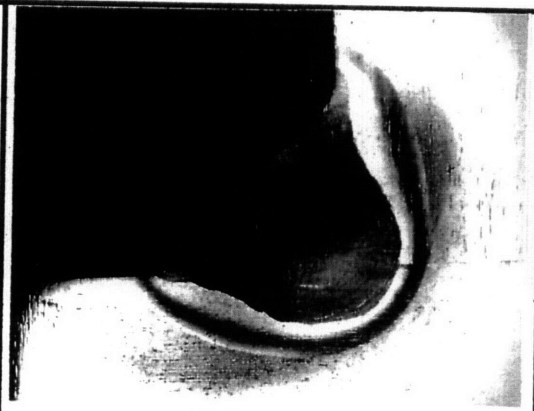 TEST 5	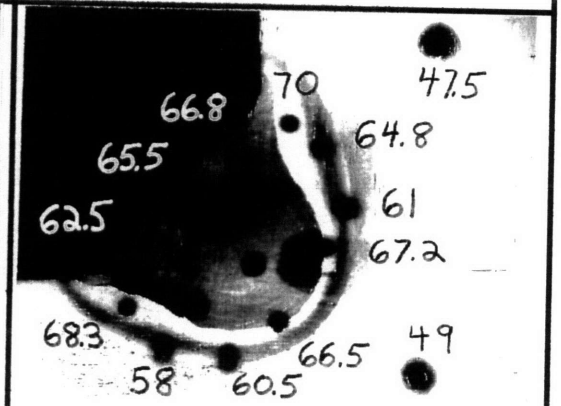 TEST 5
33	350	29.3 ipm	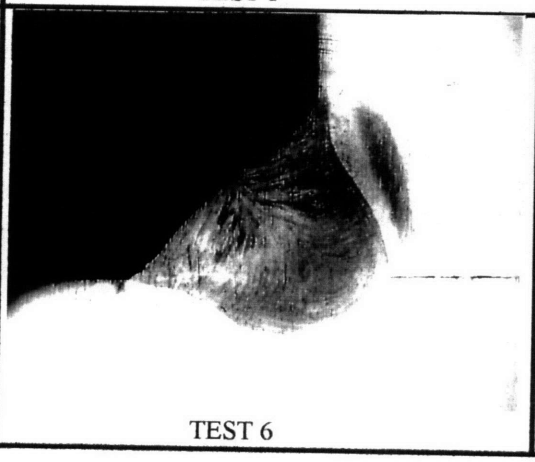 TEST 6	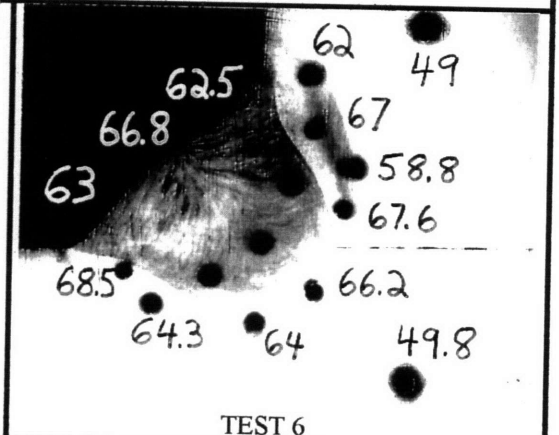 TEST 6

SCALE (MM)

0 1 2 3 4 5

VOLTS	AMPS	TRAVEL	STEEL = EH-36 WELD = E71T-1 \ Excel-Arc 71 \ CO2	HARDNESS VALUES (ROCKWELL A)
33.5	330	24.4 ipm	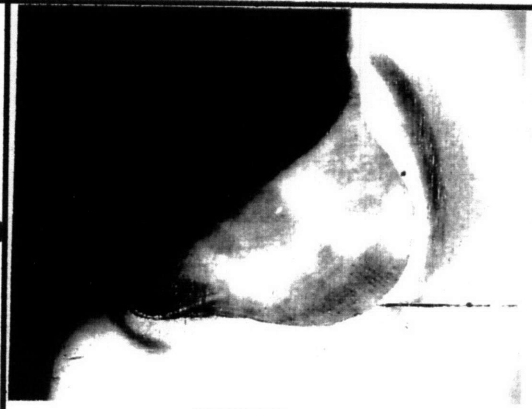 TEST 7	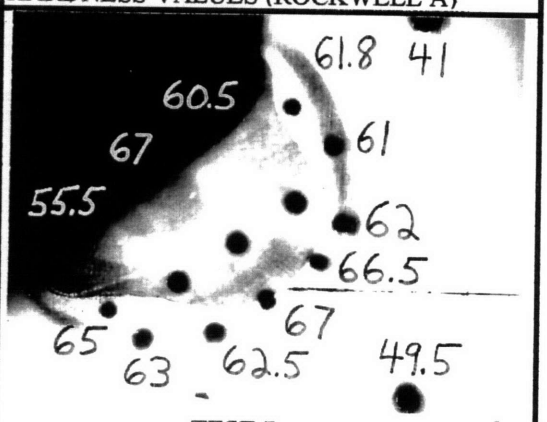 TEST 7
			Test 7 had the welding electrode located 2.5 mm above the weld joint intersection.	

SCALE (MM)

0 1 2 3 4 5

VOLTS	AMPS	TRAVEL	STEEL=DH-36 WELD=E71T-1 \ Fabco 802 \ CO2	HARDNESS VALUES (ROCKWELL A)
23	160	6.9 ipm	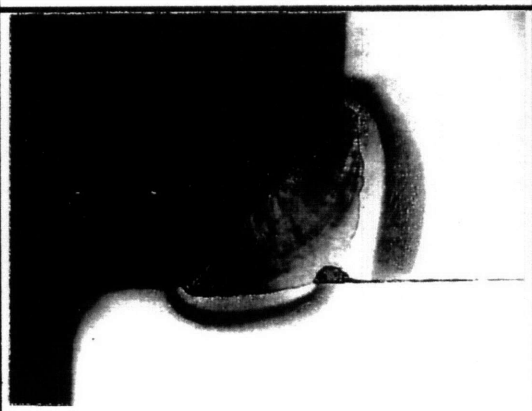 TEST 8	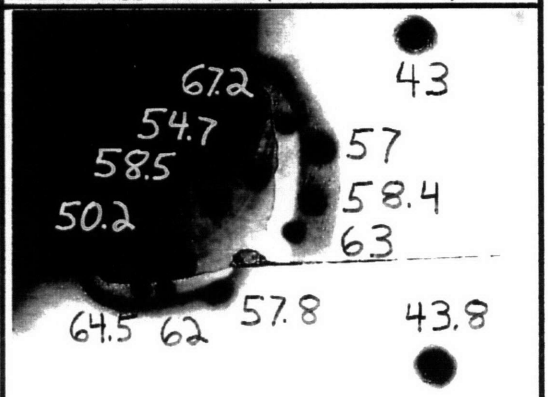 TEST 8
27	260	17.5 ipm	 TEST 9	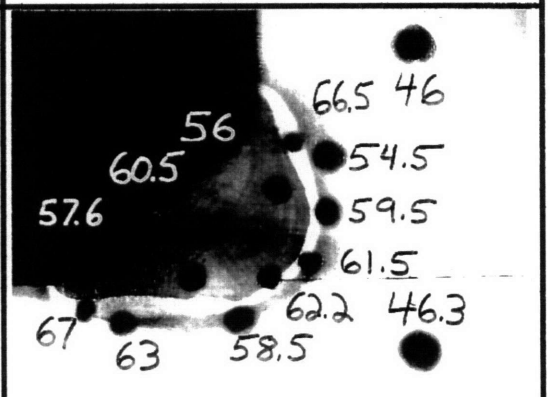 TEST 9
33	350	29.3 ipm	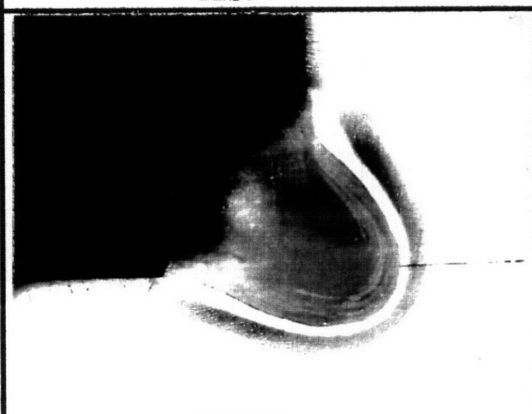 TEST 10	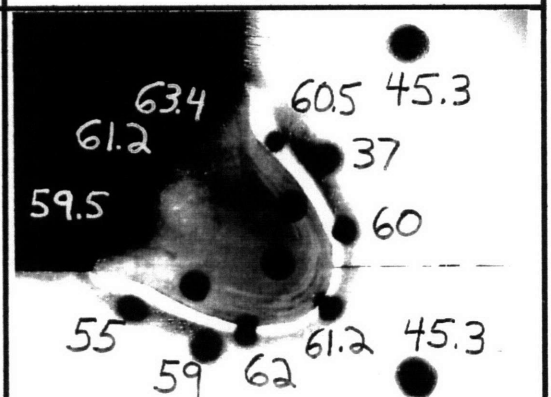 TEST 10

SCALE (MM)

0 1 2 3 4 5

APPENDIX G

Subroutine to Reduce Testing Data

Subroutine to Reduce Testing Data (Excel 5.0)

```
Sub SelectEvery5thRow()
    ColsSelection = Selection.Columns.Count
    RowsSelection = Selection.Rows.Count
    RowsBetween = 5
    Diff = Selection.Row - 1
    Selection.Resize(RowsSelection, 1).Select
    Set FinalRange = Selection. _
                        Offset(RowsBetween - 1, 0).Resize(1, ColsSelection)
    For Each xCell In Selection
        If xCell.Row Mod RowsBetween = Diff Then
            Set FinalRange = Application.Union _
                                (FinalRange, xCell.Resize(1, ColsSelection))
        End If
    Next xCell
    FinalRange.Select
End Sub
```

APPENDIX H

Upper Bound to the Weld Limit Load for Test Geometries

APPENDIX H

UPPER BOUND TO TENSILE STRENGTH FROM PLANAR SLIDING (APPLIED TO TEST SPECIMENS)

This method is from calculations included in Report 26 by McClintock (1994).
These calculations are used for the comparison of test results to theory shown in Table 5.1.

Upper Bound from Planar Sliding of Homogeneous Welds with Arbitrary Penetration and Weld Angle

A . Assigned Variables

Variable Definition

θ_w= weld angle

dx= weld leg length along the x-axis (mm)

Hv= average Vickers hardness (Kg/mm^2)

k= yield strength in shear (N/mm^2)

x_c= x-coordinte of the crack tip (mm)

y_c= y-coordinate of the crack tip

θ_{AB}= angle to the upper slip line from the x-axis (radians)

θ_{BC}= angle to the lower slip line from the x-axis (radians)

θ_{ABt}= angle from the craack tip to the upper toe (radians)

θ_{BCt}= angle from the crack tip to the lower toe (radians)

l_{AB}= length of the upper slip plane (mm)

l_{BC}= length of the lower slip plane (mm)

b= length of the tested specimen

Assigned Variable Values:

x_{c_i} = b_i = y_{c_i} = θ_{w_i} = d_{x_i} = $i = 1..10$

x_{c_i}	b_i	y_{c_i}	θ_{w_i}	d_{x_i}
0·mm	.1265·m	0·mm	.785398·rad	5.7·mm
0·mm	.128·m	0·mm	.785398·rad	5.9·mm
1.1·mm	.1275·m	0·mm	.785398·rad	7·mm
2.2·mm	.125·m	0·mm	.785398·rad	7.2·mm
2.7·mm	.125·m	0·mm	.800322·rad	6.6·mm
3.2·mm	.124·m	0·mm	.763179·rad	6.9·mm
2.1·mm	.126·m	0·mm	.765792·rad	7.8·mm
0·mm	.124·m	0·mm	.833904·rad	4.9·mm
2.2·mm	.126·m	0·mm	.725767·rad	7.1·mm
3.3·mm	.1255·m	0·mm	.844154·rad	5.6·mm

$$\theta ABt_i = \frac{\pi}{2} + \operatorname{atan}\left(\frac{x_{c_i} - 1}{d_{x_i} \cdot \tan(\theta w_i) - y_{c_i}}\right) \qquad \theta ABt_1 = 1.571$$

$$\theta BCt_i = -\operatorname{atan}\left(\frac{y_{c_i}}{d_{x_i} + x_{c_i}}\right)$$

$$\theta ABo_i = \theta ABt_i$$

$$\theta BCo_i = \theta BCt_i$$

$$l BCo_i = \frac{\left(d_{x_i} + x_{c_i} - \frac{y_{c_i}}{\tan(\theta w_i)}\right) \cdot \sin(\theta w_i)}{\sin(\theta w_i + \theta BCo_i)}$$

$$l ABo_i = l BCo_i \cdot \frac{\sin(\theta w_i + \theta BCo_i)}{\sin(\theta w_i + \theta ABo_i)}$$

If the upper slip line breaks through to the weld surface.

B. Calculations for the Shear Strength of the Fillet Weld

$TSm_i =$	$TSh_i =$
87400·psi	100000·psi
87400·psi	115000·psi
87400·psi	104000·psi
87400 psi	116000·psi
87400·psi	116300·psi
87400·psi	127000·psi
87400·psi	112000·psi
81700·psi	88000·psi
81700·psi	102000·psi
81700·psi	109000·psi

Tensile Strength
EXCEL-ARC 71(TESTS 1-7)
FABCO 802 (TESTS 8-10)
TSm(Values by electrode manufacturer)
TSh(Values by Rockwell A)

$$Km_i = \frac{TSm_i}{\sqrt{3}} \qquad Kh_i = \frac{TSh_i}{\sqrt{3}}$$

Shear strength of the weld in yield.
Km= shear strength by manufacturer test
Kh= shear strength by hardness tests

D. Calculation of the Limit Load of the Web

Limit Load Calculations from Hardness Tests.

$TS = 58000 \cdot psi$

$TS = 40.778 \cdot \frac{kgf}{mm^2}$

Ultimate Tensile Stress of EH-36 base plate.

From Rockwell A test (42.5 value)

$t = 15 \cdot mm$

Thickness of the web.(For typical tankers)

$PL_{bp} := t \cdot \frac{2}{\sqrt{3}} \cdot TS$

The 2/sqrt(3) accounts for the plane strain condition.

$PL_{bp} = 706.296 \cdot \frac{kgf}{mm}$

Limit Load Calculations from Testing on the Plate (From plate manufacturer)

$UTS = 82091.4 \cdot psi$

$UTS = 57.716 \cdot \frac{kgf}{mm^2}$

Tensile strength of EH 36 plate from manufacturer tests.

$PL_{bp} := t \cdot \frac{2}{\sqrt{3}} \cdot UTS$

Tensile Strength of web with typical tanker ship dimensions.

$PL_{bp} = 999.67 \cdot \frac{kgf}{mm}$

E. Calculation of the Limit Load of the Weld in Transverse Loading

Upper Bound Limit Load (Kgf/mm)

$$P_{ubm_i} := \frac{2 \cdot Km_i}{\sin\left(\theta ABo_i - \theta BCo_i\right)} \cdot \left(l ABo_i \cdot \left|\cos\left(\theta BCo_i\right)\right| + l BCo_i \cdot \left|\cos\left(\theta ABo_i\right)\right|\right)$$

Manufacturers weld strength.

$$P_{ubh_i} := \frac{2 \cdot Kh_i}{\sin\left(\theta ABo_i - \theta BCo_i\right)} \cdot \left(l ABo_i \cdot \left|\cos\left(\theta BCo_i\right)\right| + l BCo_i \cdot \left|\cos\left(\theta ABo_i\right)\right|\right)$$

Hardness estimates of weld strength

UPPER BOUNDS TO THE LIMIT LOAD FOR THE 10 TEST SPECIMENS

Test	Manufacturer Tensile Strength	Hardness Estimated Tensile Strength
1	$P_{ubm_1} = 404.44 \cdot \frac{kgf}{mm}$	$P_{ubh_1} = 462.746 \cdot \frac{kgf}{mm}$
2	$P_{ubm_2} = 418.631 \cdot \frac{kgf}{mm}$	$P_{ubh_2} = 550.83 \cdot \frac{kgf}{mm}$
3	$P_{ubm_3} = 599.26 \cdot \frac{kgf}{mm}$	$P_{ubh_3} = 713.079 \cdot \frac{kgf}{mm}$
4	$P_{ubm_4} = 762.365 \cdot \frac{kgf}{mm}$	$P_{ubh_4} = 1.012 \cdot 10^3 \cdot \frac{kgf}{mm}$
5	$P_{ubm_5} = 820.566 \cdot \frac{kgf}{mm}$	$P_{ubh_5} = 1.092 \cdot 10^3 \cdot \frac{kgf}{mm}$
6	$P_{ubm_6} = 925.847 \cdot \frac{kgf}{mm}$	$P_{ubh_6} = 1.345 \cdot 10^3 \cdot \frac{kgf}{mm}$
7	$P_{ubm_7} = 770.564 \cdot \frac{kgf}{mm}$	$P_{ubh_7} = 987.451 \cdot \frac{kgf}{mm}$
8	$P_{ubm_8} = 358.166 \cdot \frac{kgf}{mm}$	$P_{ubh_8} = 385.784 \cdot \frac{kgf}{mm}$
9	$P_{ubm_9} = 684.22 \cdot \frac{kgf}{mm}$	$P_{ubh_9} = 854.228 \cdot \frac{kgf}{mm}$
10	$P_{ubm_{10}} = 841.72 \cdot \frac{kgf}{mm}$	$P_{ubh_{10}} = 1.123 \cdot 10^3 \cdot \frac{kgf}{mm}$

APPENDIX I

Upper Bound to Weld Limit Load for Test Geometries

(Without Penetration)

APPENDIX I

UPPER BOUND TO TENSILE STRENGTH FROM PLANAR SLIDING (APPLIED TO TEST SPECIMEN GEOMETRY WITHOUT PENETRATION)

This method is from calculations included in Report 26 by McClintock (1994).
These calculations are used for the comparison of test results to theory shown in Table 5.1.

Upper Bound from Planar Sliding of Homogeneous Welds with Arbitrary Penetration and Weld Angle

A . Assigned Variables

Variable Definition

θ_w= weld angle

dx= weld leg length along the x-axis (mm)

Hv= average Vickers hardness (Kg/mm^2)

k= yield strength in shear (N/mm^2)

x_c= x-coordinte of the crack tip (mm)

y_c= y-coordinate of the crack tip

θ_{AB}= angle to the upper slip line from the x-axis (radians)

θ_{BC}= angle to the lower slip line from the x-axis (radians)

θ_{ABt}= angle from the craack tip to the upper toe (radians)

θ_{BCt}= angle from the crack tip to the lower toe (radians)

l_{AB}= length of the upper slip plane (mm)

l_{BC}= length of the lower slip plane (mm)

b= length of the tested specimen

Assigned Variable Values:

$i := 1..10$

$x_{c_i} :=$	$b_i :=$	$y_{c_i} :=$	$\theta_{w_i} :=$	$d_{x_i} :=$
0·mm	.1265·m	0·mm	.785398·rad	5.7·mm
0·mm	.128·m	0·mm	.785398·rad	5.9·mm
0·mm	.1275·m	0·mm	.785398·rad	7·mm
0·mm	.125·m	0·mm	.785398·rad	7.2·mm
0·mm	.125·m	0·mm	.800322·rad	6.6·mm
0·mm	.124·m	0·mm	.763179·rad	6.9·mm
0·mm	.126·m	0·mm	.765792·rad	7.8·mm
0·mm	.124·m	0·mm	.833904·rad	4.9·mm
0·mm	.126·m	0·mm	.725767·rad	7.1·mm
0·mm	.1255·m	0·mm	.844154·rad	5.6·mm

$$\theta_{ABt_i} := \frac{\pi}{2} + \operatorname{atan}\left(\frac{x_{c_i} - 1}{d_{x_i} \cdot \tan(\theta_{w_i}) - y_{c_i}}\right) \qquad \theta_{ABt_1} = 1.571$$

$$\theta_{BCt_i} := -\operatorname{atan}\left(\frac{y_{c_i}}{d_{x_i} + x_{c_i}}\right)$$

$$\theta_{ABo_i} := \theta_{ABt_i}$$

$$\theta_{BCo_i} := \theta_{BCt_i}$$

$$l_{BCo_i} := \frac{\left(d_{x_i} + x_{c_i} - \frac{y_{c_i}}{\tan(\theta_{w_i})}\right) \cdot \sin(\theta_{w_i})}{\sin(\theta_{w_i} + \theta_{BCo_i})}$$

$$l_{ABo_i} := l_{BCo_i} \cdot \frac{\sin(\theta_{w_i} + \theta_{BCo_i})}{\sin(\theta_{w_i} + \theta_{ABo_i})}$$

If the upper slip line breaks through to the weld surface.

B. Calculations for the Shear Strength of the Fillet Weld

$TSm_i :=$	$TSh_i :=$
87400·psi	100000·psi
87400·psi	115000·psi
87400·psi	104000·psi
87400·psi	116000·psi
87400·psi	116300·psi
87400·psi	127000·psi
87400·psi	112000·psi
81700·psi	88000·psi
81700·psi	102000·psi
81700·psi	109000·psi

Tensile Strength
EXCEL-ARC 71(TESTS 1-7)
FABCO 802 (TESTS 8-10)
TSm(Values by electrode manufacturer)
TSh(Values by Rockwell A)

$$Km_i := \frac{TSm_i}{\sqrt{3}} \qquad Kh_i := \frac{TSh_i}{\sqrt{3}}$$

Shear strength of the weld in yield.
Km= shear strength by manufacturer test
Kh= shear strength by hardness tests

D. Calculation of the Limit Load of the Web

Limit Load Calculations from Hardness Tests.

$TS := 58000 \cdot psi$ Ultimate Tensile Stress of EH-36 base plate.

$TS = 40.778 \cdot \frac{kgf}{mm^2}$ From Rockwell A test (42.5 value)

$t := 15 \cdot mm$ Thickness of the web.(For typical tankers)

$PL_{bp} := t \cdot \frac{2}{\sqrt{3}} \cdot TS$ The 2/sqrt(3) accounts for the plane strain condition.

$PL_{bp} = 706.296 \cdot \frac{kgf}{mm}$

Limit Load Calculations from Testing on the Plate (From plate manufacturer)

$UTS := 82091.4 \cdot psi$

$UTS = 57.716 \cdot \frac{kgf}{mm^2}$ Tensile strength of EH 36 plate from manufacturer tests.

$PL_{bp} := t \cdot \frac{2}{\sqrt{3}} \cdot UTS$ Tensile Strength of web with typical tanker ship dimensions.

$PL_{bp} = 999.67 \cdot \frac{kgf}{mm}$

E. Calculation of the Limit Load of the Weld in Transverse Loading

Upper Bound Limit Load (Kgf/mm)

$$P_{ubm_i} := \frac{2 \cdot Km_i}{\sin\left(\theta ABo_i - \theta BCo_i\right)} \cdot \left(l ABo_i \cdot \left|\cos\left(\theta BCo_i\right)\right| + l BCo_i \cdot \left|\cos\left(\theta ABo_i\right)\right|\right)$$ Manufacturers weld strength.

$$P_{ubh_i} := \frac{2 \cdot Kh_i}{\sin\left(\theta ABo_i - \theta BCo_i\right)} \cdot \left(l ABo_i \cdot \left|\cos\left(\theta BCo_i\right)\right| + l BCo_i \cdot \left|\cos\left(\theta ABo_i\right)\right|\right)$$ Hardness estimates of weld strength

UPPER BOUNDS TO THE LIMIT LOAD FOR THE 10 TEST SPECIMENS (Penetration = 0)
BLOCK SLIDING METHOD

Test	Manufacturer Tensile Strength	Hardness Estimated Tensile Strength
1	$P_{ubm_1} = 404\,44 \cdot \frac{kgf}{mm}$	$P_{ubh_1} = 462.746 \cdot \frac{kgf}{mm}$
2	$P_{ubm_2} = 418.631 \cdot \frac{kgf}{mm}$	$P_{ubh_2} = 550.83 \cdot \frac{kgf}{mm}$
3	$P_{ubm_3} = 496.68 \cdot \frac{kgf}{mm}$	$P_{ubh_3} = 591.016 \cdot \frac{kgf}{mm}$
4	$P_{ubm_4} = 510.871 \cdot \frac{kgf}{mm}$	$P_{ubh_4} = 678.044 \cdot \frac{kgf}{mm}$
5	$P_{ubm_5} = 482.489 \cdot \frac{kgf}{mm}$	$P_{ubh_5} = 642.031 \cdot \frac{kgf}{mm}$
6	$P_{ubm_6} = 468.298 \cdot \frac{kgf}{mm}$	$P_{ubh_6} = 680.479 \cdot \frac{kgf}{mm}$
7	$P_{ubm_7} = 532.157 \cdot \frac{kgf}{mm}$	$P_{ubh_7} = 681.94 \cdot \frac{kgf}{mm}$
8	$P_{ubm_8} = 358.166 \cdot \frac{kgf}{mm}$	$P_{ubh_8} = 385.784 \cdot \frac{kgf}{mm}$
9	$P_{ubm_9} = 417.859 \cdot \frac{kgf}{mm}$	$P_{ubh_9} = 521.685 \cdot \frac{kgf}{mm}$
10	$P_{ubm_{10}} = 417.86 \cdot \frac{kgf}{mm}$	$P_{ubh_{10}} = 557.487 \cdot \frac{kgf}{mm}$

Note: For welds with a weld angle greater than 45 degrees the slip line solution is determined by the following formula:

$$PL_i = Kh_i \cdot d_{X_i} \cdot \left[1 + 2 \cdot \left(\theta_{w_i} - \frac{\pi}{4} \right) \right]$$

TEST	PL (kgf/mm)
5	641.77
8	384.02
10	553.84